Low Energy Properties of Magnetic Systems

José María Román Faúndez

September 1998

Universitat de Barcelona

Departament d'Estructura i Constituents de la Matèria

Low Energy Properties of Magnetic Systems

Memoria presentada por
José María Román Faúndez
para optar al título de
Doctor en Ciencias Físicas.

Tesis realizada bajo la dirección de

Joan Soto Riera
Profesor titular de la Universitat de Barcelona,

dentro de programa de doctorado del *departament d'Estructura i Constituents de la Matèria* / Bienio 1994-96,

tutelado por

Pedro Pascual de Sans
Catedrático de la Universitat de Barcelona.

Agradecimientos

Quiero empezar estos agradecimientos, que por necesidad han de ser extensos, *agraïnt al meu director de tesi Joan Soto Riera la seva ajuda en la realització d'aquesta tesi, així com la seva paciència i sobretot aquella il.lusió per fer bé les coses fins al final, que em va encomanar poc a poc i que jo em pensava haver perdut.*

Me gustaría agradecer a Pedro Pascual de Sans la oportunidad de vivir *experiencias inolvidables* que contarle a mis nietos. Claro que no serán igual que las historias que me cuenta mi abuelo de cuando estuvo en Valladolid haciendo la mili en *tiempo normal* como ordenanza del teniente coronel don Arias Bulnes Tres Palacios, pero *Déu n'hi do!*. Quiero agradecerle a Rolf Tarrach el trabajo compartido, y a Joaquim Gomis las risas que hemos echado a cuenta de las clases y el *bazooka*. A Josep Tarón debo agradecerle su apoyo sobre todo durante el primer año, y su ayuda en las clases de problemas, así como a Ramón Miquel y Artur Polls. Continuando con los agradecimientos a profesores no puedo olvidarme de los buenos momentos y la hospitalidad recibida durante mi estancia en Madrid por parte de Germán Sierra, Jorge Dukelsky y Miguel Angel Martín-Delgado.

Ahora pasaremos a los que realmente más han sufrido conmigo. Quiero agradecer a Francesc Xavier Magdaleno, Paula Herrera, Assumpta Parreño (Assum), Marçel Porta y Arturo Martí el tiempo que me han aguantado. También a Josep Herrero y Sergi Leseduarte las caminatas y charlas compartidas, a pesar de los ríos atravesados. A Antonio Pineda por haber resultado un buen *hermano mayor*, así como espero que Dolors Eiras sea una buena *hermanita*. A Joan Simón, Julián Manzano y sus compinches la alegría que han traido al departamento, que no la pierdan. También quiero agradecer a Manuel Montejo (Manu), Marta Janeras, Jordi Llumá, José María Ruiz (Chema), M. Montserrat García del Muro (Montse), Roberto Ribas, Albert Roura y Oscar Iglesias los buenos momentos que hemos pasado juntos, sin los cuales creo que no habría podido terminar esta tesis.

Además quiero agradecer la simpatía del personal de secretaría, que menudo *personal*, Laura, Joan Ramón, y Oriol, que siempre me *escondía* las cartas.

Siempre tendré un recuerdo especial para mis amigos Maite Faúndez, Antonio Rejón (Toni), su hermana Olga, Olga Jiménez y Pilar Pereiro (Pili), que estuvieron ahí en los momentos más difíciles, y que durante este último año han sufrido la ausencia derivada de mi *suicidio*.

Para ausencia la que ha tenido que sufrir mi familia, durante cuatro años, salvo algunas visitas esporádicas. La verdad es que Amorebieta está distinta cada vez que voy, menos mal que hay teléfono, y que mi hermano Antonio me hizo una *visitilla*, de un año.

Debo agradecer la financiación durante la realización de esta tesis del Departamento de Educación, Universidades e Investigación del Gobierno Vasco por medio de una beca FPI.

Eskerrik asko gustioi. Goazen aurrera!.

Author's works

J. M. Román and R. Tarrach, *"The Regulated Four-parameter One-dimensional Point Interaction"*, *J. Phys.* **A29** (1996) 6073-6086.

J. M. Román and J. Soto, *"Effective Field Theory Approach to Ferromagnets and Antiferromagnets in Crystalline Solids"*, cond-mat/9709289.

J. M. Román and J. Soto, *"Spin Wave Mediated Non-reciprocal Effects in Antiferromagnets"*, cond-mat/9709299.

J. M. Román, G. Sierra, J. Dukelsky and M. A. Martín-Delgado, *"The Matrix Product Approach to Quantum Spin Ladders"*, cond-mat/9802150.

J. M. Román and J. Soto, *"Continuum Double Exchange Model"*, preprint no. UB-ECM-PF 98/18.

J. M. Román and J. Soto, *"Spin Waves in Canted Phases"*, preprint no. UB-ECM-PF 98/19.

Contents

Chapter 1

Introduction

This chapter is devoted to the introduction to the main points described in this thesis. First of all, we study a set of quasi-one-dimensional systems that have received considerable attention lately, namely, the quantum spin ladders. A renormalisation group variational method applied to quantum systems has been used in the study. Secondly, a continuum model is applied to the study of the ground state configuration in the crystals of doped manganites. This model gives rise to a rich variety of phases relating the magnetic and conducting properties. After that, from an effective field theory approach a formalism has been developed to describe the spin wave dynamics in magnetic ordered crystalline media. The coupling with the electromagnetic field in the microwave regime has been introduced in order to apply the formalism to the description of non-reciprocal effects in antiferromagnetic crystals.

1.1 Introduction

This thesis is devoted to the study of magnetic systems in Condensed Matter (CM) using different approaches. The first approach is a Renormalisation Group (RG) technique based on a variational modification of the Density Matrix Renormalisation Group (DMRG). DMRG is very useful in the solution of one and quasi-one-dimensional problems, leading to a great precision in the results, in particular for the ground state energy and the correlation length in spin chains [1]. After that, a continuum model is constructed to study the magnetic and conducting properties of the ground state of doped manganites, giving rise to a rich phase structure. Finally, we introduce an Effective Field Theory formalism, borrowed from Quantum Field Theory (QFT), which has been applied successfully in the description of systems where spontaneous symmetry breaking (SSB) occurs, as the pion dynamics in the low energy spectrum of QCD [2]. Notice that since the SSB occurs only in systems with dimension higher than one [3] the last effective theories cannot be applied in one-dimensional systems. However, other formalisms are suitable to work in dimension 1, among them the Matrix Product Method (MPM) to be presented here.

Let us first introduce the physical systems we are going to work with. The fundamental ingredients in a CM physical system are electrons and nuclei. These interact thorough the Coulomb law, $1/r$, which in some circumstances must be augmented with the spin-orbit and magnetic dipole interactions. The way of approaching these systems is by selecting the degrees of freedom which are relevant for the problem to be considered within a required precision. These degrees of freedom may be different of the fundamental ones as well as their interactions. For instance, the phonons, polarons or holes which turn out to be the elementary excitations in some systems, or new interactions like the Lennard-Jones interactions, $1/r^{12} - 1/r^6$. In general we will be working at such energies that an atomic crystalline structure exist and only the electrons of the external orbitals will be relevant, i.e., their state may be modified in the considered physical process. At this level, for instance, we have the free electron model, which describes some conductor metals. Another kind of model is given by the Hubbard model, which describes localised electrons with the possibility of hopping between neighbouring atoms. This model explains phenomena such as the Mott transition (insulator-conductor). The $t - J$ model, which is derived from the previous one when double occupancy is forbidden in each atom, is thought to be relevant for high-T_c

superconductivity. In a next nested level the Heisenberg model emerges from the $t-J$ model when we are at half-filling. The previous relations among these models will be discussed in the following section.

Once we have selected the "microscopic" effective model we may proceed in two ways. On the one hand, we may calculate directly some macroscopic observables, and on the other, we may construct a macroscopic model which gives us the dynamics of the system in the long distance regime. Some of these models, eventually, can be promoted to effective theories. In any case, the RG [4] is a widely used technique in order to perform these calculations. By means of a recurrent procedure RG enhances the relevant degrees of freedom in the low energy and long distance regime. In the chapter 2 we show how RG works in the first case, namely, the computation of macroscopic observables, as ground state energies or correlation lengths. With respect to the derivation of the low energy dynamics the RG gives rise to effective theories which describe the macroscopic behaviour. In particular, when it is applied to CM systems familiar equations in QFT often arise. For instance, the Majorana equation for fermions in the 2-dimensional Fermi liquid theory or the Chern-Simons theory in the quantum Hall effect (QHE) [5].

The macroscopic models that one may construct are based on phenomenological evidences. The continuum models provide a suitable description of the long wave length regime. Even though these models have not been systematically derived from an application of the RG, they incorporate the main characteristics of the system. In this sense we have construct in chapter 3 a continuum model to describe the ground state and low energy properties of the doped manganites.

In addition to the apparent degrees of freedom collective low energy excitations exist in the Hubbard or descendent models. This collective modes are generated in a crystalline lattice, like phonons, as well as in magnetic structures, like spin waves, and must be taken into account in the study of these systems. The RG application in these systems would produce these kind of degrees of freedom in the description of the macroscopic dynamics. However, since these excitations turn out to be Goldstone modes, whose dynamics is very much constrained by symmetry properties and described by a general formalism independent of the details of the underlying models, a direct application of the RG is unnecessary. Although, an indirect application is taken into account in the selection of the terms which enter the effective theory. This formalism is known since sixties [6, 7], but has not been widely used until few years

ago to describe pion physics in QCD [2]. It has been suggested recently [8] that this formalism may be useful in CM. In the chapter 4 the construction of the formalism for ferromagnetic and antiferromagnetic crystals is described.

1.2 Hubbard Model

The simplest "Hubbard model" describes the excitations produced in a crystal where the electrons are localised around atoms. The electrons interact thorough a Coulomb potential with the other electron in their orbital with an intensity U. They can hop to one of the nearest atoms with a reduction of the system energy t_{ij} [9],

$$H_{Hub} = -\sum_{<i,j>\sigma} t_{ij} c^{\dagger}_{i\sigma} c_{j\sigma} + U \sum_{i} n_{i\uparrow} n_{i\downarrow}. \tag{1.2.1}$$

Outside the atom the Coulomb interaction is screened, and the dominant term inside reads

$$U = \int d\mathbf{r} d\mathbf{r}' \phi^*_i(\mathbf{r}) \phi^*_i(\mathbf{r}') V(\mathbf{r}-\mathbf{r}') \phi_i(\mathbf{r}') \phi_i(\mathbf{r}), \tag{1.2.2}$$

where $V(\mathbf{r}-\mathbf{r}')$ represents the Coulomb interaction and $\phi_i(\mathbf{r})$ the orbital wave function corresponding to the i-th atom. The coefficient t_{ij} describes the transport between orbitals in different atoms. The hopping is taken to nearest neighbours.

$$t_{ij} = -\int d\mathbf{r} \phi^*_i(\mathbf{r}) h(\mathbf{r}) \phi_j(\mathbf{r}) = t^*_{ji}, \tag{1.2.3}$$

where $h(\mathbf{r})$ represents the one-particle part of the hamiltonian including the kinetic term and the external fields.

In the "strong coupling" limit, $|t_{ij}|/U \to 0$, the double occupancy is forbidden, since this increases very much the energy of the system. In this situation it can be proved that the Hubbard hamiltonian becomes the $t-J$ model, where the Coulomb interaction gives rise to a Heisenberg type of interaction between nearest neighbours.

$$H_{t-J} = -\sum_{<i,j>\sigma} t_{ij} c^{\dagger}_{i\sigma} c_{j\sigma} + \sum_{<i,j>} J_{ij} \left(\mathbf{S}_i \mathbf{S}_j + \frac{1}{4} \right), \tag{1.2.4}$$

where the operator $\mathbf{S}_i = \sum_i c^{\dagger}_{i\sigma} \sigma_{\sigma\sigma'} c_{i\sigma'}/2$ and the coupling $J_{ij} = 4|t_{ij}|^2/U$ arises from a return hopping between two neighbouring atoms suppressed by the Coulomb energy due to the "virtual" double occupancy. Since the Hubbard model only allows double occupancy when the two electrons have opposite spin, the Heisenberg coupling turns

out to be antiferromagnetic. From here we can see the electrostatic origin of the Heisenberg interaction. In fact, the magnetic field generated by magnetic dipoles is 10^4 times less than the one *induced* by the typical Heisenberg couplings [10].

When the system is considered at "half-filling", i.e., one electron per site, the Heisenberg model is obtained. This is due to the fact that double occupancy is forbidden in the $t-J$ model and therefore electrons cannot hop in this situation.

This kind of models describe the crystalline systems. For example, the $t-J$ model is thought to describe the high-T_c superconductivity, whereas the main physical characteristics of ferromagnetic and antiferromagnetic crystals are described by the Heisenberg model.

One of the works which this thesis is based on refers to spin ladders interacting through Heisenberg hamiltonians. The spin ladders are constructed by several coupled parallel chains. Their study may yield to a deeper understanding of the crossover between 1 and 2 dimensions. In this sense the odd-legged ladders present a continuous transition (infinite correlation length, gapless), whereas the even-legged ladders have discontinuous one (finite correlation length, gap) [11]. New materials, like VOPO, have been discovered recently whose physical characteristics are thought to be described by spin ladders. This allows to test experimentally the validity of the obtained results.

1.3 Renormalisation Group in Quantum Systems

A very powerful and widely used technique is applied in the study of spin ladders: RG. This allows us to describe the macroscopic behaviour of the system, i.e., starting with a microscopic theory we apply an algorithm known as renormalisation group transformations (RGT) which enhances the macroscopically (in the low energy and long distance regime) relevant degrees of freedom and builds the interactions among them.

1.3.1 Blocking and boundary conditions

The most usual RGT is the "blocking" procedure. In this procedure we divide the system in blocks and the relevant degrees of freedom are selected within each block (after blocking the details of the microscopic information inside each block can not be recovered any more). By iterating the procedure a stationary point may be reached

which provides the macroscopic description of the system.

In the case we have a quantum system [12] the quantum problem can be solved in the block and the representative states selected among the solutions (the low energy ones, in principle). In the resolution of the quantum problem in the block boundary conditions (BC) must be imposed. The set of wave functions obtained with particular BC will not reproduce, in general, the wave function of the global system. A way to avoid this problems is to consider the combination of boundary conditions (CBC) method. In this method the block problem is solved for several BC and a combination of all the solutions is made. The problem now is how to choose the combination criteria.

1.3.2 Density matrix renormalisation group

The density matrix renormalisation group (DMRG) developed by White in 1992 [1] is the most efficient CBC method for one-dimensional systems. The DMRG follows the renormalisation process developed by Wilson in the study of Kondo problem. This is a recursive method which generates a chain by adding a new site in each RG step, i.e., given a chain B (described by m states, $|\beta\rangle$) a new site $\bullet$ (described by m^* states, $|s\rangle$) is added to obtain a new chain B' (described by m states$|\alpha\rangle$), $B\bullet \rightarrow B'$.

The DMRG algorithm solves the system $B\bullet$ for several BC and decides the combination criteria at the same time.

1. It doubles the system $B\bullet$ forming the superblock $B \bullet \bullet B^R$, where B^R is the chain B reflexion.

2. It computes the superblock ground state $|\Psi_0\rangle$.

3. It takes the partial trace over the ampliation of the system, $\bullet B^R$, in the density matrix $|\Psi_0\rangle\langle\Psi_0|$.
$$\rho = tr_{\bullet B^R}|\Psi_0\rangle\langle\Psi_0|. \tag{1.3.1}$$

4. It diagonalises the matrix ρ, which describes the system $B\bullet$ physics.

5. It takes the m states with the highest eigenvalue in ρ as the representative ones of the new system B'.

This Hilbert space truncation is reflected in the following recurrent relations for the states:
$$|\alpha\rangle_N = \sum_{\beta s} A^{(N)}_{\alpha\beta}[s]\ |s\rangle_N \otimes |\beta\rangle_{N-1}, \tag{1.3.2}$$

where the $A^{(N)}_{\alpha\beta}[s]$ matrices are computed in each RG step and are directly related with the change of basis which diagonalises the density matrix ρ.

The expression (1.3.2) is the starting point for the work presented in the chapter 2, which is summarised in the following section.

1.4 Matrix Product Method

In the chapter 2 we present a method based on the DMRG whose purpose is to yield a deeper understanding on how DMRG works. Since DMRG is a numerical method, it is very difficult to follow the evolution of the physical process and to gain any intuition from it. The matrix product method (MPM) is a variational recurrent method which assumes that a fix point exists for the equation (1.3.2) in such a way that $\lim_{N\to\infty} A^{(N)}_{\alpha\beta}[s] = A_{\alpha\beta}[s]$. In this case, given a set of states $|\beta\rangle$ for B and $|s\rangle$ for $\bullet$, we use the recurrent formula

$$|\alpha\rangle_N = \sum_{\beta s} A_{\alpha\beta}[s]\ |s\rangle_N \otimes |\beta\rangle_{N-1} \tag{1.4.1}$$

to calculate the observables (ground state energy, correlation length, etc.) in the one-dimensional system depending on the matrices $A_{\alpha\beta}[s]$. These matrices are taken as variational parameters and are computed by minimising the ground state energy.

The system in which we will apply this formalism is the 2-leg spin ladders. These systems can be thought as quasi-one-dimensional systems provided that we consider a rung in a ladder as a site in a one-dimensional chain. The spins in these ladders interact thorough a Heisenberg hamiltonian

$$H_N = J_\perp \sum_{n=1}^{N} \mathbf{S}_1(n)\cdot\mathbf{S}_2(n) + J_\parallel \sum_{n=1}^{N-1} \left(\mathbf{S}_1(n)\cdot\mathbf{S}_1(n+1) + \mathbf{S}_2(n)\cdot\mathbf{S}_2(n+1)\right), \tag{1.4.2}$$

where $\mathbf{S}_a(n)$ is a spin S operator acting on the $n = 1,\ldots,N$ rung and the $a = 1,2$ leg of the ladder.

Since the hamiltonian commutes with the total spin operator we have chosen states with a well defined spin to describe the system,

$$|J_1 M_1\rangle_N = \sum_{\lambda J_2} A^{\lambda}_{J_1 J_2}\ |(\lambda J_2), J_1 M_1\rangle_N, \tag{1.4.3}$$

where

$$|(\lambda J_2), J_1 M_1\rangle_N = \sum_{\mu} \langle \lambda\mu, J_2 M_2 | \lambda J_2, J_1 M_1\rangle\ \ |\lambda\mu\rangle_N \otimes |J_2 M_2\rangle_{N-1} \tag{1.4.4}$$

and $A^{\lambda}_{J_1 J_2}$ are the variational parameters. In this way the formalism is greatly simplified, since we are allowed to use all the rotational group properties (Wigner-Eckart theorem).

Using this method we have computed the ground state energy, the correlation length an other similar observables for different kinds of ladders. The differences are determined by the ferromagnetic (F) or antiferromagnetic (A) nature of the Heisenberg couplings. The considered cases are $AA_{1/2}$, $AF_{1/2}$, $FA_{1/2}$, AA_1 and $AA_{3/2}$ (for example $AF_{1/2}$ is a spin 1/2 ladder with A coupling along the legs and F coupling along the rungs). Furthermore several symmetry relations proposed in [13] for the 1/2 spin ladders, called "dualities", are shown, at least in some regions of the couplings $J_{\|}$ and $J_{\perp}$.

1.5 Doped Manganites

The manganites are a generic group of alloys which present a rich magnetic structure in their ground state, from antiferromagnetism to ferromagnetism going through canted phases (i.e., the magnetisations in the even and odd sublattices form an angle θ, $0 < \theta < \pi$) or phase separation regions. These materials are based on the general formula $La_{1-x}A_xMnO_3$, where $A = Ca, Sr$ or Ba and $0 \leq x \leq 1$ represents the number of La atoms substituted by type A atoms. The valence of the different elements is La^{3+}, A^{2+}, Mn^{3+} ($[Ar]3d^4$) or Mn^{4+} ($[Ar]3d^3$) and O^{2-}. Therefore, each substitution $La^{3+} \rightarrow A^{2+}$ corresponds to a substitution in the manganese atom $Mn^{3+} \rightarrow Mn^{4+}$, which are the magnetic ions, and produces a change in the spin $S = 2 \rightarrow S = 3/2$ (Pauli principle helps to minimise the electrostatic energy in the d-shell, if the electrons are unpaired, which gives rise to the highest possible spin. This is known as the Hund's Rule).

Let us give a brief overview of the crystallographic and electronic structures of these materials. Usually the manganites crystalise in a Perovskite distorted structures, i.e., ideally, with the Mn atoms at the vertices of a cube, the other metallic elements (La, Ca, Sr or Ba) body centered in the cube, and the O in the middle of the faces. From this structure the ideal cubic space group $Pm\bar{3}m$ slightly distorts to an orthorhombic space group. The crystalline field makes that the 5-fold $3d$ bands splits into a 3-fold t_{2g} band and a 2-fold e_g band. For small x a new structural distortion (Jahn-Teller distortion) produces a further splitting of the 2-fold e_g band.

The band structure above makes that the extreme compounds, i.e., $LaMnO_3$ ($x = 0$) and $AMnO_3$ ($x = 1$) behave like semiconductors. Furthermore, they present

an AF ground state due to the antiparallel coupling produced between d-shells of neighbouring atoms. On the other hand, $0.2 < x < 0.4$ a F ground state arises. In this range of doping parameter conduction properties are also observed, which suggests that both phenomena are related. Indeed, Zener in his Double Exchange Model [14] postulates that the exchange of the electrons from Mn^{3+} to Mn^{4+} atoms through the O atoms produces a lowering in the energy of the system, and since these exchanges do not modify the spin of the electrons the most favored state is the ferromagnetic one.

The previous characteristics are incorporated in the $s-d$ model which describes a Kondo problem with a Heisenberg term. The $s-d$ model considers the electrons in the e_g band as dynamical spin 1/2 quantum fermions with a hopping amplitude t_{ij} and interacting with a classical spin, generated by the electrons in the t_{2g} band, through an onsite Heisenberg ferromagnetic interaction, which takes into account the Hund's rule. The classical spins interact antiferromagnetically with their nearest neighbours.

$$H_{s-d} = -\sum_{<i,j>\sigma} t_{ij} c^\dagger_{i\sigma} c_{j\sigma} - \frac{J_H}{2}\sum_i c^\dagger_i \boldsymbol{\sigma} c_i \mathbf{S}_i + \sum_{<i,j>} J_{ij}\mathbf{S}_i\mathbf{S}_j. \tag{1.5.1}$$

1.6 Field Theoretical Model for Doped Manganites

Based on the above model, in chapter 3, we introduce a continuum model to describe the low energy properties of the doped manganites. First of all, two slowly varying magnetisation fields are introduced, $\mathbf{M}_1(x)$ and $\mathbf{M}_2(x)$, associated to the even and odd sublattices in the crystal. Afterwards, two slowly varying fermionic fields which describe the conducting holes produced by the doping, interacting locally with the corresponding magnetisation, are considered. The number of doping holes is controled by the chemical potential.

$$\begin{aligned}\mathcal{L}(x) &= \psi_1^\dagger(x)\left[(1+i\epsilon)i\partial_0 + \frac{\partial_i^2}{2m} + \mu + J_H\frac{\boldsymbol{\sigma}}{2}\mathbf{M}_1(x)\right]\psi_1(x) \\ &\quad + \psi_2^\dagger(x)\left[(1+i\epsilon)i\partial_0 + \frac{\partial_i^2}{2m} + \mu + J_H\frac{\boldsymbol{\sigma}}{2}\mathbf{M}_2(x)\right]\psi_2(x) \\ &\quad + t\left(\psi_1^\dagger(x)\psi_2(x) + \psi_2^\dagger(x)\psi_2(x)\right) - J_{AF}\mathbf{M}_1(x)\mathbf{M}_2(x),\end{aligned} \tag{1.6.1}$$

We have consider the parabolic approximation of the band for small doping.

We assume that by setting $t = 0$ the chemical potentials associated to small dopings are bellow the filled band. It is after allowing t to take finite values that the band may

cross the chemical potential giving rise to conductivity and ferromagnetic or canted phases.

The effective potential for the $\mathbf{M}_1(x)$ and $\mathbf{M}_2(x)$ fields, obtained by integrating out the fermionic degrees of freedom in the path integral, gives rise to different phases: AFI (AF-Insulating), $AFC2$ (AF-Conducting, 2-bands), $CC2$ (Canted-Conducting, 2-bands), $CC1$ and $FC1$, as well as a phase separation region.

1.7 Spontaneous Symmetry Breaking

As it was mentioned in the introduction, certain collective low energy excitations, known as Goldstone modes, may exist in CM systems. For instance, the phonons, in any crystalline system, or spin waves, in magnetically ordered systems. These collective excitations are, in general, present in systems where a spontaneous symmetry breakdown is produced. There are effective field theories specially suitable to describe their dynamics, which is totally determined (except for some coefficients that must be measured or calculated from first principles) by symmetry considerations, which are independent of the details of any microscopic model which idealises the system.

1.7.1 Goldstone theorem

Given a system whose dynamics presents a symmetry group G, an its ground state has a smaller symmetry group H, $H \subset G$, it is said that spontaneous symmetry breaking (SSB) occurs. In this circumstances the Goldstone theorem tells us that gapless excitation modes appear in the spectrum.

These modes are described by fields which transform under the group G as elements of the coset G/H. The number of real fields describing these modes is equal to the number of broken generators, i.e., $n_G - n_H$, where n_G and n_H are the number of generators in the groups G and H respectively. Whereas the number of fields is known the number of modes described by these cannot be known *a priori*, since it depends on the kind of equation which these fields verify. A wave equation (Klein-Gordon type) describes one mode with one real field, whereas a Schödinger equation describes one mode with one complex field, or equivalently with two real fields [15]. The kind of equation which describes the dynamics is determined by the space-time transformation properties.

1.7.2 Effective lagrangians

The importance of the Goldstone modes in the description of a physical system description has already been mentioned. Due to the absence of gap in their spectrum they can be present in any phenomena. This is the reason why a formalism to describe these modes as well as their interactions is necessary. First of all we will try to describe the Goldstone modes mathematically.

The Goldstone modes, like phonons or spin waves, are fluctuations of a ground state with a symmetry group, H, smaller than that for the theory, G. This fluctuation can be imagined as an element of G, with their group parameters varying slowly thorough the space-time structure of the ground state. Those parameters which produce fluctuations along the H directions are irrelevant, since they leave invariant the ground state. Therefore the resultant element belongs to the coset G/H.

$$U(x) = \exp\left\{\frac{i}{f_\pi}\pi^a(x)X^a\right\} \quad \in \quad G/H \qquad , \qquad (a = 1, \ldots, n_G - n_H). \tag{1.7.1}$$

The coset G/H elements transform under an element of G with a non-linear transformation given by

$$U(x) \longrightarrow gU(x)h^\dagger(g,U) \qquad , \qquad h^\dagger(g,U) \in H, \tag{1.7.2}$$

in such a way that $h^\dagger(g,U)$ restores to the coset the transformed field $gU(x)$.

Now that we know the fields describing the Goldstone modes and their transformations we are in the position of constructing an effective lagrangian which describes their dynamics. The Goldstone modes are low energy solutions of the underlying theory with a symmetry group G. Therefore an effective theory which reproduces the low energy spectrum of the system must be invariant under the same group of symmetry G. The effective lagrangian is a scalar under the invariance group, therefore we must construct an expansion of invariant terms organised in powers of derivatives. In addition to these, topological terms (invariants except for a total derivative) must be admited because they give rise to invariant actions. These terms play an essential role as we will see in chapter 4.

The number of Goldstone modes described by $U(x)$ is determined by the transformation properties under the space-time symmetry group. These properties are related to the way in which the spontaneous breaking of the space-time symmetry is produced. In relativistic systems [6] the space-time symmetry is given by the Poincaré

group, which induces wave equations (Klein-Gordon type) for the Goldstone modes, where each mode is described by one field. Moreover the ground state does not break the Poincaré invariance. A more complex situation appears in the non-relativistic case. We could think that the Galileo group is the relevant one and therefore the Goldstone modes would follow a Schrödinger equation (there would be twice fields than modes). This is not generally true: crystallographic space groups are the relevant ones. The crystallographic space symmetry can also be spontaneously broken by the ground state, which allows for the appearance of wave equations in the description of Goldstone modes.

1.8 Spin Waves in Magnetic Crystals

In the chapter 4 we develop the theory presented in the previous section for spin waves in ferromagnetic and antiferromagnetic crystals. The spin waves are the Goldstone modes of the SSB $SU(2) \to U(1)$, i.e., from the invariance under spin rotations to the invariance under only one direction, that of the alignment of the spins in the ferromagnet or antiferromagnet. We choose the third direction of the spin as the alignment one $U(1) = \langle e^{i\theta S^3} \rangle$. In this case the spin waves are described by

$$U(x) = exp\left\{ \frac{i\sqrt{2}}{f_\pi} \left[\pi_1(x) S^1 + \pi_2(x) S^2 \right] \right\}, \tag{1.8.1}$$

where S^i are the $SU(2)$ generators and $\pi_i(x)$ are the spin wave fields (f_π is a dimensionful factor).

For convenience, due to the application developed in the chapter 5, we have chosen $R\bar{3}c \otimes T$ as the space-time transformation group, which is that enjoyed by Cr_2O_3. This group is broken in a different way by the ferromagnetic and antiferromagnetic ground state. In the ferromagnet the spin points to the same direction in all the sites of the crystal, and therefore $U(x)$ can be considered invariant under any spatial transformation. On the other hand, in an antiferromagnet two sublattices exist with opposite spin, and therefore a space transformation mapping the two sublattices (the spatial inversion I in the Cr_2O_3) must affect the $U(x)$ transformation. In fact, in this case $U(x) \to U(x)C$, where $C = e^{-i\pi S^2}$ is a matrix which produces the spin flip.

These transformations together with one of the topological terms mentioned in the previous section give rise to the differences between ferromagnetic and antiferromagnetic spin waves. Consider $a_0^3(x) \sim tr(U^\dagger(x) i\partial_0 U(x) P_+)$ (P_+ is a projector over the

highest component of the spin), under the transformation (1.7.2) turns out to be a topological term. This is the only one that can yield a first order equation in time derivatives. This is the case for the ferromagnet since $a_0^3(x)$ is invariant under spatial transformations, in particular I. On the other hand, in the antiferromagnetic case $a_0^3(x) \to -a_0^3(x)$ under I, which forbids this term in the effective lagrangian, giving rise to a second order equation in time derivatives. This produces a wave equation for the antiferromagnetic spin waves.

In chapter 4 small perturbations are also introduced from the spin-orbit and magnetic dipole interactions. These interactions do not preserve the $SU(2)$ symmetry, they are said to break explicitly the symmetry. These perturbations give rise to a gap in the spin wave spectrum, which depends on the coupling parameter.

Finally, in connexion with the work to be presented in the chapter 5, the electromagnetic field coupling to spin waves is introduced. There are two mechanisms which produce this coupling. The first one is the Pauli coupling which breaks explicitly the $SU(2)$ symmetry, and the other one is a non-minimal coupling, i.e., direct coupling to electromagnetic field strength tensor, $F_{\mu\nu}$ ($\mathbf{E}$ and $\mathbf{B}$).

In chapter 5 we apply the previous formalism to the study of non-reciprocal effects in antiferromagnetic crystals in the microwave region, where the spectrum is dominated by the spin waves. Non-reciprocal effects are those not invariant under time reversal. In our case sending a light beam with wave number $\mathbf{k}$ or $-\mathbf{k}$ different physical effects are produced. These effects are observed in the second harmonic generation and in the gyrotropic birefringence.

Bibliography

[1] S. R. White, *Phys. Rev. Lett.* **69** (1992) 2863;

S. R. White, *Phys. Rev.* **B48** (1993) 10345.

[2] J. Gasser and H. Leutwyler, *Ann. Phys. (N.Y.)* **158** (1984) 142.

[3] N. D. Mermin and H. Wagner, *Phys. Rev. Lett.* **22** (1966) 1133.

[4] K. G. Wilson, *Rev. Mod. Phys.* **47** (1975) 773.

[5] R. Shankar, *"Effective Field Theory in Condensed Matter Physics"*, cond-mat/9703210.

[6] J. Goldstone, *Nuovo Cim.* **19** (1961) 145.

[7] G. S. Guralnik, C. R. Hagen and T. W. B. Kibble, *"Advances in Particle Physics"*, Vol.2, p.567, ed. R. L. Cool and R. E. Marshak (Willey, New York, 1968).

[8] H. Leutwyler, *Phys. Rev.* **D49** (1994) 3033.

[9] Balachandran *et al.*, *"Hubbard Model and Anyon Superconductivity"* (World Scientific, Singapore, 1990).

[10] N. W. Ashcroft and N. D. Mermin, *"Solid State Physics"* (Saunders College Publishing, Forth Worth, 1976);

C. Kittel, *"Introduction to Solid State Physics"* (John Wiley & Sons, Inc., New York, 1971);

G. Burns, *"Solid State Physics"* (Academic Press, Inc., San Diego, 1985).

[11] G. Sierra, *J. Phys.* **A29** (1996) 3299.

[12] J. González *et al.*, *"Quantum Electron Liquids and High-T_c Superconductuvity"* (Springer, Berlin, 1995).

[13] G. Sierra, M. A. Martín-Delgado, *"Dualities in Spin Ladders"*, cond-mat/9706104, to appear in *J. Phys.* **A**.

[14] C. Zener, *Phys. Rev.* **82** (1951) 403.

[15] H. B. Nielsen and S. Chada, *Nucl. Phys.* **B105** (1976) 445.

Chapter 2

The Matrix Product Approach to Quantum Spin Ladders

In this chapter we present a manifestly rotational invariant formulation of the matrix product method valid for spin chains and ladders. We apply it to 2-legged spin ladders with spins 1/2, 1 and 3/2 and different magnetic structures labelled by the exchange coupling constants, which can be ferromagnetic or antiferromagnetic along the legs and the rungs of the ladder. We compute ground state energy densities, correlation lengths and string order parameters. We present numerical evidence of the duality properties of the three different non ferromagnetic spin 1/2 ladders. We show that the long range topological order characteristic of isolated spin 1 chains is broken by the interchain coupling. The string order correlation function decays exponentially with a finite correlation length that we compute. A physical picture of the spin 1 ladder is given in terms of a collection of resonating spin 1 chains. Finally for ladders with spin equal or greater than 3/2 we define a class of AKLT states whose matrix product coefficients are given by rotation group 9-j symbols.

2.1 Introduction

The matrix product method (MPM) is a variational approach appropriate to study the ground state and excitations of a variety of one-dimensional lattice systems in Condensed Matter and Statistical Mechanics. The theoretical and experimental interest of these systems has grown spectacularly in the last years, due to the discovery of interesting and unexpected physical properties in spin chains and ladders.

The basic idea behind the MPM is the construction of the ground state and excitations of 1D or quasi 1D systems in a recursive way, by relating the states of the system with length N to that of length $N-1$. This simple idea has appeared in the past in different places. First of all, in the Wilson's real space renormalisation group the 1D-lattice is built up by the addition of a single site at every RG step [1]. This procedure is also used in the density matrix renormalisation group method (DMRG) of White [2]. Other source of the MPM is the well known AKLT state of the spin 1 chain [3]. This is a simple but non trivial example of a matrix product state, which has motivated various generalisations as the ones of Klumper *et al.* [4], Ostlund and Rommer [5], etc. We shall follow in this chapter the formulation of the MPM due to the latter authors, which is based on the analysis of the fixed point structure of the DMRG ground state in the thermodynamic limit [5]. A closely related approach is that of Fannes *et al.* [6]. The MPM offers an alternative formulation of the DMRG method in the regime where the latter reaches a fixed point after many RG iterations [7].

Whereas the DMRG is a purely numerical method, the MPM offers the possibility of an analytical approach to elucidate the actual structure of the ground state (GS) and excitations. The MPM is a standard variational method which determines the variational parameters by minimising the GS energy. Minimisation problems are in general harder than diagonalisation ones. In this respect the MPM is so far less performant than the DMRG. However we believe that the analytical insights gained with the MPM could be used to boost the numerical precision and applications of both the MPM and the DMRG.

In this chapter we apply the MPM to the 2-leg spin ladder. Spin ladders with diagonal couplings have been studied with the MPM of Klumper *et al.* in ref. [8]. Spin ladders were first studied as theoretical labs to test ideas concerning the crossover from 1D to 2D, with the surprising result that this crossover is far from being smooth: the even and odd ladders display quite different properties converging only when the

number of legs goes to infinity (for an introduction to the subject see [9]). Even spin ladders are spin liquids with a finite spin gap and finite spin correlation length, while odd spin ladders belong to the same universality class than the spin 1/2 antiferromagnetic Heisenberg chain, which has no gap and the correlations decay algebraically. Another reason to study ladder systems is that materials actually exists with that structure and hence the theoretical predictions can in principle be compared with experimental data concerning the spectrum, susceptibility, etc.

We study in this chapter five different spin ladders characterised by their local spin $S = 1/2$, 1 and 3/2 and the signs of the exchange of coupling constants along the legs, $J_{\|}$, and the rungs, $J_{\perp}$.

In the case of the spin 1/2 ladders we discuss the following topics: i) the RVB picture of the antiferromagnetic ladder, ii) the equivalence between the ladder state and the Haldane state of the spin 1 chain, and iii) the duality properties relating the different magnetic structures.

In the case of the spin 1 ladder we show that the long range topological order characteristic of isolated spin 1 chains disappears and the string correlator decays exponentially with a finite correlation length.

The study of the spin 3/2 ladder motivates the definition of an AKLT state characterised in terms of rotation group 9-j symbols.

We compute GS energy densities, spin correlation lengths and string order parameters and compare our results with those existing in the current literature.

The organisation of the chapter is as follows. In section 2.2 we review the MPM. In section 2.3 we particularise the MPM to systems which are rotational invariant, where the use of group theory leads to a simplification of the formalism. In section 2.4 we present our numerical results concerning five different spin ladders. In section 2.5 we summarise our results and present some prospects of our work. There are three appendices which contain technical details or proofs of results presented in the main body of the chapter.

2.2 Review of the Matrix Product Method

Some of the results presented in this section are known and can be found in references [5, 6]. We also present a full account of the formulas and derivations used in reference [7] where the MPM was compared with the DMRG method in the case of the

antiferromagnetic spin 1 chain.

Let us consider a spin chain or a ladder B_N with open boundary conditions, where N denotes the number of sites of a chain or the number of rungs of a ladder. To describe the low energy properties of B_N one introduces a collection of m states $\{|\alpha\rangle_N\}_{\alpha=1}^m$, which form an orthonormal basis, i.e., ${}_N\langle\alpha|\alpha'\rangle_N = \delta_{\alpha\alpha'}$. In the DMRG these states are the most probable ones to contribute to the GS of the superblock $B_{N-1}\bullet\bullet B_{N-1}^R$ of length $2N$, formed by adding two sites (or rungs), $\bullet\bullet$, and a mirror image B_{N-1}^R to the original lattice B_{N-1}. The basic assumption of the MPM is that the basis associated with B_N and B_{N-1} are related in a simple manner by the equation

$$|\alpha\rangle_N = \sum_{\beta s} A_{\alpha\beta}[s]\ |s\rangle_N \otimes |\beta\rangle_{N-1} \quad , \quad N \geq 2, \tag{2.2.1}$$

where $|s\rangle_N$ $(s = 1, \ldots, m^*)$ denotes a complete set of m^* states associated to the N^{th} site (resp. rung) added to the chain (resp. ladder). Eq. (2.2.1) has to be supplemented with the initial data $|\beta\rangle_1$. The quantities $A_{\alpha\beta}[s]$ are the variational parameters of the MPM, and their determination is the central problem one has to solve. This is done by the standard variational method. The important point about eq. (2.2.1) is that $A_{\alpha\beta}[s]$ does not depend on N. Eq. (2.2.1) is motivated by the truncation method used in the DMRG where $A_{\alpha\beta}[s]$ depended on N,i.e., $A_{\alpha\beta}^{(N)}[s]$. When N is large enough one reaches a fixed point, i.e., $A_{\alpha\beta}^{(N)}[s] \to A_{\alpha\beta}[s]$. In this manner the thermodynamic limit of the DMRG leads to a translational invariant MPM state.

The condition that both $|\alpha\rangle_N$ and $|\beta\rangle_{N-1}$ form orthonormal basis imposes a normalisation condition on $A_{\alpha,\beta}[s]$,

$$\sum_{\beta s} A_{\alpha\beta}^*[s]\ A_{\alpha'\beta}[s] = \delta_{\alpha\alpha'}. \tag{2.2.2}$$

It is interesting to count how many variational parameters there are in (2.2.1). The quantities $A_{\alpha\beta}[s]$ represent a total of m^2m^* variables. We shall assume that all of them may be non vanishing. The normalisation constraints (2.2.2) represent a total of $m+m(m-1)/2$ constraints (m coming from the diagonal terms $\alpha = \alpha'$ and $m(m-1)/2$ coming from the off-diagonal ones). On the other hand, one can rotate the basis of states $\{|\alpha\rangle\}_{\alpha=1}^m$ by an element of the orthogonal group $O(m)$ reducing by $m(m-1)/2$ the number of independent MPM variables. The total number of variational degrees of freedom, N_A, is then given by

$$N_A = m^2m^* - m - 2m(m-1)/2 = m^2(m^* - 1). \tag{2.2.3}$$

We show in appendix 2.A that the set of $A_{\alpha\beta}[s]$ belongs to the grassmanian manifold,

$$A \in \frac{O(mm^*)}{O(m) \otimes O(m(m^*-1))}. \tag{2.2.4}$$

As an exercise one can check that the dimension of (2.2.4) coincides with N_A given in (2.2.3).

In ref. [5] eq. (2.2.1) is used to generate an ansatz for the GS of periodic chains. In this chapter we shall rather use this equation to generate states with open boundary conditions, in the spirit of the DMRG. We shall show below that the set $|\alpha\rangle$ corresponds to ground states with different boundary conditions. The use of open boundary conditions leads to a simplification of the MPM which is very close to the more abstract formalism proposed in [6].

2.2.1 Correlators of local operators

Let us use eq. (2.2.1) to compute the expectation values of local operators in a recursive way. We shall first consider a local operator $\mathcal{O}_n$ acting at the position $n = 1, \ldots, N$ of the lattice. It is easy to get from (2.2.1) the expectation value

$${}_N\langle\alpha|\mathcal{O}_n|\alpha'\rangle_N = \begin{cases} \sum_{\beta\beta'} T_{\alpha\alpha',\beta\beta'}\ {}_{N-1}\langle\beta|\mathcal{O}_n|\beta'\rangle_{N-1} & \text{for } n < N \\ \sum_\beta \hat{\mathcal{O}}_{\alpha\alpha',\beta\beta} & \text{for } n = N \end{cases}, \tag{2.2.5}$$

where

$$T_{\alpha\alpha'\beta\beta'} = \sum_s A^*_{\alpha\beta}[s]\ A_{\alpha'\beta'}[s], \tag{2.2.6}$$

$$\hat{\mathcal{O}}_{\alpha\alpha',\beta\beta'} = \sum_{ss'} A^*_{\alpha\beta}[s]\ \ A_{\alpha'\beta'}[s']\ \ \langle s|\mathcal{O}|s'\rangle. \tag{2.2.7}$$

T can be identified with $\widehat{1}$. Eqs. (2.2.5), (2.2.6) and (2.2.7) suggest to interpret the expectation value ${}_N\langle\alpha|\mathcal{O}_n|\alpha'\rangle_N$ as a vector labeled by the pair $\alpha\alpha'$, in which case T and $\hat{\mathcal{O}}$ become $m^2 \times m^2$ matrices. Upon iteration of (2.2.5) one finds

$${}_N\langle\alpha|\mathcal{O}_n|\alpha'\rangle_N = \sum_\beta \left(T^{N-n}\ \hat{\mathcal{O}}\right)_{\alpha\alpha',\beta\beta}. \tag{2.2.8}$$

More generally, the expectation value of a product of local operators is given by

$${}_N\langle\alpha|\mathcal{O}^{(1)}_{n_1}\ \mathcal{O}^{(2)}_{n_2} \cdots \mathcal{O}^{(r)}_{n_r}|\alpha'\rangle_N = \sum_\beta \left(T^{N-n_1}\ \hat{\mathcal{O}}^{(1)} T^{n_1-n_2-1} \hat{\mathcal{O}}^{(2)} \cdots T^{n_{r-1}-n_r-1} \hat{\mathcal{O}}^{(r)}\right)_{\alpha\alpha',\beta\beta}, \tag{2.2.9}$$

where $N \geq n_1 > n_2 > \cdots > n_r \geq 1$. The matrix T plays a very important role in the MPM. Eqs (2.2.5) and (2.2.9) imply that T behaves as a shift operator by one lattice space. The basic properties of T follow from the normalisation condition (2.2.2) which can be expressed as

$$\sum_{\beta} T_{\alpha\alpha',\beta\beta} = \delta_{\alpha\alpha'} \tag{2.2.10}$$

which implies that T has a eigenvalue equal to 1. Let us call $|v\rangle$ the right eigenvector corresponding to this eigenvalue. Eq.(2.2.10) can be written in matrix notation as

$$T\ |v\rangle = |v\rangle \quad , \quad v_{\alpha\alpha'} = \delta_{\alpha\alpha'}. \tag{2.2.11}$$

On the other hand, let $\langle\rho|$ denote the left eigenvector of T corresponding to the eigenvalue 1, i.e.,

$$\langle\rho|T = \langle\rho| \quad \longleftrightarrow \quad \sum_{\alpha\alpha'} \rho_{\alpha\alpha'} T_{\alpha\alpha',\beta\beta'} = \rho_{\beta\beta'}. \tag{2.2.12}$$

A convenient normalisation of $\langle\rho|$ is given by

$$\langle\rho|v\rangle = 1 \quad \longleftrightarrow \quad \sum_{\alpha} \rho_{\alpha\alpha} = 1. \tag{2.2.13}$$

For later use we shall diagonalise T as follows,

$$T = \sum_{p} x_p |v_p\rangle\langle\rho_p| \quad , \quad \langle\rho_p|v_{p'}\rangle = \delta_{pp'}, \tag{2.2.14}$$

where $|v_p\rangle$ and $\langle\rho_p|$ are the right and left eigenvectors of T with eigenvalue x_p ($x_1 = 1$, $|v_1\rangle = |v\rangle$, $\langle\rho_1| = \langle\rho|$). As a matter of fact all the remaining eigenvalues of T are less than one, i.e., $|x_p| < 1 \ \ \forall p \neq 1$.

In the limit $N \to \infty$ one gets

$$\lim_{N\to\infty} \langle\alpha|\mathcal{O}_{n_1}^{(1)}\ \mathcal{O}_{n_2}^{(2)} \cdots \mathcal{O}_{n_r}^{(r)}|\alpha'\rangle_N = \ \delta_{\alpha\alpha'}\ \langle\rho|\ \widehat{\mathcal{O}}^{(1)} T^{n_1-n_2-1} \widehat{\mathcal{O}}^{(2)} \cdots T^{n_{r-1}-n_r-1} \widehat{\mathcal{O}}^{(r)}|v\rangle. \tag{2.2.15}$$

The delta function on the r.h.s. of this equation means that the local operators $\widehat{\mathcal{O}}^{(n)}$ acting in the bulk do not modify the boundary conditions associated to the various choices of α.

Assuming that T is invertible, one can rewrite eq. (2.2.15) in the following manner:

$$\lim_{N\to\infty_N} \langle\alpha|\mathcal{O}_{n_1}^{(1)}\ \mathcal{O}_{n_2}^{(2)} \cdots \mathcal{O}_{n_r}^{(r)}|\alpha'\rangle_N = \ \delta_{\alpha\alpha'}\ \langle\rho|\ \tilde{\mathcal{O}}^{(1)}(n_1)\tilde{\mathcal{O}}^{(2)}(n_2) \cdots \tilde{\mathcal{O}}^{(r)}(n_r)|v\rangle, \tag{2.2.16}$$

where $\tilde{\mathcal{O}}(n)$ is defined as

$$\tilde{\mathcal{O}}(n) = T^{-n-1}\ \hat{\mathcal{O}}\ T^n. \tag{2.2.17}$$

Observe that $\tilde{1} = 1$. The r.h.s. of (2.2.16) is nothing but a spatial ordered product of local operators $\tilde{\mathcal{O}}(n)$, which is reminiscent of the radial ordered product that appears in Conformal Field Theory. This connection supports the interpretation of T as an euclidean version of the shift operator. Under this viewpoint the states $|v\rangle$ and $\langle\rho|$ appear as incoming $|0\rangle$ and outgoing vacua $\langle 0|$ that are left invariant by the shift operator T.

We have shown above that the MPM leads in the thermodynamic limit to a sort of discretised field theory characterised by a shift or spatial transfer operator T and local operators $\tilde{\mathcal{O}}(n)$. We can now try to exploit these interpretation to extract some physical quantities.

First of all let us consider the correlator of two operators $\mathcal{O}^{(1)}(n_1)$ and $\mathcal{O}^{(2)}(n_2)$. From (2.2.14) and (2.2.15) one has

$$\langle\rho|\ \hat{\mathcal{O}}^{(1)}\ T^{n_1-n_2-1}\hat{\mathcal{O}}^{(2)}|v\rangle = \sum_p x_p^{n_1-n_2-1}\ \langle\rho|\hat{\mathcal{O}}^{(1)}|v_p\rangle\ \langle\rho_p|\hat{\mathcal{O}}^{(2)}|v\rangle. \tag{2.2.18}$$

In the limit when $|n_1 - n_2| >> 1$ the sum over p is dominated by the highest eigenvalue $|x_p|$ of T for which the corresponding matrix elements $\langle\rho|\hat{\mathcal{O}}^{(1)}|v_p\rangle$ and $\langle\rho_p|\hat{\mathcal{O}}^{(2)}|v\rangle$ are non zero. If $x_p < 1$ one gets a finite correlation length ξ given by the formula,

$$\xi = -1/\ln|x_p|. \tag{2.2.19}$$

In the case where $\hat{\mathcal{O}}^{(1)}$ and $\hat{\mathcal{O}}^{(2)}$ are both the spin operator $\mathbf{S}$, it turns out that the matrix element $\langle\rho|\hat{\mathbf{S}}|v\rangle$ vanishes, and hence the spin-spin correlator is short ranged with a finite spin correlation length ξ given by the formula (2.2.19) with $|x_p| < 1$. The finiteness of ξ does indeed occur for MP ansatzs which preserve the rotational invariance. However if the latter is broken, as in a Neel like state, then ξ may become infinite.

In section 2.3 we shall give a formula to compute ξ in the case of rotational invariant MP ansatzs.

Another interesting application of (2.2.16) is provided by the computation of the string order parameter.

2.2.2 String order parameter

A spin 1 chain has a long range topological order (LRTO) characterised by a non vanishing value of a non local operator $g(\infty)$ defined as follows [10],

$$\begin{aligned} g(\infty) &= \lim_{\ell\to\infty}\ g(\ell) \\ g(\ell) &= \langle S^z(\ell)\ \prod_{k=1}^{\ell-1} e^{\pi \mathrm{i} S^z(k)}\ S^z(0)\ \rangle. \end{aligned} \tag{2.2.20}$$

The AKLT state has $g_{AKLT}(\infty) = -(2/3)^2$, while the spin 1 antiferromagnetic spin chain has $g(\infty) = -0.374325$ [11]. From eq. (2.2.15) we deduce the following expression for (2.2.20),

$$g(\ell) = \langle \rho | \widehat{S^z} \left(\widehat{e^{\mathrm{i}\pi S^z}} \right)^{\ell-1}\ \widehat{S^z} | v \rangle. \tag{2.2.21}$$

In appendix 2.C we show that the operator $\widehat{e^{\mathrm{i}\pi S^z}}$ has an eigenvalue equal to 1. Denoting by $|v^{\mathrm{st}}\rangle$ and $\langle \rho^{\mathrm{st}}|$ the associated right and left eigenvectors we obtain the following expression for the string order parameter,

$$g(\infty) = \langle \rho |\ \widehat{S^z}\ |v^{\mathrm{st}}\rangle\ \langle \rho^{\mathrm{st}}|\ \widehat{S^z}\ |v\rangle \tag{2.2.22}$$

which suggests that $g(\infty)$ measures a sort of off-diagonal order.

For antiferromagnetic spin 1 ladders we shall see that the LRTO disappears and that the correlator (2.2.20) is short ranged with a finite correlation length ξ^{st}.

2.2.3 Ground state energy density

Let us suppose we have a translational invariant Hamiltonian of the form

$$H_N = \sum_{n=1}^{N}\ h_n^{(1)} + \sum_{n=1}^{N-1}\ h_{n,n+1}^{(2)}, \tag{2.2.23}$$

where $h^{(1)}$ is an on site (rung) operator while $h^{(2)}$ couples two nearest neighbour sites (rungs). We define the expectation value

$$E^N_{\alpha\alpha'} = {}_N\langle \alpha | H_N | \alpha' \rangle_N, \tag{2.2.24}$$

which can be computed recursively. From eqs. (2.2.1) and (2.2.5) one gets

$$E^N_{\alpha\alpha'} = \sum_{\beta\beta'} T_{\alpha\alpha',\beta\beta'}\ E^{N-1}_{\beta\beta'} + \sum_{\beta} \widehat{h}_{\alpha\alpha',\beta\beta} \qquad , \qquad (N \geq 2), \tag{2.2.25}$$

where $\widehat{h} = \widehat{h}^{(1)} + \widehat{h}^{(2)}$. The hated representation of the site hamiltonian $h^{(1)}$ is given by eq. (2.2.7), while the hated representation of the hamiltonian $h^{(2)}$ is given by

$$\widehat{h}^{(2)}_{\alpha\alpha',\beta\beta'} = \sum_{\gamma\gamma' s' s} {}_{N-1,N}\langle s_2 s_1 | h^{(2)}_{N-1,N} | s'_1 s'_2 \rangle_{N,N-1} \; A^*_{\alpha\gamma}[s_1] A^*_{\gamma\beta}[s_2] A_{\alpha'\gamma'}[s'_1] A_{\gamma'\beta'}[s'_2]. \tag{2.2.26}$$

It should be clear from eqs. (2.2.7) and (2.2.26) which is the hated representative of an operator involving an arbitrary number of sites. Eq. (2.2.25) can be conveniently written in matrix notation as

$$|E^N\rangle = T \; |E^{N-1}\rangle + \widehat{h} \; |v\rangle \qquad , \qquad (N \geq 2), \tag{2.2.27}$$

where $|E^N\rangle$ is a vector with components $E^N_{\alpha\alpha'}$. Iterating (2.2.27) one gets

$$|E^N\rangle = (1 + T + T^2 + \cdots + T^{N-2}) \; \widehat{h} \; |v\rangle + T^{N-1} \; |E^1\rangle. \tag{2.2.28}$$

The geometric series in T can be sumed up and due to the eigenvalue equal to 1 it contributes a term proportional to N, i.e.,

$$\lim_{N\to\infty} \frac{1}{N} |E^N\rangle = e_\infty \; |v\rangle. \tag{2.2.29}$$

This equation implies that all the states $|\alpha\rangle_N$ have the same energy density in the thermodynamic limit, i.e., $E^N_{\alpha\alpha'} = \delta_{\alpha\alpha'} \; e_\infty$. Hence e_∞ can be identified with the GS energy per site for chains or per rung for ladders and it is given by

$$e_\infty = \langle \rho | \; \widehat{h} \; |v\rangle = \sum_{\alpha\alpha'\beta} \rho_{\alpha\alpha'} \; \widehat{h}_{\alpha\alpha',\beta\beta}. \tag{2.2.30}$$

This is the quantity one has to minimise respect to the MPM parameters.

The formalism presented above is closely related to the DMRG. Even though this relation is not the main subject of the chapter we shall make some remarks on it (see [7]).

2.2.4 MPM versus the DMRG

Let us suppose that we diagonalise ρ, as a $m \times m$ matrix, denoting its eigenvalues as w^2_α, i.e.,

$$\rho_{\alpha\alpha'} = w^2_\alpha \, \delta_{\alpha\alpha'}. \tag{2.2.31}$$

The eigenvalue eq. (2.2.12) becomes then

$$\sum_{\alpha s} w_\alpha^2 A_{\alpha\beta}[s]\ A^*_{\alpha\beta'}[s] = \delta_{\beta\beta'} w_\beta^2. \tag{2.2.32}$$

There is a close analogy between eqs. (2.2.2) and (2.2.32), except for the fact that the order of the labels is exchanged. Given the tensor product decomposition $s\otimes\beta \to \alpha$, we shall assume that one can reverse the order between the states α and β in terms of "charge conjugate states" α^c and β^c, as follows: $s \otimes \alpha^c \to \beta^c$. For example the charge conjugate of a state with spin M is another state with spin $-M$. Using this concept we can impose the following symmetry condition [12]

$$w_\alpha A_{\alpha\beta}[s] = \pm w_{\beta^c} A_{\beta^c\alpha^c}[s] \quad , \quad w_{\beta^c} = w_\beta, \tag{2.2.33}$$

which leads to the equivalence between eqs. (2.2.2) and (2.2.32).

The relation between the MPM and the DMRG is made clear by the construction of the GS of the superblock $B_N \bullet B_N^R$ in the following way:

$$\begin{aligned} |\psi_0\rangle &= \sum \psi_{\alpha s\beta}\ \ |\alpha^R\rangle \otimes |s\rangle \otimes |\beta\rangle \\ \psi_{\alpha s\beta} &= w_\alpha\ A_{\alpha\beta}[s]. \end{aligned} \tag{2.2.34}$$

The density matrix that induces $\psi_{\alpha s\beta}$ on the block B, and which is obtained by tracing over the states in $\bullet B_N^R$, coincides with $\rho_{\alpha\alpha'} = w_\alpha^2\, \delta_{\alpha\alpha'}$.

Condition (2.2.33) guarantees that $|\psi_0\rangle$ is a state invariant under the parity transformation that interchanges the blocks B_N and B_N^R, while leaving invariant the site $\bullet$.

It is interesting to observe that the MPM leads to a superblock of the form $B_N \bullet B_N^R$, rather than to the standard superblock $B_N \bullet \bullet B_N^R$ [7].

2.3 The MPM applied to spin ladders

In this section we shall apply the MPM to the 2-leg spin ladder with a spin S at each site of the chain. The collection $|\alpha\rangle_N$ will be given by the set $|JM\rangle_N$ ($J \le J_{\max}$) of states with total spin J and third component M. For the sake of simplicity we have only considered one state per angular momenta J and M. This will allow us to show more clearly the analytic structure of the MPM, which can later on be numerically improved by considering multiplicity. This has already been done in the case of spin chains in references [5, 7].

The states added at each step of the MPM are the ones that appear in the tensor product decomposition of two spin S irreps, i.e., $S \otimes S = 0 \oplus 1 \oplus \cdots \oplus 2S$. These states are labelled by $|\lambda\mu\rangle$ where $\lambda = 0, \cdots, 2S$ is the total spin and $\mu = -\lambda, \ldots, \lambda$ is its third component.

Using these notations we propose the following recurrence relation for the states $|JM\rangle_N$:

$$|J_1 M_1\rangle_N = \sum_{\lambda J_2} A^{\lambda}_{J_1 J_2} \, |(\lambda J_2), J_1 M_1\rangle_N, \tag{2.3.1}$$

where

$$|(\lambda J_2), J_1 M_1\rangle_N = \sum_{\mu} \langle \lambda\mu, J_2 M_2 | \lambda J_2, J_1 M_1\rangle \;\; |\lambda\mu\rangle_N \otimes |J_2 M_2\rangle_{N-1}. \tag{2.3.2}$$

In (2.3.2) the quantity $\langle \lambda\mu, J_2 M_2 | \lambda J_2, J_1 M_1\rangle$ is the Clebsch-Gordan coefficient corresponding to the decomposition $\lambda \otimes J_2 \to J_1$. Comparing eqs. (2.2.1) and (2.3.1) we obtain the following relation between the symbols $A_{J_1 M_1, J_2 M_2}[\lambda\mu]$ and the rotational invariant symbols $A^{\lambda}_{J_1 J_2}$:

$$A_{J_1 M_1, J_2 M_2}[\lambda\mu] = A^{\lambda}_{J_1 J_2} \, \langle \lambda\mu, J_2 M_2 | \lambda J_2, J_1 M_1\rangle. \tag{2.3.3}$$

The use of rotational invariant basis reduces considerably the number of independent variational parameters and consequently increases the power of the MPM [5, 7].

The variational parameters $A^{\lambda}_{J_1 J_2}$ are subject to the CG condition,

$$A^{\lambda}_{J_1 J_2} = 0 \quad \text{unless} \quad |\lambda - J_2| \leq J_1 \leq |\lambda + J_2|. \tag{2.3.4}$$

Using (2.3.3) and the orthogonality properties of the CG coefficients, the normalisation conditions (2.2.2) become

$$\sum_{\lambda, J_2} |A^{\lambda}_{J_1 J_2}|^2 = 1, \quad \forall \; J_1. \tag{2.3.5}$$

At this point we can just take eq. (2.3.3) and plug it into the corresponding formulas of section 2.2 in order to derive expectation values, the GS energy density, etc. in terms of $A^{\lambda}_{J_1 J_2}$. There is however a more efficient way to do this by using group theory. The application of the Wigner-Eckart theorem will allow us to express all the results in terms of reduced matrix elements of the operators involved as well as the rotation group $6j$-symbols. In our derivations we shall follow the same steps as in section 2.2, leaving the technical details to appendix 2.B.

2.3.1 Correlators of Invariant Tensors

Let us denote by $\mathcal{O}^{(k)}$ an irreducible tensor of total angular momentum k, whose components are labeled by $\mathcal{O}^{(k)}_M, M = -k, \ldots, k$. The spin operators $\mathbf{S}$ correspond to $k = 1$. Let us suppose we have two irreducible tensors with the same total angular momenta k, $\mathcal{O}^{(k,A)}(n)$ and $\mathcal{O}^{(k,B)}(m)$, acting at the positions n and m ($N \geq n > m \geq 1$) of the ladder. The scalar product of these two operators is defined as

$$\mathcal{O}^{(k,A)}(n) \cdot \mathcal{O}^{(k,B)}(m) = \sum_{M=-k}^{k} (-1)^{-M} \mathcal{O}^{(k,A)}_M(n) \cdot \mathcal{O}^{(k,B)}_{-M}(m). \tag{2.3.6}$$

The basic result we derive in appendix 2.B is

$$\begin{aligned} {}_N\langle J_1 M| \, \mathcal{O}^{(k,A)}(n) \cdots \mathcal{O}^{(k,B)}(m) \, |J_1 M\rangle_N = \\ \sum_{J_2,\ldots,J_7} T^{N-n}_{J_1 J_2} \, \widehat{\mathcal{O}}^{(k,A)}_{J_2,J_3 J_4} \, \left(T^{n-m-1}_k\right)_{J_3 J_4, J_5 J_6} \, \widehat{\mathcal{O}}^{(k,B)}_{J_5 J_6, J_7}, \end{aligned} \tag{2.3.7}$$

where T and $T^{(k)}$ are defined as

$$T_{J_1 J_2} = \sum_{\lambda} \left(A^{\lambda}_{J_1 J_2}\right)^* A^{\lambda}_{J_1 J_2}, \tag{2.3.8}$$

$$(T_k)_{J_1 J_2, J_3 J_4} = \sum_{\lambda} \left(A^{\lambda}_{J_1 J_3}\right)^* A^{\lambda}_{J_2 J_4} \, (-1)^{\lambda + k + J_1 + J_4} \sqrt{(2J_1+1)(2J_2+1)} \begin{Bmatrix} J_3 & J_1 & \lambda \\ J_2 & J_4 & k \end{Bmatrix}, \tag{2.3.9}$$

while $\widehat{\mathcal{O}}^{(k,A)}$ and $\widehat{\mathcal{O}}^{(k,B)}$ are defined in appendix 2.B.

Eq. (2.3.7) is the invariant version of (2.2.9) involving only two operators. In order to obtain the thermodynamic properties of (2.3.7) we use the properties of the transfer operator T. The normalisation conditions (2.3.5) imply the following conditions on T:

$$\sum_{J_2} T_{J_1 J_2} = 1 \quad , \quad \forall \; J_1. \tag{2.3.10}$$

Let us call ρ_J the left eigenvector of $T_{J_1 J_2}$ with eigenvalue 1, i.e.,

$$\sum_{J_1} \rho_{J_1} \, T_{J_1 J_2} = \rho_{J_2}. \tag{2.3.11}$$

Using eqs. (2.3.10) and (2.3.11) into (2.3.7) and taking $N >> 1$ we get

$$\lim_{N\to\infty} \; {}_N\langle J_1 M| \, \mathcal{O}^{(k,A)}(n) \cdot \mathcal{O}^{(k,B)}(m) \, |J_1 M\rangle_N = \langle \rho| \, \widehat{\mathcal{O}}^{(k,A)} \, T^{n-m-1}_k \, \widehat{\mathcal{O}}^{(k,B)} |v\rangle, \tag{2.3.12}$$

where we use a matrix notation in J-space with the convention $v_J = 1,\ \forall J$. From eq. (2.3.12) we deduce that the correlation length associated to the scalar product of two irreducible operators with angular momentum k, is given by the highest eigenvalue of the matrix T_k defined in (2.3.9). The spin-spin correlation length is obtained by looking at the highest absolute eigenvalue of T_1.

2.3.2 Ground state energy density

The Hamiltonian of the 2-leg ladder has the form proposed in (2.2.23) where $h^{(1)}$ is the rung Hamiltonian and $h^{(2)}$ is the leg Hamiltonian,

$$h_n^{(1)} = J_\perp\ \mathbf{S}_1(n)\cdot\mathbf{S}_2(n) \tag{2.3.13a}$$

$$h_{n,n+1}^{(2)} = J_\parallel\ \left(\mathbf{S}_1(n)\cdot\mathbf{S}_1(n+1) + \mathbf{S}_2(n)\cdot\mathbf{S}_2(n+1)\right), \tag{2.3.13b}$$

$\mathbf{S}_a(n)$ is a spin S operator acting on the $n = 1,\ldots,N$ rung and the $a = 1,2$ leg of the ladder.

As in (2.2.24) we define the expectation value of the ladder Hamiltonian as,

$$E_J^N =_N \langle JM|H_N|JM\rangle_N. \tag{2.3.14}$$

Using (2.3.1) we find

$$E_{J_1}^N = \sum_{J_2}\ \left(T_{J_1J_2}\ E_{J_2}^{N-1} + \widehat{h}_{J_1J_2}\right) \quad , \quad (N \geq 2), \tag{2.3.15}$$

where $\widehat{h} = \widehat{h}^{(1)} + \widehat{h}^{(2)}$ ($\widehat{h}^{(1)}$ and $\widehat{h}^{(2)}$ can be found in appendix 2.B).

Iterating eq. (2.3.15) and using the properties of the matrix T we can inmediately get the large N limit of the energy (2.3.14),

$$\lim_{N\to\infty}\frac{1}{N}E_J^N = e_\infty \quad , \quad \forall\ J, \tag{2.3.16}$$

where the GS energy density is given by,

$$e_\infty = \langle\rho|\ \widehat{h}\ |v\rangle = \sum_{J_1,J_2}\ \rho_{J_1}\ \widehat{h}_{J_1J_2}. \tag{2.3.17}$$

2.3.3 Main steps of the MPM algorithm

Let us summarise the main steps of the MP algorithm hereby proposed,

1. Solve the normalisation conditions (2.3.5) expressing $A^{\lambda}_{J_1 J_2}$ in terms of a set of linearly independent variational parameters.
2. Find the eigenvector ρ_J of the matrix T.
3. Minimise the GS energy density (2.3.17) with respect to the independent variational parameters.

We will now comment on how these three steps can be implemented.

Solution of the normalisation conditions

We shall suppose in the rest of the chapter that the parameters $A^{\lambda}_{J_1 J_2}$ are all real. Hence the normalisation conditions

$$\sum_{\lambda, J_2} (A^{\lambda}_{J_1 J_2})^2 = 1 \quad , \quad \forall\ J_1 \tag{2.3.18}$$

imply that the set $\{A^{\lambda}_{J_1 J_2}\}$ for J_1 fixed are the coordinates of a sphere whose dimension depends on the allowed values of J and the CG conditions (2.3.4). Let us call $A^{\max}_{J_1}$ the highest coordinate, in absolute value, i.e.,

$$A^{\max}_{J_1} = A^{\lambda_0}_{J_1 L_0} \quad \text{such that} \quad |A^{\lambda_0}_{J_1 L_0}| \geq |A^{\lambda}_{J_1 J_2}| \ \ \forall\ \lambda, J_2. \tag{2.3.19}$$

If $A^{\max}_{J_1} > 0$ (resp. $A^{\max}_{J_1} < 0$) we can think of it as the north (resp. south) pole of a sphere, whose neaghbourhood can be described by the stereographic coordinates,

$$x^{\lambda}_{J_1 J_2} = A^{\lambda}_{J_1 J_2} / A^{\max}_{J_1} \quad , \quad |x^{\lambda}_{J_1 J_2}| \leq 1. \tag{2.3.20}$$

Notice that $x^{\lambda_0}_{J_1 L_0} = 1$. The remaining coordinates are the independent variational parameters used in the minimisation of the GS energy. The solution of the constraint (2.3.18) finally reads

$$A^{\lambda}_{J_1 J_2} = \epsilon_{J_1}\ x^{\lambda}_{J_1 J_2} \left(\sum_{\lambda', J_2'} \left(x^{\lambda'}_{J_1 J_2'} \right)^2 \right)^{-1/2} \quad , \quad \epsilon_J = \pm 1, \tag{2.3.21}$$

where $\epsilon_{J_1} = 1(-1)$ corresponding to the north (south) pole of the above mentioned sphere.

Determination of ρ_J

The solution of the eigenvalue problem of eq. (2.3.11) can be done numerically. However for a ladder with spin $S = 1/2$ it can also be solved analytically which will allow us to make some considerations on the nature of ρ_J. In the case where $S = 1/2$ the allowed values for λ are 0 and 1. Hence the unique non-vanishing entries of $A^{\lambda}_{J_1 J_2}$ are A^0_{JJ}, A^1_{JJ}, A^1_{JJ+1} and A^1_{JJ-1}. Similarly from eq. (2.3.8) the non-vanishing entries of T are T_{JJ}, T_{JJ+1} and T_{JJ-1}. The set of equations we have therefore to solve read explicitly as

$$\begin{gathered} T_{J,J} + T_{J,J+1} + T_{J,J-1} = 1 \\ \rho_J\, T_{J,J} + \rho_{J+1}\, T_{J+1,J} + \rho_{J-1} T_{J-1,J} = \rho_J \\ \textstyle\sum_{J=0}^{J_{\max}}\ \rho_j = 1. \end{gathered} \tag{2.3.22}$$

The solution of these equations is given by

$$\rho_J = \frac{u_J}{\sum_L u_L}, \tag{2.3.23}$$

where

$$u_0 = 1 \quad , \quad u_J = \prod_{L=0}^{J} \frac{T_{L,L+1}}{T_{L+1,L}} \ \ (J > 0); \tag{2.3.24}$$

we are assuming that $J = 0, \cdots, J_{\max}$.

Eqs. (2.3.23) and (2.3.24) imply that ρ_J is always positive, in agreement with the Perron-Frobenius theorem applied to the matrix T, whose entries are all non-negative. In ref. [7] it was shown that the values of ρ_J are intimately related to the eigenvalues of the density matrix that appear in the DMRG. These and other facts suggest that the MPM is in fact equivalent to the DMRG, specially when the number of states kept m becomes large.

2.4 Numerical Results

In this section we shall apply the MPM formalism, presented in the previous sections, to five different spin ladders, corresponding to different choices of the spin S and signs of the coupling constants $J_{\|}$ and $J_{\perp}$. We shall denote every of these ladders as AA_S, AF_S, and FA_S where A and F stands for antiferromagnetic or ferromagnetic couplings. Thus for example AF_S is a spin S ladder with antiferromagnetic couplings

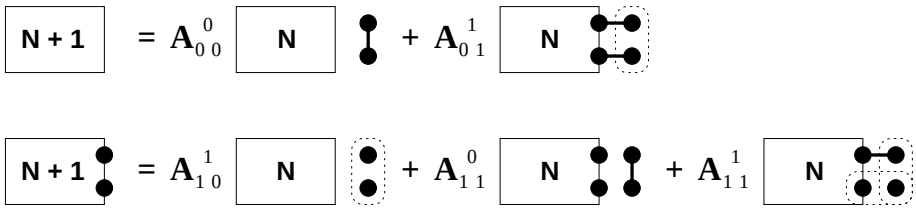

Figure 2.1. Graphical representation of the MP ansatz in the case of the spin 1/2 ladder and basis $|JM\rangle_N$ with $J = 0$ and 1. Every dot represents a spin 1/2. A link between two dots denotes the formation of a singlet between the spins. Doted lines denote symetrisation of the spins encircled by them.

along the legs and ferromagnetic couplings along the rungs. With these notations we will study below the following cases: $AA_{1/2}$, $AF_{1/2}$, $FA_{1/2}$, AA_1 and $AA_{3/2}$. Within each case we will highlight a particular aspect, which the MPM helps to clarify.

2.4.1 $AA_{1/2}$-ladder: The dimer-RVB state

This is the most studied spin ladder. Its properties are well known and can be summarised as follows. In the weak coupling regime, i.e., $J_\perp << J_{||}$, the gapless spin 1/2 chains become massive by the interchain coupling which is a relevant operator of dimension 1 [13, 14, 15]. The magnitude of the gap is proportional to $J_\perp$. In the intermediate coupling regime, i.e., $J_\perp \simeq J_{||}$ the spin ladder can be mapped into the $O(3)$-*non-linear sigma model* (NLSM) with no topological term [16, 17, 18]. This model is known to have a spin gap. From numerical studies the magnitude of the spin gap Δ and the spin correlation length, in the isotropic case $J_\perp = J_{||} = J$, are given by $\Delta = 0.502J$ and $\xi = 3.2$ respectively [19, 20, 21, 22]. In the strong coupling regime $J_\perp >> J_{||}$, the most appropriate physical picture of the GS and excitations is given by the RVB scenario proposed in [20], and supported by DMRG [20], mean field [23] and variational calculations [24]. In a recent work a recurrent variational ansatz (RVA) was proposed to generate the dimer-RVB and generalisations of it. The RVA method is a MPM based on 2^{nd} and higher order recurrent relations, while the standard MPM is based on a 1^{st} order relation. We shall see below that the MPM applied to ladders essentially contains the RVA, and that the numerical results are improved.

Let us first consider the case where the MPM states $|JM\rangle_N$ are chosen to be a singlet and a triplet, i.e., $J = 0$ and 1. In this case eq. (2.3.1) is depicted in fig. 2.1.

$J_\parallel/J_\perp$	$J_{\max}=1$	$J_{\max}=2$	RVA	Mean Field	Lanczos
0.0	0.375000	0.375000	0.375000	0.375000	
0.2	0.383199	0.383199	0.383195	0.382548	
0.4	0.409607	0.409608	0.409442	0.405430	
0.6	0.453509	0.453513	0.45252	0.442424	
0.8	0.510504	0.510523	0.507909	0.489552	
1.0	0.575924	0.575970	0.571314	0.542848	0.578
1.25	0.664776	0.664867	0.657551	0.614473	0.6687
1.66	0.819656	0.819834	0.808438	0.738360	0.8333
2.5	1.152056	1.152416	1.13384	1.002856	1.18
5.0	2.172002	2.172878	2.13608		2.265

Table 2.1. GS energy per site $-e_\infty/2J_\perp$ of the ladder $AA_{1/2}$. The first two columns are the MPM results. The RVA results are obtained with a third order recursion formula [24]. The mean field and Lanczos results have been obtained in references [23] and [25] respectively.

$J_\parallel/J_\perp$	$J_{\max}=1$	$J_{\max}=2$	RVA
0.0	0.0000	0.0000	0.000000
0.2	0.5300	0.5303	0.437166
0.4	0.8057	0.8081	0.608323
0.6	1.0652	1.0740	0.751286
0.8	1.2753	1.2945	0.866958
1.0	1.4282	1.4593	0.959249
1.25	1.5572	1.6018	1.04877
1.66	1.6802	1.7413	1.15205
2.5	1.7903	1.8698	1.26951
5.0	1.8747	1.9711	1.38532

Table 2.2. Spin correlation length of the ladder $AA_{1/2}$. The first two columns are the MPM results. The RVA results are those of ref. [24].

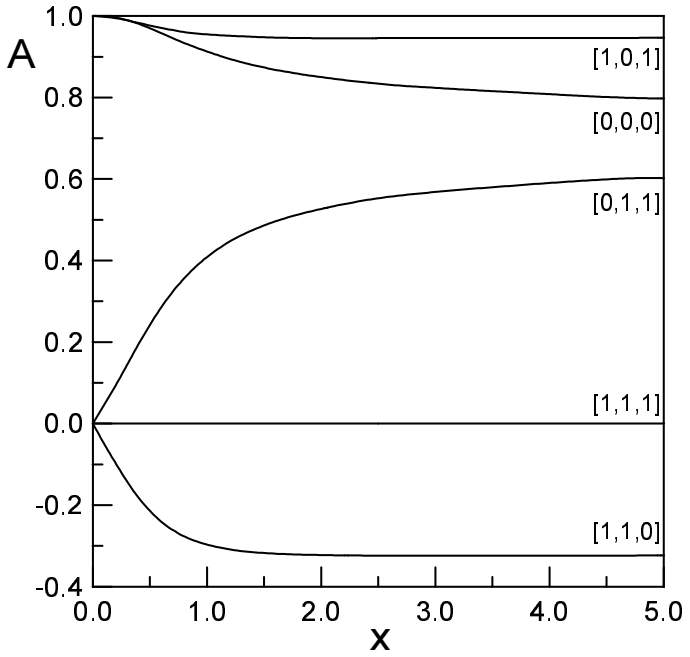

Figure 2.2. The MP parameters for the ladder $AA_{1/2}$. In figures 2.2 to 2.10 we adopt the notation $x = |J_{||}/J_{\perp}|$. The curve $A^{\lambda}_{J_1 J_2}$ is labelled as $[J_1, J_2, \lambda]$.

There are a priori five non vanishing MP parameters subjected to two normalisation constraints, leaving a total of three independent parameters.

Fig. 2.2 shows $A^{\lambda}_{J_1 J_2}$ as functions of $x = J_{||}/J_{\perp}$. In the whole range of coupling constants the most important amplitudes are A^0_{00} and A^1_{10} while A^1_{11} is essentially zero. The latter amplitude correspond to having only a single bond among two rungs (see fig. 2.1), which is forbidden in the dimer-RVB picture of refs. [20] and [24].

In table 2.1 we show the GS energy density obtained with the MPM for $J_{\max} = 1$ and 2, together with the RVA, mean field and Lanczos results. In table 2.2 we give the spin correlation length computed with the MPM and the RVA.

There is an appreciable improvement in the numerical results of the MPM respect to the RVA, specially for the spin correlation length.

2.4.2 $AF_{1/2}$-ladder: Relation with the spin 1 chain

The ladder with magnetic structure AF is interesting because it is intimately related to the spin 1 chain [26]. This relation can be clearly seen in the strong coupling limit

$-J_\perp >> J_\parallel$, since it leads to an effective spin 1 on every rung, which are effectively coupled antiferromagnetically along the legs. An effective Hamiltonian can be derived from (2.3.13a) and (2.3.13b), and reads [26]

$$H_{\rm eff}^{\rm ladder} = -\frac{1}{4}\,|J_\perp|\,N + \frac{1}{2}\,J_\parallel \sum_n \mathbf{S}_{\rm eff}\cdot\mathbf{S}_{\rm eff}, \tag{2.4.1}$$

where $\mathbf{S}_{\rm eff}(n) = \mathbf{S}_1(n) + \mathbf{S}_2(n)$ is the spin 1 operator acting on the $n^{\rm th}$ rung. The term proportional to $J_\perp$ comes from the rung Hamiltonian when diagonalised in the spin 1 sector. This equation implies the following relation between the energies per site of the AF-ladder and the spin 1 chain $e_\infty^{\rm eff}$:

$$e_\infty^{AF} = -\frac{1}{8}\,|J_\perp| + \frac{1}{4}\,J_\parallel\,e_\infty^{\rm eff}. \tag{2.4.2}$$

In table 2.3 we give the GS energies of the ladder parametrised in terms of the effective energy $e_\infty^{\rm eff}$. We also give the spin correlation length. We have made two choices of MP states $|JM\rangle_N$. One for which $J = 0$ and 1 and the other for which $J = 1/2$ and $3/2$. The latter one corresponds to having a single spin $1/2$ at the boundary of the ladder. These two choices have an analogue for the spin 1 chain. For integer $J's$ the MP parameters do not vary in the whole interval $0 < J_\parallel < 1.66$ and take the values,

$$\begin{aligned} A_{00}^0 = A_{11}^0 = 0.000 \qquad A_{01}^1 = 1.000 \\ A_{10}^1 = -0.577 \qquad A_{11}^1 = 0.816. \end{aligned} \tag{2.4.3}$$

For half-integer $J's$ the MP parameters do not vary in the whole interval $0 < J_\parallel < 5$ and take the values,

$$\begin{aligned} A_{\frac{1}{2}\frac{1}{2}}^0 = A_{\frac{3}{2}\frac{3}{2}}^0 = 0.000 \qquad A_{\frac{1}{2}\frac{1}{2}}^1 = 0.989 \\ A_{\frac{1}{2}\frac{3}{2}}^1 = 0.148 \qquad A_{\frac{3}{2}\frac{1}{2}}^1 = -0.953 \qquad A_{\frac{3}{2}\frac{3}{2}}^1 = -0.303. \end{aligned} \tag{2.4.4}$$

Note that for half integers J there is one more variational parameter. The most important amplitudes indeed correspond to the formation of an AKLT state with a single bond connecting every effective spin 1.

The values of $e_\infty^{\rm eff}$ and ξ in the integer J case coincide with those of the AKLT state, while the ones of the half-integer J case coincide with those obtained with a MPM method applied to the spin 1 chain [7] where one keeps two MPM states with $J = 1/2$ and $3/2$. These results provide additional support for the equivalence between the $AF_{1/2}$-ladder and the spin 1 chain in the strong and intermediate coupling regimes observed previously by other authors [26].

$-J_{\|}/J_{\perp}$	$-e_{\infty}^{\text{eff,int}}$	$-e_{\infty}^{\text{eff,half}}$	ξ^{int}	ξ^{half}
(0.0, 1.66)	1.333333	1.399659	0.910	2.5997
2.5	1.363970	1.399659	1.9682	2.5997
5.0	1.498539	1.399659	1.9607	2.5997

Table 2.3. The exact values of the GS energy density of a spin 1 chain and its correlation length are given by $e_{\infty} = -1.4014845$ and $\xi = 6.03$ [11].

2.4.3 $FA_{1/2}$-ladder

In the strong coupling regime the ladders $FA_{1/2}$ and $AA_{1/2}$ have similar GS energies and correlation lengths (see tables 2.1, 2.2 and 2.4). The MP parameters display also a similar behaviour although some of them are interchanged (see figures 2.2 and 2.3). The physical reason of this is the common GS in the case where $J_{\|} = 0$, given by the coherent superposition of valence bonds in the rungs.

The relation between $FA_{1/2}$ and $AA_{1/2}$ is part of a more general relation involving also the ladder $AF_{1/2}$ and can be established by means of a type of transformations called dualities in ref. [27].

2.4.4 Duality properties of spin ladders

On a 2-leg ladder one can define three types of dualities called U, T and S, which mix or leave invariant the ladder's magnetic structures AA, AF and FA [27]. These are based on a generalisation of the Migdal-Kadanoff transformations [28], which consist in the substitution of couplings (bond moving) between nearest neigbouring (n.n.) sites and other n.n. or n.n.n. couplings. This is achieved by adding a potential V to he hamiltionian H, so that the transformed hamiltonian $H' = H + V$ has a GS energy smaller than the GS energy of H, provided that $\langle V \rangle = 0$, where the expectation value is taken respect with to the GS of H.

$$\begin{aligned} e^{-\beta F'} = e^{-\beta F}\langle e^{-\beta V}\rangle \quad &\longrightarrow \quad e^{-\beta F'} \geq e^{-\beta F} e^{-\beta \langle V \rangle} \\ F' \leq F \quad &when \quad \langle V \rangle = 0. \end{aligned} \tag{2.4.5}$$

In ladders the bond moving potential is built by adding a new interaction and subtracting an original one. After imposing that the expectation value vanishes we obtain the relation between the transformed coupling constants and the original ones.

$-J_{\parallel}/J_{\perp}$	$-e_{\infty}/2J_{\perp}$	ξ
0.0	0.375000	0.0000
0.2	0.381754	0.5140
0.4	0.399295	0.7577
0.6	0.424396	1.010
0.8	0.454891	1.277
1.0	0.489324	1.554
1.25	0.536374	1.895
1.66	0.619895	2.381
2.5	0.803434	2.992
5.0	1.376973	3.520

Table 2.4. GS energy per site and correlation length of the ladder $FA_{1/2}$.

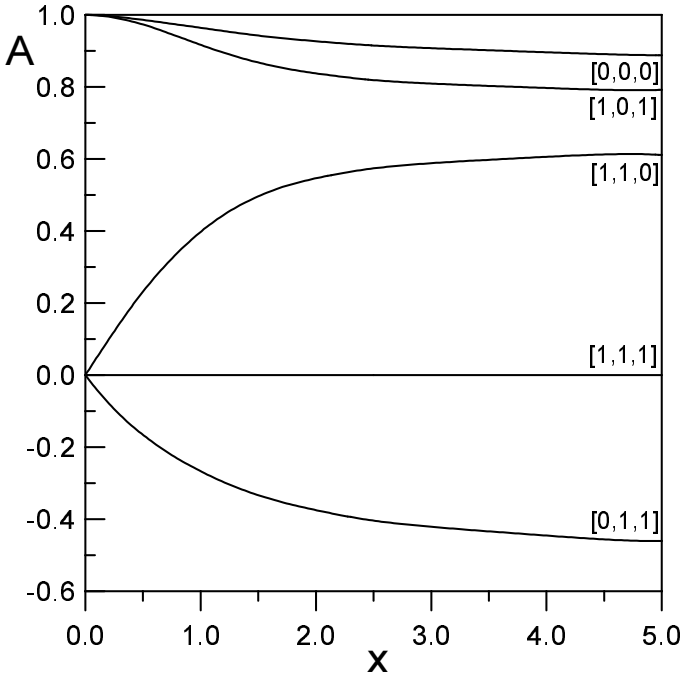

Figure 2.3. Same notations as in fig. 2.2 but for the $FA_{1/2}$-ladder.

U-duality

The U duality maps a Hamiltonian with couplings constants $J_{\|}, J_{\perp}$ into a ladder with couplings constants $J_{\|}^U, J_{\perp}^U$ where,

$$\begin{aligned} J_{\|}^U &= J_{\|} \langle \mathbf{S}_1(n) \cdot \mathbf{S}_1(n+1) \rangle / \langle \mathbf{S}_1(n) \cdot \mathbf{S}_2(n+1) \rangle \\ J_{\perp}^U &= J_{\perp}. \end{aligned} \tag{2.4.6}$$

Under U the leg-bonds are transformed into diagonal ones while the rung-bonds are left invariant. The signs of $\langle \mathbf{S}_1(n) \cdot \mathbf{S}_1(n+1) \rangle$ and $\langle \mathbf{S}_1(n) \cdot \mathbf{S}_2(n+1) \rangle$ are determined by those of $J_{\|}$ and $J_{\perp}$ respectively. Thus U acts on the magnetic structures as follows:

$$\begin{aligned} AA \quad &\stackrel{U}{\longrightarrow} \quad FA \\ J_{\|}(AA) > 0 \quad &\longrightarrow \quad J_{\|}^U(FA) < 0 \\ J_{\perp}(AA) > 0 \quad &\longrightarrow \quad J_{\perp}^U(FA) > 0 \end{aligned} \tag{2.4.7a}$$

$$\begin{aligned} AF \quad &\stackrel{U}{\longrightarrow} \quad AF \\ J_{\|}(AF) > 0 \quad &\longrightarrow \quad J_{\|}^U(AF) > 0 \\ J_{\perp}(AF) < 0 \quad &\longrightarrow \quad J_{\perp}^U(AF) < 0. \end{aligned} \tag{2.4.7b}$$

In fig. 2.4 we show $J_{\|}^U(FA)$ and $J_{\|}^U(AF)$ as functions of $J_{\|}(AA)$ and $J_{\|}(AF)$ respectively.

The GS energy density of the ladder with coupling constants $J_{\|}^U, J_{\perp}^U$ is a lower bound of the original GS energy [27], i.e.,

$$\begin{aligned} e_\infty(J_{\|}^U(FA), J_{\perp}^U(FA)) &\leq e_\infty(J_{\|}(AA), J_{\perp}(AA)) \\ e_\infty(J_{\|}^U(AF), J_{\perp}^U(AF)) &\leq e_\infty(J_{\|}(AF), J_{\perp}(AF)). \end{aligned} \tag{2.4.8}$$

In fig. 2.5 we show the validity of these inequalities, which in the strong coupling limit almost become identities. In fig. 2.6 we show the correlation lengths for both AA and the transformed FA-ladders. Again in the strong coupling limit they become very close.

T-duality

The T transformation consists in the replacement of the vertical bonds by diagonal ones, i.e.,

$$\begin{aligned} J_{\|}^T &= J_{\|} \\ J_{\perp}^T &= J_{\perp} \langle \mathbf{S}_1(n) \cdot \mathbf{S}_1(n+1) \rangle / \langle \mathbf{S}_1(n) \cdot \mathbf{S}_2(n+1) \rangle, \end{aligned} \tag{2.4.9}$$

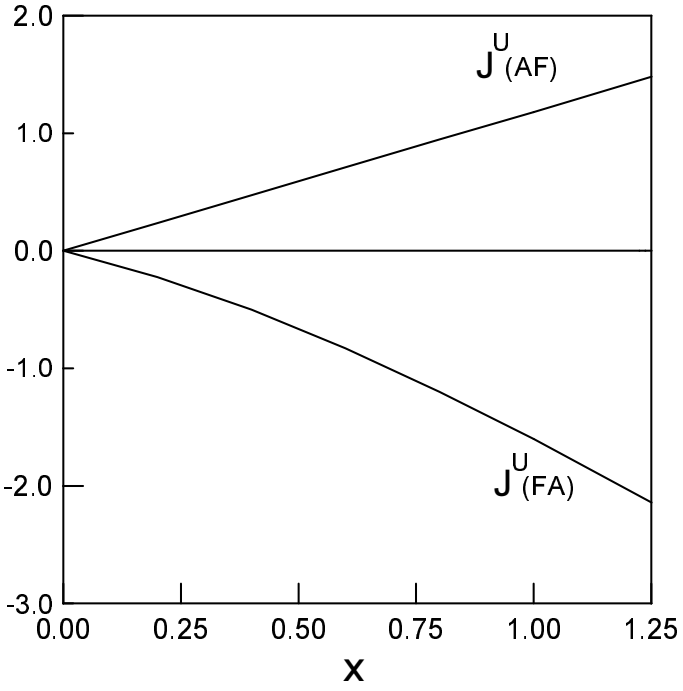

Figure 2.4. $J^U(AF) \equiv J^U_{||}(AF)$ and $J^U(FA) \equiv J^U_{||}(FA)$.

which leads to the following action on magnetic structures,

$$\begin{array}{ccc} AA & \xrightarrow{T} & AF \\ J_{||}(AA) > 0 & \longrightarrow & J^T_{||}(AF) > 0 \\ J_{\perp}(AA) > 0 & \longrightarrow & J^T_{\perp}(AF) < 0 \end{array} \tag{2.4.10a}$$

$$\begin{array}{ccc} FA & \xrightarrow{T} & FA \\ J_{||}(FA) < 0 & \longrightarrow & J^T_{||}(FA) < 0 \\ J_{\perp}(FA) > 0 & \longrightarrow & J^T_{\perp}(FA) > 0. \end{array} \tag{2.4.10b}$$

In fig. 2.7 we plot the energies associated to the FA-ladder and its T transformed, which satisfies the inequality

$$e_\infty(J^T_{||}(FA), J^T_{\perp}(FA)) \leq e_\infty(J_{||}(FA), J_{\perp}(FA)). \tag{2.4.11}$$

The convergence of both curves in the weak coupling is in agreement with the bosonisation arguments employed in [27].

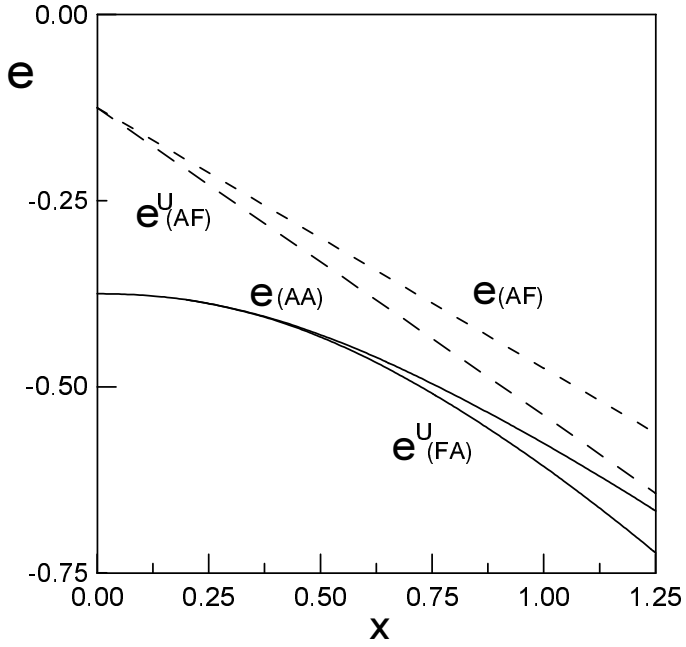

Figure 2.5. GS energy per site of the AA and AF-ladders and their U-dual models.

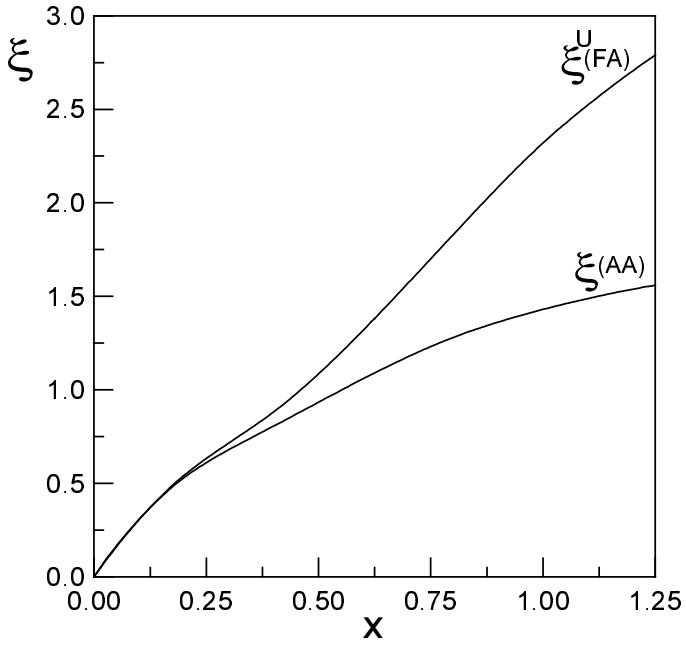

Figure 2.6. Spin-correlation lengths of the AA-ladder and its U-dual.

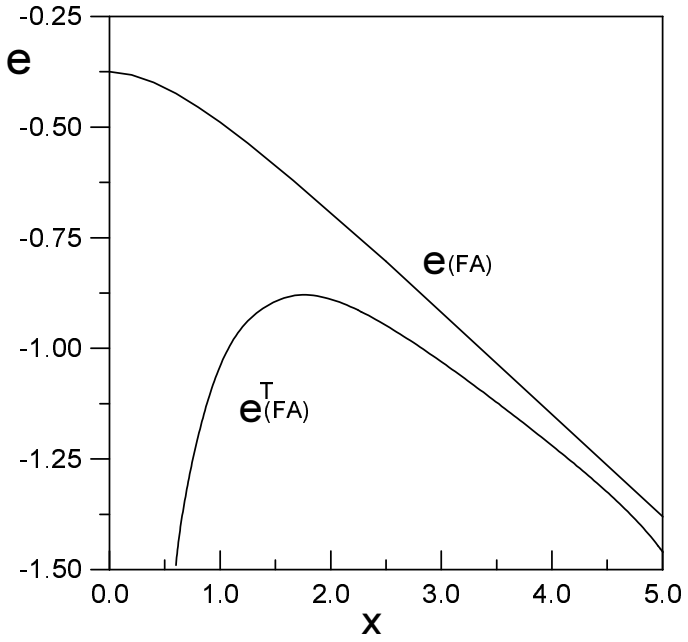

Figure 2.7. GS energy per site of the AF-ladder and its T-dual given by the FA-ladder.

S-duality

Finally the S transformation is defined by the replacement of vertical bonds by horizontal ones and viceversa,

$$\begin{aligned} J_{\|}^{S} &= \tfrac{1}{2}\, J_{\perp}\, \langle \mathbf{S}_1(n)\cdot\mathbf{S}_2(n)\rangle / \langle \mathbf{S}_1(n)\cdot\mathbf{S}_1(n+1)\rangle \\ J_{\perp}^{S} &= 2\, J_{\|}\, \langle \mathbf{S}_1(n)\cdot\mathbf{S}_1(n+1)\rangle / \langle \mathbf{S}_1(n)\cdot\mathbf{S}_2(n)\rangle. \end{aligned} \tag{2.4.12}$$

The factors 2 and 1/2 are explained by the fact that there are two leg-bonds for each rung-bond. Eqs. (2.4.12) imply,

$$\begin{array}{ccc} AF & \stackrel{S}{\longrightarrow} & FA \\ J_{\|}(AF) > 0 & \longrightarrow & J_{\|}^{S}(FA) < 0 \\ J_{\perp}(AF) < 0 & \longrightarrow & J_{\perp}^{S}(FA) > 0 \end{array} \tag{2.4.13a}$$

$$\begin{array}{ccc} AA & \stackrel{S}{\longrightarrow} & AA \\ J_{\|}(AA) > 0 & \longrightarrow & J_{\|}^{S}(AA) > 0 \\ J_{\perp}(AA) > 0 & \longrightarrow & J_{\perp}^{S}(AA) > 0. \end{array} \tag{2.4.13b}$$

In fig. 2.8 we plot the energies of the AA-ladder and its transformed which satisfy

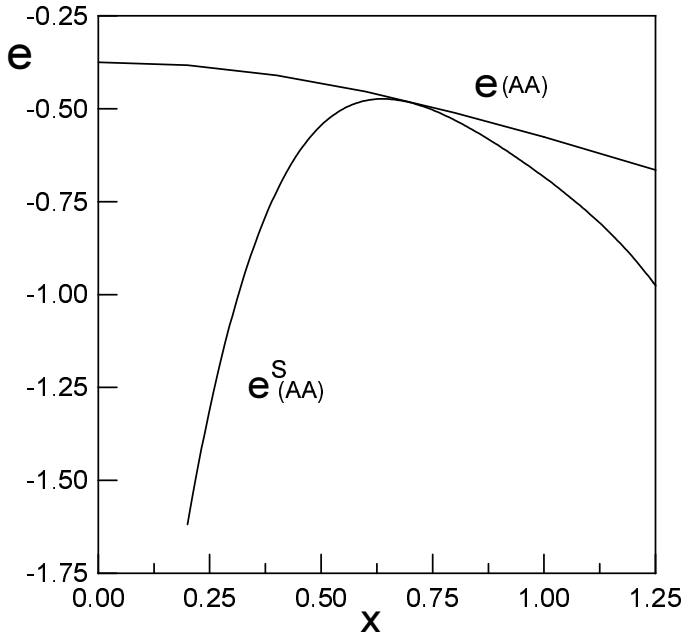

Figure 2.8. GS energy per site of the AA-ladder and its S-dual.

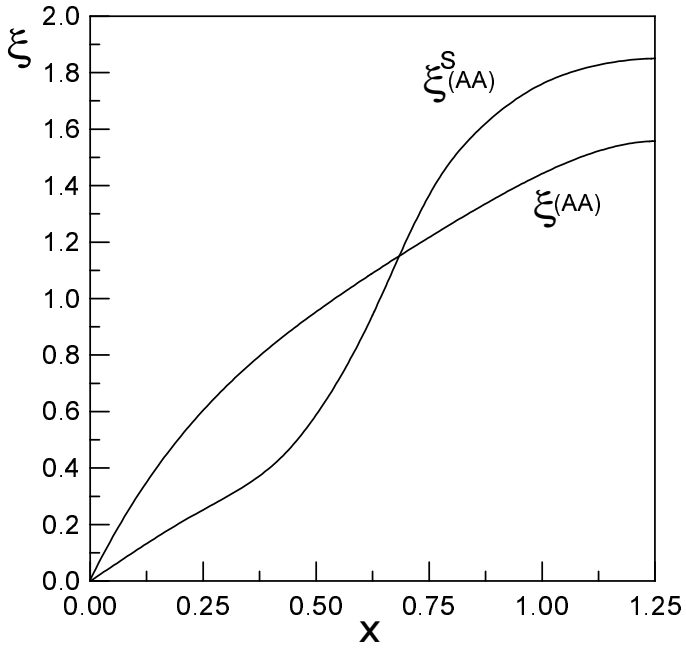

Figure 2.9. Spin-correlation length of the AA-ladder and its S-dual.

the inequality

$$e_\infty(J_\parallel^S(AA), J_\perp^S(AA)) \leq e_\infty(J_\parallel(AA), J_\perp(AA)). \tag{2.4.14}$$

Note that in the region $J_\parallel \sim J_\perp$ both energies get very closed. Fig. 2.9 shows the spin correlation length for the AA-ladder and its S transformed, displaying the same pattern as fig. 2.8. In summary we have found further numerical evidence of the duality properties of the 2-leg ladder proposed in [27].

2.4.5 AA_1-ladder: Short-range string order

In table 2.5 we show the GS energy density and the spin-correlation length of the ladder AA_1. Observe that the correlation length is longer that the one of the spin 1/2 ladder.

As mentioned in the introduction a spin 1 chain has a long range topological order (LRTO) characterised by a non-vanishing $g(\infty)$. In appendix 2.C we give an analytical expression for $g(\infty)$ in terms of the MP parameters of the spin 1 chain.

However when two spin 1 chains are coupled antiferromagnetically the LRTO disappears and the string order parameter $g(\ell)$ decays exponentially as $e^{-\ell/\xi^{\rm st}}$. We call $\xi^{\rm st}$ the string correlation length, and its value together with the spin correlation length are shown in fig. 2.10 as functions of the ratio $J_\parallel/J_\perp$. In the weak coupling limit where $J_\parallel/J_\perp \to \infty$ we expect $\xi^{\rm st}$ to diverge, recovering in that way the LRTO of the uncoupled chains. The value of $\xi^{\rm st}$ is obtained by the formula (2.2.19) with x_p the highest eigenvalue of the operator $\widehat{e^{i\pi S_1^z}}$ (see appendix 2.C).

An intuitive way to understand the breaking of the LRTO is given by the AKLT picture of ref. [3]. An AKLT state is a valence bond state where every spin 1 is represented as a symmetrised product of two spins 1/2, and such that every of these "elementary" spins is linked by a bond to one of the spins 1/2 on its neighbours. In this way all the spins of the chain are connected by a succession of nearest neighbour links. When we couple antiferromagnetically two spin 1 chains there is the possibility that two parallel bonds along the legs become two parallel bonds along the rungs as shown in fig. 2.11. Thus the two infinite parallel arrays of connected bonds, characteristic of the uncoupled chains, effectively break into a collection of fluctuating islands whose size is of the order of $\xi^{\rm st}$. Everyone of these islands is a sort of closed spin 1 chain (fig. 2.11).

$J_\parallel/J_\perp$	$-e_\infty/2J_\perp$	ξ
0.0	1.000000	0.0000
0.2	1.055719	1.0114
0.4	1.206557	1.8318
0.6	1.407358	2.3852
0.8	1.631166	2.6762
1.0	1.867327	2.8227
1.25	2.172905	2.9042
1.66	2.688880	2.9286

Table 2.5. GS energy per site and correlation length of the AA_1-ladder.

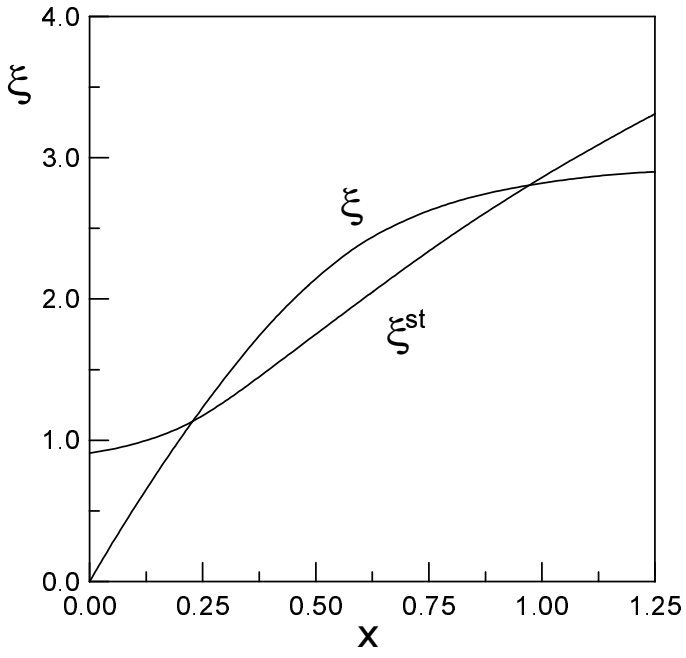

Figure 2.10. Plots of the spin-correlation length ξ and the string correlation length $\xi^{\rm st}$ of the ladder AA_1.

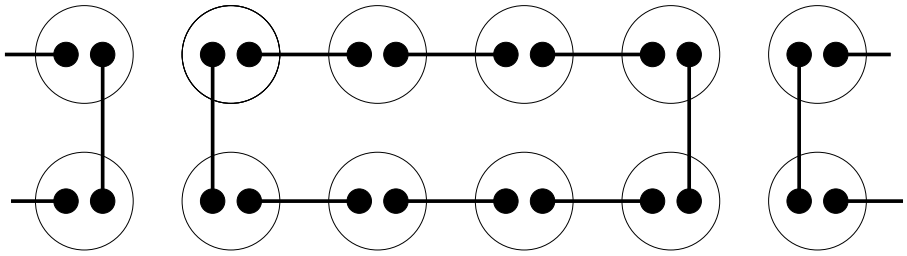

Figure 2.11. Pictorical representation of a possible AKLT state of the spin 1 ladder.

The finite value of $\xi^{\rm st}$ at the origin of fig. 2.10 is due to the fact that $e^{i\pi S_1^z}$ has indeed a finite value when computed on the singlet formed by two spins 1 on a rung,

$$\langle e^{i\pi S_1^z}\rangle_{\rm rung} = \sum_{m=\pm 1,0} (-1)^m \langle 1m1-m|00\rangle^2 = -\frac{1}{3}, \tag{2.4.15}$$

which leads to $\xi^{\rm st}(J_{||}=0) = 1/\ln 3$. Fig. 2.10 suggests the existence of three different regimes. In the weak coupling regime where $\xi^{\rm st} > \xi$ the ladder can be effectively considered as a collection of weakly interacting closed spin 1 chains. In the strong coupling regime where $\xi^{\rm st} > \xi$ the bonds are meanly along the rungs and the interbond coupling is small. Finally, there is an intermediate region, with $\xi^{\rm st} < \xi$, where the islands of spins interact strongly with their neighbours.

2.4.6 $AA_{3/2}$-ladder

In table 2.6 we give the GS energy densities and spin correlation lengths of the ladder $AA_{3/2}$. As one may expect the correlation length is longer than for the spin 1 and 1/2 ladders. This fact agrees with the results obtained by mapping the spin ladders into the NLSM [16, 17, 18].

AKLT states for ladders

The spin 3/2 2-ladder offers the possibility of constructing an AKLT state with a valence bond connecting every spin 3/2 to its three nearest neighbours. More generally, let us consider a ladder with spin $S \geq 3/2$ and three integers $p, q, r \geq 1$ satisfying the relation $p+q+r = 2S$. Then one can define an AKLT state, denoted by the triplet (p, q, r), by linking the $2S$ "elementary spinors" of each spin to the ones in its neighbours following the pattern shown in fig. 2.12. The AKLT states (p, q, r) and (q, p, r) when

$J_\parallel/J_\perp$	$-e_\infty/2J_\perp$	ξ
0.0	1.875000	0.0000
0.2	2.054760	1.8760
0.4	2.449827	3.3099
0.6	2.911353	3.9475
0.8	3.400562	4.2401
1.0	3.904988	4.3829
1.25	4.548607	4.4624
1.66	5.623131	4.4900

Table 2.6. GS energy per site and correlation length of the $AA_{3/2}$-ladder.

$p \neq q$ correspond to dimerised ladders and they differ by the translation of one unit space along the legs.

The spin 3/2 AKLT ladder corresponds in the above notation to $(1,1,1)$. This state contains in fact a spin 0 and a spin 1 state which can be generated by the MP equation (2.3.1) where the amplitudes $A^\lambda_{J_1 J_2}$ are given by rotation group 9-j symbols

$$A^\lambda_{J_1 J_2} = 3\sqrt{(2J_2+1)(2\lambda+1)} \begin{Bmatrix} 1/2 & 1/2 & J_2 \\ 3/2 & 3/2 & \lambda \\ 1 & 1 & J_1 \end{Bmatrix}. \tag{2.4.16}$$

In this equation $J_1, J_2 = 0$ and 1, while $\lambda = 0, 1, 2$.

The proof of (2.4.16) follows from the definition of the 9-j symbols as the coefficients that give the change of basis when coupling in two different ways four angular momenta, namely, [29]

$$\begin{aligned} \psi\left(j_1 j_3 (J_{13}) j_2 j_4 (J_{24}) J\right) &= \sum_{J_{12} J_{34}} \sqrt{(2J_{12}+1)(2J_{34}+1)(2J_{13}+1)(2J_{24}+1)} \\ &\times \begin{Bmatrix} j_1 & j_2 & J_{12} \\ j_3 & j_4 & J_{34} \\ J_{13} & J_{24} & J \end{Bmatrix} \psi\left(j_1 j_2 (J_{12}) j_3 j_4 (J_{34}) J\right), \end{aligned} \tag{2.4.17}$$

where $\psi\left(j_1 j_3 (J_{13}) j_2 j_4 (J_{24}) J\right)$ is a state with angular momentum J obtained by the tensor product decomposition $J_{13} \otimes J_{24} \to J$, which in turn are obtained by the decompositions $j_1 \otimes j_3 \to J_{13}$ and $j_2 \otimes j_4 \to J_{24}$.

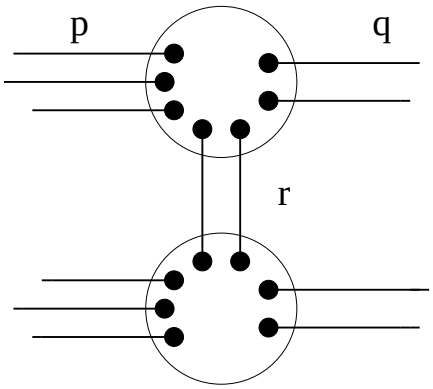

Figure 2.12. Graphical representation of a generic AKLT state of a ladder denoted as (p, q, r). There are a total of $p + q + r$ dots inside every circle representing a total spin $S = (p + q + r)/2$.

One may check that the normalisation conditions (2.3.5) holds for (2.4.16), as a consequence of the orthogonality conditions satisfied by the 9-j symbols [29]. The GS energy per site and the spin correlation length of the AKLT state (2.4.16) in the case where $J_{\|} = J_{\perp} = J$ are given by,

$$e_{\infty}^{\mathrm{AKLT}}/2J = -3.263536 \quad , \quad \xi^{\mathrm{AKLT}} = 1.116221. \tag{2.4.18}$$

This state has a much shorter correlation length than the MP state that minimises the GS energy of the $AA_{3/2}$-ladder (see table 2.6). The GS energies of both states are also quite different. We conclude from these facts that the spin 3/2 AKLT state does not give a good description of the GS of the $AA_{3/2}$-ladder.

A generic AKLT state of the type (p, q, r) when $p \neq q$ has to be described by alternating MP amplitudes depending on the eveness of the site. Thus for even sites one has

$$A^{\lambda}_{J_1 J_2} = (q + r + 1)\sqrt{(2J_2 + 1)(2\lambda + 1)} \begin{Bmatrix} \frac{p}{2} & \frac{p}{2} & J_2 \\ S & S & \lambda \\ \frac{q+r}{2} & \frac{q+r}{2} & J_1 \end{Bmatrix}, \tag{2.4.19}$$

where $J_1 = 0, \ldots, q$; $J_2 = 0, \ldots, p$ and $\lambda = 0, \ldots, 2S - r$. For odd sites the corresponding MP amplitudes are obtained by interchanging p and q in (2.4.19).

2.5 Conclusions and Prospects

Let us summarise the main results obtained in this chapter.

(i) We have presented a rotational invariant formulation of the MPM which allow us to express the GS energy density, the correlation length and the string order parameter, in terms of invariant objects. This reduces considerably the number of independent MP parameters used in the minimisation process.

(ii) We have improved the numerical results concerning the GS energy density and spin correlation length obtained previously with other approximate methods as those of references [24, 23]. The consideration of MP ansatzs with multiple states per spin will certainly lead to better results.

(iii) We have shown the equivalence between the ladder $AF_{1/2}$ and the spin 1 antiferromagnetic Heisenberg chain. The MPM applied to both systems shows strong numerical coincidences for the GS energy and correlation length. This agrees with the results obtained previously by other methods [26, 30, 31]

(iv) We have found numerical evidences for the duality properties proposed in [27] for the spin ladders with magnetic structures AA, AF and FA.

(v) We have shown that there is a breaking of the long range topological order of the spin 1 chains when they are coupled in a 2-legged ladder. A physical picture of the GS of the spin 1 ladder is given in terms of resonating closed spin 1 chains.

(vi) We have constructed AKLT states for 2-legged ladders with spin $S \geq 3/2$, showing that the corresponding MP parameters are given by rotation group 9-j symbols.

(vii) We have suggested a relation between the MPM and the DMRG based on the density matrix that appear in both methods (see also [7]). We conjecture that the minimisation of the GS energy e_∞ can be transformed into an eigenvalue problem on a superblock $B_N \bullet B_N^R$.

In summary we have shown the adequacy of the MPM to study the 2-legged ladder, specially in the strong and intermediate coupling regimes. This is made possible from the fact that these ladders are finitely correlated. Hence one may expect that even

spin ladders with a finite number of legs could be described by the same technique, although with a larger number of states m. On the other hand, odd legged ladders are not finitely correlated and they cannot be properly described in the large N limit within the actual formulation of the MPM. An interesting problem is the application of the MPM to 2D systems, which can be thought of as ladders with a large number of legs. It is clear that one should choose a collection of the most representative states for the rungs to be added after each iteration of the MP recurrence equation.

2.A The MP ansatz and the Grassmannian manifolds

In this appendix we shall give a proof of eq. (2.2.4) which gives a precise mathematical meaning of the coefficients $A_{\alpha\beta}[s]$ defining a generic MP ansatz.

In the r.h.s. of eq. (2.2.1) we have a generic vector of dimension $n = mm^*$ while on its l.h.s. the vector has dimension m. Hence eq. (2.2.1) amounts to a choice of a m-dimensional linear subspace of $\mathbf{R}^n$ in the case of $A_{\alpha\beta}[s]$ real or a complex subspace of $\mathbf{C}^n$ in the case of $A_{\alpha\beta}[s]$ complex. Let us call the set of all these subspaces as $M_{n,m}(\mathbf{R})$ and $M_{n,m}(\mathbf{C})$ for $A_{\alpha\beta}[s]$ real and complex respectively. The group $O(n)$ (resp. $U(n)$) acts transitively on $M_{n,m}(\mathbf{R})$ (resp. $M_{n,m}(\mathbf{C})$), which leads to the result [32]

$$M_{n,m}(\mathbf{R}) = \frac{O(n)}{O(m) \otimes O(n-m)} \tag{2.A.1a}$$

$$M_{n,m}(\mathbf{C}) = \frac{U(n)}{U(m) \otimes U(n-m)}. \tag{2.A.1b}$$

In (2.A.1a) the groups $O(m)$ and $O(n-m)$ are identified with the subgroups of $O(n)$ consisting of those elements leaving fixed every vector of a given $(n-m)$-dimensional subspace and of its orthogonal complement, respectively. Similar arguments lead to eq.(2.A.1b). $M_{n,m}(\mathbf{R})$ ($M_{n,m}(\mathbf{C})$) are called the real (complex) Grassmannian manifolds. Taking $n = mm^*$ in (2.A.1a) we get eq. (2.2.4).

As a simple illustration of these equations let us consider the case of a MP ansatz that generates a single state $|GS\rangle_N$ ($m = 1$), i.e.,

$$|GS\rangle_N = \sum_s A[s]\ |s\rangle_N \otimes |GS\rangle_{N-1}, \tag{2.A.2}$$

with $A[s] \in \mathbf{R}$. The normalisation condition (2.2.2) reads

$$\sum_{s=1}^{m^*} A[s]^2 = 1. \tag{2.A.3}$$

Thus $A[s]$ belongs to the (m^*-1)-dimensional sphere $SO(m^*)/SO(m^*-1)$. Upon the identification of $A[s]$ and $-A[s]$ we get the (m^*-1)-real projective space $M_{m^*,1}(\mathbf{R}) = SO(m^*)/SO(m^*-1) \otimes \mathbf{Z}_2$.

2.B The Rotational Invariant MPM

Group theoretical preliminaries

Before we give the proof of the main formulas of section 2.3 we shall review some basic definitions and results in the rotation group theory [29].

An irreducible tensor with angular momentum k is an operator $T^{(k)}_M$, where $M = -k, \cdots, k$, which satisfies the following commutation relations with the total angular momentum operator $\mathbf{J}$,

$$[J_z, T^{(k)}_M] = M\, T^{(k)}_M \tag{2.B.1a}$$

$$[J_x \pm i\, J_y, T^{(k)}_M] = \sqrt{k(k+1) - M(M \pm 1)}\, T^{(k)}_{M\pm 1}. \tag{2.B.1b}$$

The scalar product of two irreducible tensors $\mathbf{T}^{(k)}$ and $\mathbf{U}^{(k)}$ with the same spin k is defined by

$$\mathbf{T}^{(k)} \cdot \mathbf{U}^{(k)} = \sum_{M=-k}^{k} (-1)^{-M}\, T^{(k)}_M\, U^{(k)}_{-M}. \tag{2.B.2}$$

The Wigner-Eckart theorem reads

$$\langle JM|T^{(k)}_\mu|J'M'\rangle = (-1)^{J-M} \begin{pmatrix} J & k & J' \\ -M & \mu & M' \end{pmatrix} (J||\mathbf{T}^{(k)}||J'), \tag{2.B.3}$$

where the 3-j symbol is related to the CG coefficient by

$$\begin{pmatrix} J & k & J' \\ -M & \mu & M' \end{pmatrix} = \frac{(-1)^{J-k-M'}}{\sqrt{2J'+1}}\, \langle J - M k\mu | J' - M'\rangle. \tag{2.B.4}$$

The quantity $(J||\mathbf{T}^{(k)}||J')$ in (2.B.3) is called the reduced matrix element of the operator $\mathbf{T}^{(k)}$. As an example we give the reduced matrix element of the spin operator $\mathbf{S}$,

$$(S||\mathbf{S}||S) = \sqrt{S(S+1)(2S+1)}. \tag{2.B.5}$$

Let $|\alpha_1 j_1 \alpha_2 j_2 JM\rangle$ be a state with total angular momenta J and third component M, appearing in the tensor product decomposition $(\alpha_1 j_1) \otimes (\alpha_2 j_2)$, where (αj) denotes a state with total angular momentum j and α labels other possible quantum numbers. We shall need below the following results:

$$\langle \alpha_1 j_1 \alpha_2 j_2 JM | (\mathbf{T}_1^{(k)} \cdot \mathbf{T}_2^{(k)}) | \alpha_1' j_1' \alpha_2' j_2' J' M' \rangle = \tag{2.B.6a}$$
$$\delta_{JJ'}\, \delta_{MM'}\, (-1)^{j_2+J+j_1'} \left\{ \begin{array}{ccc} j_1 & j_2 & J \\ j_2' & j_1' & k \end{array} \right\} (\alpha_1 j_1 || \mathbf{T}_1^{(k)} || \alpha_1' j_1')\, (\alpha_2 j_2 || \mathbf{T}_2^{(k)} || \alpha_2' j_2')$$

$$(\alpha_1 j_1 \alpha_2 j_2 J || \mathbf{T}_1^{(k)} || \alpha_1' j_1' \alpha_2' j_2' J') = \tag{2.B.6b}$$
$$\delta_{\alpha_2 \alpha_2'} \delta_{j_2 j_2'}\ (-1)^{j_1+j_2+J'+k} \left\{ \begin{array}{ccc} j_1 & J & j_2 \\ J' & j_1' & k \end{array} \right\} \sqrt{(2J+1)(2J'+1)}\, (\alpha_1 j_1 || \mathbf{T}_1^{(k)} || \alpha_1' j_1')$$

$$(\alpha_1 j_1 \alpha_2 j_2 J || \mathbf{T}_2^{(k)} || \alpha_1' j_1' \alpha_2' j_2' J') = \tag{2.B.6c}$$
$$\delta_{\alpha_1 \alpha_1'} \delta_{j_1 j_1'}\ (-1)^{j_1+j_2'+J+k} \left\{ \begin{array}{ccc} j_2 & J & j_1 \\ J' & j_2' & k \end{array} \right\} \sqrt{(2J+1)(2J'+1)}\, (\alpha_2 j_2 || \mathbf{T}_2^{(k)} || \alpha_2' j_2').$$

The subindices 1 and 2 in $\mathbf{T}_1^{(k)}$ and $\mathbf{T}_2^{(k)}$ mean that the corresponding operators acts on the states labelled as $(\alpha_1 j_1)$ and $(\alpha_2 j_2)$ respectively.

Recursion relations for the scalar product of invariant tensors

Here we shall procede to prove eq. (2.3.7).

Using eq. (2.3.1) we easily get for $N > n > m$

$$ {}_N\langle J_1 M|\, \mathcal{O}^{(k,A)}(n) \cdot \mathcal{O}^{(k,B)}(m)\, |J_1 M\rangle_N = $$
$$\sum_{J_2} T_{J_1 J_2}\ {}_{N-1}\langle J_2 M|\, \mathcal{O}^{(k,A)}(n) \cdot \mathcal{O}^{(k,B)}(m)\, |J_2 M\rangle_{N-1}, \tag{2.B.7}$$

where $T_{J_1 J_2}$ is given in (2.3.8). Iterating (2.B.7) $N-n$ times we reach the situation where $N = n$. This produces the term $T_{J_1 J_2}^{N-n}$ in (2.3.7). Next we need to compute the matrix element,

$$ {}_n\langle J_1 M|\, \mathcal{O}^{(k,A)}(n) \cdot \mathcal{O}^{(k,B)}(m)\, |J_1 M\rangle_n = \tag{2.B.8}$$
$$\sum_{J_2 J_3 \lambda_2 \lambda_3} \left(A_{J_1 J_2}^{\lambda_2}\right)^*\ A_{J_1 J_3}^{\lambda_3}\ {}_n\langle (\lambda_2 J_2), J_1 M|\, \mathcal{O}^{(k,A)}(n) \cdot \mathcal{O}^{(k,B)}(m)\, |(\lambda_3 J_3), J_1 M\rangle_n.$$

The matrix element on the r.h.s. of (2.B.8) has the form described in (2.B.6a), which yields

$$ {}_n\langle (\lambda_2 J_2), J_1 M|\, \mathcal{O}^{(k,A)}(n) \cdot \mathcal{O}^{(k,B)}(m)\, |(\lambda_3 J_3), J_1 M\rangle_n = \tag{2.B.9}$$
$$(-1)^{J_1+J_2+\lambda_3} \left\{ \begin{array}{ccc} \lambda_2 & J_2 & J_1 \\ J_3 & \lambda_3 & k \end{array} \right\}\ {}_n(\lambda_2 || \mathcal{O}^{(k,A)}(n) || \lambda_3)_n\ {}_{n-1}(J_2 || \mathcal{O}^{(k,B)}(m) || J_3)_{n-1}.$$

Introducing (2.B.9) into (2.B.8) we find

$$ {}_n\langle J_1 M|\ \mathcal{O}^{(k,A)}(n)\cdot\mathcal{O}^{(k,B)}(m)\ |J_1 M\rangle_n = \sum_{J_2 J_3} \widehat{\mathcal{O}}^{(k,A)}_{J_1,J_2 J_3}\ {}_{n-1}(J_2||\mathcal{O}^{(k,B)}(m)||J_3)_{n-1}, \tag{2.B.10} $$

where

$$ \widehat{\mathcal{O}}^{(k,A)}_{J_1,J_2 J_3} = \sum_{\lambda_2,\lambda_3} \left(A^{\lambda_2}_{J_1 J_2}\right)^* A^{\lambda_3}_{J_1 J_3}\ (-1)^{\lambda_3+J_1+J_2} \left\{ \begin{array}{ccc} \lambda_2 & J_2 & J_1 \\ J_3 & \lambda_3 & k \end{array} \right\} (\lambda_2||\mathcal{O}^{(k,A)}||\lambda_3). \tag{2.B.11} $$

The next step is to apply the MP ansatz (2.3.1) to

$$ {}_n(J_1||\mathcal{O}^{(k,B)}(m)||J_2)_n = \sum_{\lambda_1\lambda_2} \left(A^{\lambda_1}_{J_1 J_3}\right)^*\ A^{\lambda_2}_{J_2 J_4}\ {}_n((\lambda_1 J_3), J_1||\ \mathcal{O}^{(k,B)}(m)\ ||(\lambda_2 J_4), J_2)_n. \tag{2.B.12} $$

For $n > m$ we can use (2.B.6c), getting

$$ {}_n((\lambda_1 J_3), J_1||\ \mathcal{O}^{(k,B)}(m)\ ||(\lambda_2 J_4), J_2)_n = \tag{2.B.13} $$
$$ \delta_{\lambda_1\lambda_2}(-1)^{\lambda_1+J_1+J_4+k}\sqrt{(2J_1+1)(2J_2+1)} \left\{ \begin{array}{ccc} J_3 & J_1 & \lambda_1 \\ J_2 & J_4 & k \end{array} \right\} {}_{n-1}(J_3||\ \mathcal{O}^{(k,B)}(m)\ ||J_4)_{n-1}. $$

Plugging (2.B.13) into (2.B.12) we get,

$$ {}_n(J_1||\mathcal{O}^{(k,B)}(m)||J_2)_n = \sum_{J_3 J_4} (T_k)_{J_1 J_2, J_3 J_4}\ {}_{n-1}(J_3||\mathcal{O}^{(k,B)}(m)||J_4)_{n-1},\ \ (n > m), \tag{2.B.14} $$

where $(T_k)_{J_1 J_2, J_3 J_4}$ is defined in (2.3.9). The term T_k^{n-m-1} in (2.3.7) results from the iteration of (2.B.14) until one gets $n = m$. In the case when $n = m$ in (2.B.13) we should apply (2.B.6b) obtaining

$$ {}_n((\lambda_1 J_3), J_1||\ \mathcal{O}^{(k,B)}(n)\ ||(\lambda_2 J_4), J_2)_n = \tag{2.B.15} $$
$$ \delta_{J_3 J_4}\ (-1)^{\lambda_1+J_2+J_3+k}\ \sqrt{(2J_1+1)(2J_2+1)}\ \left\{ \begin{array}{ccc} \lambda_1 & J_1 & J_3 \\ J_2 & \lambda_2 & k \end{array} \right\}\ {}_n(\lambda_1||\ \mathcal{O}^{(k,B)}(n)\ ||\lambda_2)_n. $$

Introducing (2.B.15) into (2.B.12) we get

$$ {}_n(J_1||\mathcal{O}^{(k,B)}(n)||J_2)_n = \sum_{J_3}\ \widehat{\mathcal{O}}^{(k,B)}_{J_1 J_2, J_3}, \tag{2.B.16} $$

where

$$ \begin{aligned} \widehat{\mathcal{O}}^{(k,B)}_{J_1 J_2, J_3} \ &= \ \sum_{\lambda_1\lambda_2} \left(A^{\lambda_1}_{J_1 J_3}\right)^*\ A^{\lambda_2}_{J_2 J_3}\ (-1)^{\lambda_1+J_2+J_3+k} \\ &\quad \times\sqrt{(2J_1+1)(2J_2+1)}\ \left\{ \begin{array}{ccc} \lambda_1 & J_1 & J_3 \\ J_2 & \lambda_2 & k \end{array} \right\} (\lambda_1||\mathcal{O}^{(k,B)}||\lambda_2). \end{aligned} \tag{2.B.17} $$

Recursion relation of the energy expectation values

We shall not give here the explicit proof of eq. (2.3.15) since it is quite analogous to the one performed in the previous paragraph. We shall simply state the result.

The matrix $\hat{h}_{J_1J_2}$ appearing in (2.3.15) is given by the sum

$$\hat{h}_{J_1J_2} = \hat{h}^{(1)}_{J_1J_2} + \hat{h}^{(2)}_{J_1J_2}, \tag{2.B.18}$$

where

$$\hat{h}^{(1)}_{J_1J_2} = J_\perp \sum_\lambda \left(\frac{1}{2}\lambda(\lambda+1) - S(S+1)\right) |A^\lambda_{J_1J_2}|^2 \tag{2.B.19a}$$

$$\hat{h}^{(2)}_{J_1J_4} = 2J_\parallel \sum_{J_2J_3,\lambda_1,\ldots,\lambda_4} (A^{\lambda_1}_{J_1J_2}A^{\lambda_3}_{J_2J_4})^* A^{\lambda_2}_{J_1J_3}A^{\lambda_4}_{J_3J_4}(-1)^{1+\lambda_3+\lambda_4}\, \xi^{\lambda_2\lambda_1}_{J_2J_3J_1}\, \xi^{\lambda_3\lambda_4}_{J_3J_2J_4} \tag{2.B.19b}$$

with

$$\begin{aligned}\xi^{\lambda_1\lambda_2}_{J_1J_2J_3} &= (-1)^{J_1+J_3}\sqrt{(2J_1+1)(2\lambda_1+1)(2\lambda_2+1)} \\ &\quad\times\sqrt{S(S+1)(2S+1)}\begin{Bmatrix} \lambda_1 & \lambda_2 & 1 \\ J_1 & J_2 & J_3 \end{Bmatrix}\begin{Bmatrix} \lambda_1 & \lambda_2 & 1 \\ S & S & S \end{Bmatrix},\end{aligned} \tag{2.B.20}$$

where the following property for the 6-j symbol with an element equal 1 has been used [29]:

$$\begin{Bmatrix} \lambda_1 & \lambda_2 & 1 \\ J_1 & J_2 & J_3 \end{Bmatrix} = \begin{Bmatrix} \lambda_2 & \lambda_1 & 1 \\ J_2 & J_1 & J_3 \end{Bmatrix}. \tag{2.B.21}$$

2.C The string order parameter of spin 1 chain and ladder

Spin 1 chain

Let us first consider the spin 1 chain. The MP ansatz is given simply by

$$|J_1M_1\rangle_N = \sum_{J_2} A_{J_1J_2}\, |(1J_2), J_1M_1\rangle_N, \tag{2.C.1}$$

where the state $|(1J_2), J_1M_1\rangle_N$ reads as in (2.3.2) with $\lambda = 1$. We shall choose half-integer values of the angular momenta J_1 and J_2 which amounts to have a spin 1/2 at one end of the chain [5, 7].

We shall next show that the operators $T = \widehat{1}$ and $e^{\widehat{i\pi S^z}}$ have both an eigenvalue equal to 1. Let us first of all write out explicitly their components,

$$\begin{aligned}(T)_{J_1M_1J_1'M_1',J_2M_2J_2'M_2'} &= \delta_{M_1-M_2,M_1'-M_2'}\ A_{J_1J_2}\ A_{J_1'J_2'} \qquad (2.C.2a)\\ &\quad\times\langle 1M_1-M_2, J_2M_2|J_1M_1\rangle\langle 1M_1'-M_2', J_2'M_2'|J_1'M_1'\rangle\end{aligned}$$

$$\begin{aligned}\left(e^{\widehat{i\pi S^z}}\right)_{J_1M_1J_1'M_1',J_2M_2J_2'M_2'} &= \delta_{M_1-M_2,M_1'-M_2'}\ (-1)^{M_1-M_2}\ A_{J_1J_2}\ A_{J_1'J_2'} \qquad (2.C.2b)\\ &\quad\times\langle 1M_1-M_2, J_2M_2|J_1M_1\rangle\langle 1M_1'-M_2', J_2'M_2'|J_1'M_1'\rangle.\end{aligned}$$

The normalisation conditions on $A_{J_1J_2}$ reads

$$\sum_{J_2} A^2_{J_1J_2} = 1 \quad , \quad \forall\ J_1. \qquad (2.C.3)$$

Using these equations and the properties of the CG coefficients, one can verify that v and $v^{\rm st}$ defined as

$$\begin{aligned}v_{J_1M_1J_1'M_1'} &= \delta_{J_1J_1'}\ \delta_{M_1M_1'} \qquad (2.C.4a)\\ v^{\rm st}_{J_1M_1J_1'M_1'} &= \delta_{J_1J_1'}\ \delta_{M_1M_1'}(-1)^{M_1-1/2} \qquad (2.C.4b)\end{aligned}$$

are right eigenvectors with eigenvalue 1 of the matrices T and $e^{\widehat{i\pi S^z}}$ respectively.

Similarly the left eigenvectors associated to this eigenvalue are given by

$$\begin{aligned}\rho_{J_1M_1J_1'M_1'} &= \delta_{J_1J_1'}\ \delta_{M_1M_1'}\ \rho_{J_1}/(2J_1+1) \qquad (2.C.5a)\\ \rho^{\rm st}_{J_1M_1J_1'M_1'} &= \delta_{J_1J_1'}\ \delta_{M_1M_1'}(-1)^{M_1-1/2}\ \rho_{J_1}/(2J_1+1), \qquad (2.C.5b)\end{aligned}$$

where ρ_J is the left eigenvector with eigenvalue 1 of the matrix $T_{J_1J_2} = A^2_{J_1J_2}$.

According to eq. (2.2.22) the string order parameter $g(\infty)$ is given by the product of two matrix elements which we compute below.

Let us first consider

$$\langle\rho|\widehat{S^z}|v^{\rm st}\rangle = \sum \rho_{J_1M_1J_1'M_1'}\ \widehat{S^z}_{J_1M_1J_1'M_1',J_2M_2J_2'M_2'}\ v^{\rm st}_{J_2M_2J_2'M_2'}. \qquad (2.C.6)$$

The hated version of S^z is given by

$$\begin{aligned}\left(\widehat{S^z}\right)_{J_1M_1J_1'M_1',J_2M_2J_2'M_2'} &= \delta_{M_1-M_2,M_1'-M_2'}\ (M_1-M_2)\ A_{J_1J_2}\ A_{J_1'J_2'} \qquad (2.C.7)\\ &\quad\times\langle 1M_1-M_2, J_2M_2|J_1M_1\rangle\langle 1M_1'-M_2', J_2'M_2'|J_1'M_1'\rangle,\end{aligned}$$

which together with (2.C.4b) and(2.C.5a) yields the expression for (2.C.6),

$$\langle\rho|\widehat{S^z}|v^{\rm st}\rangle = \sum \frac{\rho_{J_1}}{2J_1+1} A^2_{J_1J_2} (-1)^{M_2-1/2}\,(M_1-M_2)\,(\langle 1M_1-M_2, J_2M_2|J_1M_1\rangle)^2\,. \tag{2.C.8}$$

Similarly we get

$$\langle\rho^{\rm st}|\widehat{S^z}|v\rangle = \sum \frac{\rho_{J_1}}{2J_1+1} A^2_{J_1J_2}\,(-1)^{M_1-1/2}\,(M_1-M_2)\,(\langle 1M_1-M_2, J_2M_2|J_1M_1\rangle)^2\,. \tag{2.C.9}$$

Observing that

$$(-1)^{M_1-1/2}\,(M_1-M_2) = -(-1)^{M_2-1/2}\,(M_1-M_2), \tag{2.C.10}$$

where $M_1-M_2 = 0, \pm 1$, we obtain

$$\langle\rho^{\rm st}|\widehat{S^z}|v\rangle = -\langle\rho|\widehat{S^z}|v^{\rm st}\rangle, \tag{2.C.11}$$

which in turn implies

$$g(\infty) = -\left(\langle\rho|\widehat{S^z}|v^{\rm st}\rangle\right)^2. \tag{2.C.12}$$

Let us come back to eq. (2.C.8), which can be written as

$$\sum \frac{-\rho_{J_1}}{2J_1+1} A^2_{J_1J_2}\,(-1)^{M_1-1/2}\,\langle(1J_2)J_1M_1|S^z_1|(1J_2)J_1M_1\rangle, \tag{2.C.13}$$

where S^z_1 denotes the spin operator acting on the spin 1. Using the Wigner-Eckart theorem we get

$$\begin{aligned}\langle(1J_2)J_1M_1|S^z_1|(1J_2)J_1M_1\rangle &= (-1)^{J_1-M_1}\begin{pmatrix} J_1 & 1 & J_1 \\ -M_1 & 0 & M_1\end{pmatrix}((1J_2)J_1||\mathbf{S}_1||(1J_2)J_1) \\ &= \frac{M_1}{\sqrt{J_1(2J_1+1)(J_1+1)}}\,((1J_2)J_1||\mathbf{S}_1||(1J_2)J_1).\end{aligned} \tag{2.C.14}$$

The reduced matrix element appearing in (2.C.14) can be computed using (2.B.6b),

$$\begin{aligned}((1J_2)J_1||\mathbf{S}_1||(1J_2)J_1) &= \sqrt{6}\,(-1)^{J_1+J_2}\,(2J_1+1)\begin{Bmatrix} 1 & J_1 & J_2 \\ J_1 & 1 & 1\end{Bmatrix} \\ &= \frac{\sqrt{2J_1+1}\,(2+J_1(J_1+1)-J_2(J_2+1))}{2\sqrt{J_1(J_1+1)}}.\end{aligned} \tag{2.C.15}$$

Substituting (2.C.14) and (2.C.15) into (2.C.13) and performing the sum over M_1 with the aid of the formula

$$\sum_{M=-J}^{J} M(-1)^{M-\frac{1}{2}} = (J+\frac{1}{2})\,(-1)^{J-1/2} \quad , \quad (J : \text{half integer}) \tag{2.C.16}$$

we get finally

$$\langle\rho|\widehat{S^z}|v^{\rm st}\rangle = \frac{1}{4}\sum \rho_{J_1}\, A^2_{J_1 J_2}\,(-1)^{J_1-1/2}\,\frac{2+J_1(J_1+1)-J_2(J_2+1)}{J_1(J_1+1)}. \tag{2.C.17}$$

From eqs. (2.C.12) and (2.C.17) we immediately get the value of $g(\infty)$ in the AKLT case,

$$\text{AKLT} : A_{\frac{1}{2}\frac{1}{2}} = 1 \quad \longrightarrow \quad g(\infty) = -(2/3)^2. \tag{2.C.18}$$

In ref. [7] the spin 1 Heisenberg chain was studied with a MP ansatz built up with two states with $J = 1/2$ and $3/2$. The values of the MP parameters obtained in [7] are reproduced below.

$$\begin{aligned} A_{\frac{1}{2}\frac{1}{2}} &= 0.988995 & A_{\frac{1}{2}\frac{3}{2}} &= 0.14795 \\ A_{\frac{3}{2}\frac{1}{2}} &= -0.952887 & A_{\frac{3}{2}\frac{3}{2}} &= -0.303325 \\ \rho_{\frac{1}{2}} &= 0.97646 & \rho_{\frac{3}{2}} &= 0.023539. \end{aligned} \tag{2.C.19}$$

Introducing (2.C.19) into eqs. (2.C.12) and (2.C.17) we get $g(\infty) = -0.387$, which can be compared with the exact value given by -0.374325 [11]. In [5] the spin 1 chain was studied with a MP ansatz with two spin $1/2$ and two spin $3/2$ states, which yields $g(\infty) = -0.3759$. This shows again that MP ansatzs with multiplicity improve considerably the accuracy of the numerical results [5, 7].

Spin 1 2-legs ladder

Let us go now to the spin 1 ladder. In section 2.4 we gave an intuitive argument which suggested that the LRTO of the single spin 1 chains is destroyed by the interchain coupling. Next we show that this is indeed what happens.

Let us first write eqs. (2.C.2) in the case of ladders.

$$\begin{aligned} (T)_{J_1 M_1 J_1' M_1', J_2 M_2 J_2' M_2'} &= \delta_{M_1-M_2, M_1'-M_2'} \sum_{\lambda} A^{\lambda}_{J_1 J_2}\, A^{\lambda}_{J_1' J_2'} \\ &\quad \times \langle \lambda M_1 - M_2, J_2 M_2 | J_1 M_1\rangle \langle \lambda M_1' - M_2', J_2' M_2' | J_1' M_1'\rangle \end{aligned} \tag{2.C.20a}$$

$$\left(\widehat{e^{i\pi S_1^z}}\right)_{J_1M_1J_1'M_1',J_2M_2J_2'M_2'} = \delta_{M_1-M_2,M_1'-M_2'} \sum_{\lambda\lambda'} A^{\lambda}_{J_1J_2}\, A^{\lambda'}_{J_1'J_2'} \times\langle 1M_1-M_2, J_2M_2|J_1M_1\rangle\langle 1M_1'-M_2', J_2'M_2'|J_1'M_1'\rangle \times \langle \lambda M_1-M_2|e^{i\pi S_1^z}|\lambda' M_1M_2\rangle, \quad (2.C.20b)$$

where S_1^z denotes the spin operator acting on the first leg of the ladder. The vector $v_{J_1M_1J_1'M_1'}$ given in (2.C.4a) is an eigenvector with eigenvalue 1 of the matrix T defined by (2.C.20a). This property is a consequence of the normalisation condition (2.3.5). For the spin 1 chain the latter condition also guarantees the existence of an eigenvalue 1 of the operator (2.C.2b). However this is not generally the case for the operator (2.C.20b).

The last matrix element in (2.C.20b) can be deduced expressing the state $|\lambda\mu\rangle$ of the rung in terms of the spin 1 states of every site,

$$|\lambda\mu\rangle = \sum_{m_1m_2} |1m_1\rangle_1\, |sm_2\rangle_2\langle 1m_1 1m_2|\lambda\mu\rangle. \quad (2.C.21)$$

We thus get

$$\left(\widehat{e^{i\pi S_1^z}}\right)_{J_1M_1J_1'M_1',J_2M_2J_2'M_2'} = \delta_{M_1-M_2,M_1'-M_2'} \sum_{\lambda\lambda' m_1m_2} A^{\lambda}_{J_1J_2}\, A^{\lambda'}_{J_1'J_2'}(-1)^{m_1} \times\langle 1M_1-M_2, J_2M_2|J_1M_1\rangle\langle 1M_1'-M_2', J_2'M_2'|J_1'M_1'\rangle \times \langle 1m_1 1m_2|\lambda M_1-M_2\rangle\langle 1m_1 1m_2|\lambda' M_1-M_2\rangle \quad (2.C.22)$$

We can actually set up $M_1 = M_1'$ and $M_2 = M_2'$ in (2.C.22) since in the computation of the string order parameter, the third component of the angular momenta is preserved. We have computed the highest eigenvalue $x_{\rm st}$ of the matrix (2.C.22), which turns out to be smaller than one. This shows that $g(\ell)$ decays exponentially with a correlation length $\xi^{\rm st}$ whose value is obtained by the equation

$$\xi^{\rm st} = -1/\ln|x_{\rm st}|. \quad (2.C.23)$$

Bibliography

[1] K. G. Wilson, *Rev. Mod. Phys.* **47** (1975) 773.

[2] S. R. White, *Phys. Rev. Lett.* **69** (1992) 2863;

S. R. White, *Phys. Rev.* **B48** (1993) 10345.

[3] I. Affleck, T. Kennedy, E.H. Lieb and H. Tasaki, *Commun. Math. Phys.* **115** (1988) 477.

[4] A. Klümper, A. Schadschneider and J. Zittartz, *Europhyis. Lett.* **24** (1993) 293.

[5] S. Ostlund and S. Rommer, *Phys. Rev. Lett.* **75** (1995) 3537;

S. Rommer and S. Ostlund, *Phys. Rev.* **B55** (1997) 2164.

[6] M. Fannes, B. Nachtergaele and R.F. Werner, *Commun. Math. Phys.* **144** (1992) 443, (see references therein on the MPM).

[7] J. Dukelsky, M.A. Martín-Delgado, T. Nishino and G. Sierra, cond-mat/9710310.

[8] S. Brehmer, H.-J. Mikeska and U. Neugebauer, *J. Phys.: Cond. Matter* **8** (1996) 7161.

[9] E. Dagotto and T. M. Rice, *Science* **271** (1996) 618.

[10] M. den Nijs and K. Rommelse, *Phys. Rev.* **B40** (1989) 4709.

[11] S.R. White and D.A. Huse, *Phys. Rev.* **B48** (1993) 3844.

[12] T. Nishino and K. Okunishi, *J. Phys. Soc. Jpn.* **65** (1996) 891.

[13] H.J. Schulz, *Phys. Rev.* **B34** (1996) 6372.

[14] S. P. Strong and A. J. Millis, *Phys. Rev. Lett.* **69** (1992) 2419.

[15] D. G. Shelton, A. A. Nersesyan and A. M. Tsvelik, *Phys. Rev.* **B53** (1996) 8521.

[16] D. Senechal, *Phys. Rev.* **B52** (1995) 15319.

[17] G. Sierra, *J. Phys.* **A29** (1996) 3299.

[18] S. Dell'Aringa, E. Ercolessi, G. Morandi, P. Pieri and M. Roncaglia, *Phys. Rev. Lett.* **78** (1997) 2457.

[19] E. Dagotto, J. Riera and D. J. Scalapino, *Phys. Rev.* **B45** (1992) 5744.

[20] S. R. White, R. M. Noack and D. J. Scalapino, *Phys. Rev. Lett.* **73** (1994) 886.

[21] B. Frischmuth, B. Ammon and M. Troyer, *Phys. Rev.* **B54** (1996) R3714.

[22] M. Greven, R.J. Birgeneau and U.-J. Wiese, *Phys. Rev. Lett.* **77** (1996) 1865.

[23] S. Gopalan, T. M. Rice and M. Sigrist, *Phys. Rev.* **B49** (1994) 8901;
Corrected version by B. Normand and T. M. Rice cond-mat/9701202.

[24] G. Sierra, M.A. Martín-Delgado, *Phys. Rev.* **B56** (1997) 8774.

[25] T. Barnes, E. Dagotto, J. Riera and E. S. Swanson, *Phys. Rev.* **B47** (1993) 3196.

[26] K. Hida, *J. Phys. Soc. Jpn.* **60** (1991) 1347.

[27] G. Sierra, M.A. Martín-Delgado, *"Dualities in Spin Ladders"*, cond-mat/9706104, to appear in *J. Phys.* **A**.

[28] R.J. Creswick, H.A. Farach and C.P. Pooler, Jr., *"Introduction to Renormalization Group Methods in Physics"* (John Wiley and Sons, New York, 1992).

[29] D. A. Varshalovich, A. N. Moskalev and V. K. Khersonskii, *"Quantum Theory of Angular Momenta"*, World Scientific (1988).

[30] S. R. White, *Phys. Rev.* **B53** (1996) 52.

[31] H. Watanabe, *Phys. Rev.* **B52** (1995) 12508.

[32] *"Encyclopedic Dictionary of Mathematics"*, edited by S. Iyanaga and Y. Kawada (MIT Press, London, 1977).

Chapter 3

Continuum Double Exchange Model

We present in this chapter a continuum model for doped manganites which consist of two species of quantum spin 1/2 fermions interacting with classical spin fields. The phase structure at zero temperature turns out to be considerably rich: antiferromagnetic insulator, antiferromagnetic two band conducting, canted two band conducting, canted one band conducting and ferromagnetic one band conducting phases are identified, all of them being stable against phase separation. There is also a region in the phase diagram where phase separation occurs.

3.1 Introduction

Doped manganites $La_{1-x}A_xMnO_3$ (A divalent) [1] are receiving quite a lot of both theoretical [2, 3, 4, 5, 6, 7, 8, 9] and experimental [10] attention lately. These materials show an interesting interplay between magnetism and conductivity with intrincated phase diagrams which are still controversial.

In a cubic lattice the $3d$ orbitals of Mn split into a t_{2g} triplet and an upper e_g doublet. Due to the electronic repulsion and the Fermi statistics (Hund's rule) the three t_{2g} levels are always single occupied forming a core $S = 3/2$ spin. The e_g orbitals may be further splitted by a static Jahn-Teller distortion at small doping [11].

The above features are encoded in the so called double exchange models of different degrees of complexity. The simpler ones assume a strong Jahn-Teller distortion so that only the lower e_g level is consider. Hence there is a single fermion field in each site, with a spin independent hopping term and a local interaction with the core spin [4, 5]. Core spins also interact among themselves with the usual Heisenberg term. Under certain assumptions [12] the interaction with the core spin can be traded for an angle dependent hopping term [2, 13]. The next level of complexity consist of taking into account the two e_g levels [6, 7], and only very recently, the Jahn-Teller distortion has been incorporated dynamically by some authors [9].

It is the aim of this chapter to present a simple continuum model for doped manganites which also encodes the basic features above and, moreover, is exactly solvable for classical core spins. It produces a rich phase diagram which is in qualitative agreement with recent results and it shows, in addition, that stable canted phases exist. The main advantage with respect to previous approaches is that all the parameters of the material (lattice spacing, band curvature, Hund coupling, Heisenberg coupling and doping) combine into only two constants. This allows to present a two dimensional phase diagram which holds for a large amount of materials.

3.2 The Model

Cooperative phenomena are amenable of a field theoretical description. When the phenomena do not depend on the details of the microscopic system but only on its long wave length behaviour a continuum field theory description is appropriated. The field theoretical continuum model must contain the relevant degrees of freedom at

long wavelengths, which depend on the particular systems and phenomena that are to be studied. In our case, these are doped manganites and their phase diagram at zero temperature. These systems are known to undergo a number of phase transitions when the doping is increased. They are insulating antiferromagnets (AFI) at zero doping and become conducting ferromagnets (FC) at large enough doping. What happens between these two regimes is still controversial, though most of authors agree that the phase diagram is very rich and non-trivial. Early works on the subject suggested that an interesting intermediate conducting canted phase exists [13], but recent experimental [10] and theoretical [2, 4] results indicate that the canted phase appears to be unstable against phase separation.

Theoretical work on the subject is based on variations of the double exchange models. The phase structure of the system is obtained from these models using certain simplifying assumptions (slave boson formalism [2], trial wave functions [4],...) or extensive numerical simulations [9], the scope of which is difficult to evaluate. We present below a continuum field theoretical model which, as we shall argue, contains the relevant long wavelength degrees of freedom of the system. Then our main assumption is going to be that the rich phase diagram of manganites can be understood from long wavelength physics only. As the model is exactly solvable, there are no further uncertainties due to uncontrolled approximations.

Since we wish our model to include the well established AFI and FC phases, we need at least an AF order parameter field, a F order parameter field, and a $I-C$ order parameter field. For the AF and F order parameter fields we shall use $\mathbf{M}_1(x)$ and $\mathbf{M}_2(x)$ the local magnetisations in the even and odd sublattices respectively. Both in the AF and F phases these local magnetisations are smoothly varying fields. In the AF phase $\mathbf{M}_1(x)\mathbf{M}_2(x) \sim -1$ whereas in the F phase $\mathbf{M}_1(x)\mathbf{M}_2(x) \sim 1$. For the $I-C$ order parameter one could think of introducing a single slowly varying spin $1/2$ fermion field together with a chemical potential which regulates the doping. When the chemical potential is below the energy gap of the lowest spin state we have an I phase, when it overtakes this energy gap we have a one band C phase, and when it overtakes the energy gap of the highest spin state we have a two band C phase. However, a spin $1/2$ field naturally couples to the local magnetisation, which changes abruptly from the even to the odd sublattice in the AF phase. Hence in this phase a single spin $1/2$ field cannot be slowly varying over the system. We need at least two slowly varying spin $1/2$ fermionic fields, $\psi_1(x)$ which couples to the magnetisation in the even sublattice

$\mathbf{M}_1(x)$ and $\psi_2(x)$ which couples to the magnetisation in the odd sublattice $\mathbf{M}_2(x)$. Since the conductivity is due to fermions moving from one sublattice to the other one a (spin independent) hopping term is introduced. The allowed values of the chemical potential will be limited by the physical condition that no conduction must exist when the hopping parameter vanishes.

The model must be $SU(2)$ spin invariant since the magnetic interactions emerge from the usual superexchange mechanism together with the Hund's rule. The space-time symmetries of the underlying crystal must also be impleted and will be the only remain of the microscopic lattice structure. For simplicity we shall take a cubic lattice and comment later on the slight modifications that occur for other crystals.

The lagrangian of the model reads

$$\begin{aligned}\mathcal{L}(x) &= \psi_1^\dagger(x)\left[(1+i\epsilon)i\partial_0 + \frac{\partial_i^2}{2m} + \mu + J_H\frac{\boldsymbol{\sigma}}{2}\mathbf{M}_1(x)\right]\psi_1(x) \\ &\quad + \psi_2^\dagger(x)\left[(1+i\epsilon)i\partial_0 + \frac{\partial_i^2}{2m} + \mu + J_H\frac{\boldsymbol{\sigma}}{2}\mathbf{M}_2(x)\right]\psi_2(x) \\ &\quad + t\left(\psi_1^\dagger(x)\psi_2(x) + \psi_2^\dagger(x)\psi_2(x)\right) - J_{AF}\mathbf{M}_1(x)\mathbf{M}_2(x).\end{aligned} \tag{3.2.1}$$

The size of the parameters in the model are estimated by comparing them with the naïve continuum limit of lattice double exchange models. For a cubic lattice we have $2m \sim 1/a^2t^l$, $t \sim zt^l$, $J_H \sim J_H^l$ and $J_{AF} \sim zJ_{AF}^l/a^3 > 0$, where a is the lattice spacing, $z = 6$ is the coordination number and the superscript l means the analogous lattice quantity. The fields $\psi_i(x)$ may describe either electrons or holes. Since the conduction in actual doped manganites is due to holes, one should better figure out $\psi_i(x)$ as hole annihilating fields. Recall that for holes J_H is negative whereas it is positive for electrons. This sign however is going to be irrelevant as far as the phase diagram is concerned.

The lagrangian above is invariant under the following transformations:

(i) Global $SU(2)$ spin transformations,

$$\begin{aligned}\psi_i(x) &\longrightarrow g\psi_i(x) \\ M_i^a(x) &\longrightarrow R_b^a M_i^b(x),\end{aligned} \qquad (i=1,2) \tag{3.2.2}$$

(ii) Primitive translations,

$$\begin{aligned}\psi_1(x) &\longrightarrow \psi_2(x) \qquad \psi_2(x) \longrightarrow \psi_1(x) \\ \mathbf{M}_1(x) &\longrightarrow \mathbf{M}_2(x) \qquad \mathbf{M}_2(x) \longrightarrow \mathbf{M}_1(x),\end{aligned} \tag{3.2.3}$$

(iii) Point group transformations, given by the group $m\bar{3}m$

$$\begin{array}{rcl} \psi_i(x) & \longrightarrow & g_\xi \psi_i(\xi^{-1}x) \\ M_i^a(x) & \longrightarrow & R_b^a(\xi) M_i^b(\xi^{-1}x) \end{array} \qquad (i=1,2), \tag{3.2.4}$$

when the point group transformation ξ maps points in the same sublattice, and

$$\begin{array}{rcl} \psi_1(x) & \longrightarrow & g_\xi \psi_2(\xi^{-1}x) \\ M_1^a(x) & \longrightarrow & R_b^a(\xi) M_2^b(\xi^{-1}x) \end{array} \qquad \begin{array}{rcl} \psi_2(x) & \longrightarrow & g_\xi \psi_1(\xi^{-1}x) \\ M_2^a(x) & \longrightarrow & R_b^a(\xi) M_1^b(\xi^{-1}x), \end{array} \tag{3.2.5}$$

when the transformation ξ maps points of different sublattices. Anyway, the rotations g_ξ and $R_b^a(\xi)$ can be absorbed by a $SU(2)$ transformation and the change of sublattice in (3.2.5) by a primitive translation. Hence, in practice, we only have to care about the transformation of the coordinates.

(iv) Time reversal,

$$\begin{array}{rcl} \psi_i(x) & \longrightarrow & C\psi_i^*(Tx) \\ \mathbf{M}_i(x) & \longrightarrow & -\mathbf{M}_i(Tx) \end{array} \qquad C = e^{-i\pi\sigma^2/2} = -i\sigma^2 \quad , \quad (i=1,2), \tag{3.2.6}$$

where $Tx = (-t, \mathbf{x})$.

3.3 Effective Potential

In order to find out how the ground state of the system changes as a function of the chemical potential, we shall calculate the effective potential and minimise it with respect to the order parameters $\mathbf{M}_1$ and $\mathbf{M}_2$. We shall assume that the ground state configuration corresponds to constant magnetisations both in the odd and even sublattices. Hence, the effective potential is to be minimised with respect to the angle θ between $\mathbf{M}_1$ and $\mathbf{M}_2$ only. We use $y = \cos(\theta/2)$. When $y = 0$, $0 < y < 1$ and $y = 1$ we have an antiferromagnetic, canted and ferromagnetic phase respectively.

The effective potential is obtained by integrating out the fermion fields in the path integral, and it is formally given by

$$V_{\mathit{eff}} = J_{AF}\mathbf{M}_1\mathbf{M}_2 + itr\log\hat{O}/VT, \tag{3.3.1}$$

where

$$\hat{O} = \begin{pmatrix} (1+i\epsilon)i\partial_0 + \partial_i^2/2m + \mu + \frac{J_H}{2}\boldsymbol{\sigma}\mathbf{M}_1 & t \\ t & (1+i\epsilon)i\partial_0 + \partial_i^2/2m + \mu + \frac{J_H}{2}\boldsymbol{\sigma}\mathbf{M}_2 \end{pmatrix}, \tag{3.3.2}$$

and the trace is both on spin indices and space-time coordinates. VT is the volume of the space-time.

If $\hat{O}$ has eigenvalues λ_n

$$tr \log \hat{O} = \sum_n \log \lambda_n. \tag{3.3.3}$$

We have then to diagonalise the operator $\hat{O}$. Since it contains only constant fields the diagonalisation with respect to the space-time is trivially attained by plane waves. The diagonalisation with respect to the spin indices is a simple linear algebra problem. We obtain

$$\lambda_n = O_i(q) \;=\; (1 + i\epsilon)\,\omega - \frac{\mathbf{k}^2}{2m} - \Omega_i \tag{3.3.4}$$

$$\Omega_i \;=\; \pm\frac{|J_H|M}{2}\sqrt{1 + \gamma^2 \pm 2\gamma\cos\frac{\theta}{2}} - \mu \quad , \quad \gamma \equiv \frac{2t}{|J_H|M}. \tag{3.3.5}$$

$q = (\omega, \mathbf{k})$ and $M = |\mathbf{M}_1| = |\mathbf{M}_2| = 3/2$. The restriction for the values of the chemical potential in the model implies that at most the two lower eigenvalues in (3.3.5) may contribute. This motivates the following reparametrisation of the chemical potential:

$$\mu = -\frac{|J_H|M}{2}\sqrt{1 + \gamma^2 - 2\gamma y_0} \qquad (-1 < y_0 < y_0^{max} = \gamma/2), \tag{3.3.6}$$

which eases comparison with the energy levels in (3.3.5) ($y = \cos(\theta/2)$). In order to simplify the analysis we assume γ small and keep only linear terms in γ in the relevant eigenvalues above. Namely,

$$\Omega_i = -\frac{|J_H|M}{2}\,\gamma\,(y_0 \pm y). \tag{3.3.7}$$

This is justified for $t \ll J_H$, as it turns out to be the case for the actual materials [14]. Anyway, this simplification can be lifted with the only drawback that the few analytic expressions below must also be substituted by numerical analysis.

In order to calculate the sum (3.3.3) we have used ζ-function techniques [15], which are explained in the appendix. We obtain the effective potential (for $\mu < 0$)

$$V_{\mathit{eff}} = V_0\left[(2y^2 - 1) - A\left((y_o + y)^{5/2}\theta(y_0 + y) + (y_0 - y)^{5/2}\theta(y_o - y)\right)\right], \tag{3.3.8}$$

where we have defined

$$V_0 = J_{AF}M^2 \qquad , \qquad A = \frac{(2m)^{3/2}\,t^{5/2}}{15\pi^2 J_{AF}M^2} = \frac{z^{3/2}\,t}{15\pi^2(J_{AF}a^3M^2)}. \tag{3.3.9}$$

3.4 Phase Structure

The possible phases of the model are obtained by minimising (3.3.8) with respect to y for the different values of the parameters A and y_0. The number of conducting bands is given by the number of θ-functions in (3.3.8) which contribute to the effective potential at the minimum.

In order to gain some qualitative understanding and to make the minimisation procedure systematic we shall first separate the cases $y_0 < 0$ and $y_0 > 0$. For each case we shall work out the stability conditions for AF ($y = 0$), canted ($0 < y < 1$) and F ($x = 1$) phases. After that we shall compare the energy of the stable phases and obtain the curves which separate them.

The stability conditions are given for the different phases by

$$\begin{aligned} AF: &\quad V'_{\mathit{eff}}(0) > 0 \quad or \quad V'_{\mathit{eff}}(0) = 0 \;\; V''_{\mathit{eff}}(0) > 0 \\ C: &\quad V'_{\mathit{eff}}(y_c) = 0 \;\; V''_{\mathit{eff}}(y_c) > 0 \\ F: &\quad V'_{\mathit{eff}}(1) < 0. \end{aligned} \tag{3.4.1}$$

Let us then consider first the case $y_0 < 0$. Clearly for $y_0 < -1$ the unique existing phase is the AFI phase. In the case $-1 < y_0 < 0$ only the lowest of the four spin eigenvalues may contribute to the effective potential. The stability conditions yield the following stable phases:

$$\begin{aligned} AFI: &\quad y = 0 \\ FC: &\quad y = 1 \qquad A(1+y_0)^{3/2} > 8/5. \end{aligned} \tag{3.4.2}$$

The canted phase is not stable as it can be seen from the condition $V'_{\mathit{eff}}(y_c) = 0$,

$$y_c = \frac{5}{8} A (y_0 + y_c)^{3/2}, \tag{3.4.3}$$

which has at most one solution $y_c \in [-y_0, 1]$. Since V_{eff} is continuous, and increasing at $y = 0$ this solution must be a maximum when it exists.

The curve $V_{\mathit{eff}}(0) = V_{\mathit{eff}}(1)$ in the plain (y_0, A), which separates the AF and F phases, reads

$$A(1+y_0)^{5/2} = 2 \qquad (-1 < y_0 < 0). \tag{3.4.4}$$

Above this curve the F phase is favored against the AF phase and viceversa.

Consider next the case $0 < y_0 < 1$. The stability conditions are given by

$$\begin{array}{lcll} AFC2: & y=0 & Ay_0^{1/2} < 8/15 & \\ CC2: & 5A(y_c^2+3y_0^2)/4 = (y_0+y_c)^{3/2}+(y_0-y_c)^{3/2} & 8/15 < Ay_0^{1/2} < 2\sqrt{2}/5 & \\ CC1: & y_c = 5A(y_0+y_c)^{3/2}/8 & Ay_0^{1/2} > 2\sqrt{2}/5 & (3.4.5) \\ FC1: & y=1 & A(1+y_0)^{3/2} > 8/5, & \end{array}$$

where $AFC2$, $CC2$, $CC1$ and $FC1$ stand for antiferromagnetic two band conducting, canted two band conducting, canted one band conducting and ferromagnetic one band conducting respectively. Notice that AF and canted phases do not compete among them, but only with the F phase. The curves providing the boundary between the different phases are given by

$$\begin{array}{lcll} AFC2-FC1: & A[(1+y_0)^{5/2}-2y_0^{5/2}]=2 & 0<y_0<0.127 & \\ AFC2-CC2: & Ay_0^{1/2}=8/15 & 0.127<y_0<1 & \\ CC2-FC1: & 5A(y_2^2+3y_0^2)/4=(y_0+y_2)^{3/2}+(y_0-y_2)^{3/2} & 0.127<y_0<0.168 & \\ CC2-CC1: & Ay_0^{1/2}=2\sqrt{2}/5 & 0.168<y_0<1 & (3.4.6) \\ CC1-FC1: & 5A(y_0+y_1)^{3/2}/8=y_1 & 0.168<y_0<0.5 & \\ CC1-FC1: & 5A(1+y_0)^{3/2}/8=1 & 0.5<y_0<1, & \end{array}$$

where y_1 and y_2 are given implicitly by the equations

$$\begin{aligned} &[(1+y_0)^{5/2}-(y_0+y_2)^{5/2}-(y_0-y_2)^{5/2}][(y_0+y_2)^{3/2}+(y_0-y_2)^{3/2}] = \\ &\qquad \frac{5}{2}(1-y_2^2)(y_2^2+3y_0^2) \end{aligned}$$

$$\begin{aligned} &(y_1+y_0)^{5/2}+2(1+y_0)^{1/2}(y_1+y_0)^2 \\ &\qquad +3(1-y_0)(y_1+y_0)^{3/2}+4(1-2y_0)(1+y_0)^{1/2}(y_1+y_0) \\ &\qquad -8y_0(1+y_0)(y_1+y_0)^{1/2}-4y_0(1+y_0)^{3/2}=0. \end{aligned} \tag{3.4.7}$$

The outcome is plotted in fig. 3.1.

Recall that fig. 3.1 actually does not plot a phase diagram against doping but against y_0 which is related to the chemical potential rather than to the number of conducting fermions or doping. Recall also that V_{eff} is to be regarded as a (zero temperature) grand canonical potential rather than as a free energy. The doping is introduced via

$$x = -a^3\,\frac{\partial V_{\mathit{eff}}}{\partial \mu} = -\frac{a^3}{t}\,\frac{\partial V_{\mathit{eff}}}{\partial y_0} \tag{3.4.8}$$

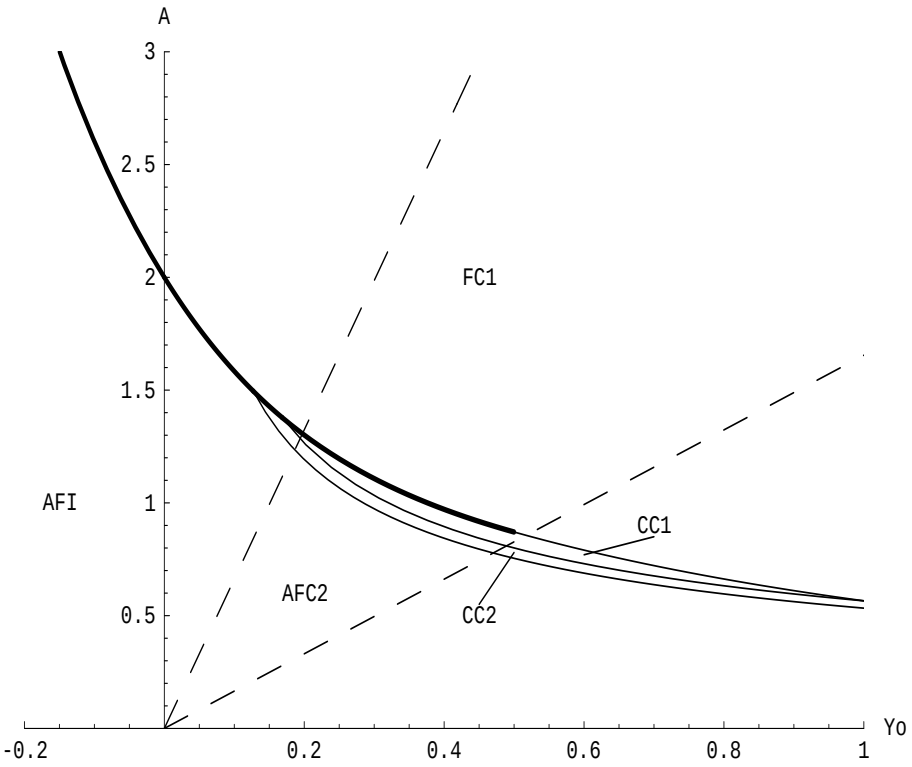

Figure 3.1. Phase diagram in the (y_0, A) plane. The thick solid line corresponds to first order transitions whereas the remaining solid lines to second order ones. The two dashed lines are the boundaries for the reliability of our model for $z|J_H|M/2(J_{AF}a^3M^2) \sim 50 - 200$.

provided that one molecule exists per unit cell with a lattice parameter a. Taking into account (3.3.9) the doping corresponding to the different phases reads

$$\begin{aligned}
AFI: \quad x &= 0 \\
AFC2: \quad x &= \frac{z^{3/2}}{6\pi^2}\, 2y_0^{3/2} \\
CC2: \quad x &= \frac{z^{3/2}}{6\pi^2}\, [(y_0+y)^{3/2} + (y_0-y)^{3/2}] \\
CC1: \quad x &= \frac{z^{3/2}}{6\pi^2}\, (y_0+y)^{3/2} \\
FC1: \quad x &= \frac{z^{3/2}}{6\pi^2}\, (1+y_0)^{3/2}.
\end{aligned} \tag{3.4.9}$$

where the y_c for the $CC2$ and $CC1$ phases are given in (3.4.5).

These expressions for the doping permit us to establish that all our phases are thermodynamically stable, unlike the ones observed in ref. [3, 4]. This is easily proven from the stability condition $\partial\mu/\partial x > 0$. For the F and AF phases this is trivially obtained, whereas canted phases are stable if they are below the curves

$$\begin{aligned} CC2: \quad & 5Ay/3 = (y_0+y)^{1/2} - (y_0-y)^{1/2} \\ & y^2 - 5y_0^2 + 4y_0(y_0^2-y^2)^{1/2} = 0 \qquad (y < y_0) \\ CC1: \quad & Ay_0^{1/2} = 16/15\sqrt{3}. \end{aligned} \tag{3.4.10}$$

This is always the case as it can be shown by plotting these curves in fig. 3.1.

Once we have the expressions (3.4.9) for the doping it is straightforward to translate fig. 3.1 to a more conventional phase diagram where the doping, x, appears in one of the axes. This is given in fig. 3.2 (recall $z = 6$).

It is interesting to notice that in fig. 3.2 a new region arises, which we have denoted PS, between the $FC1$, AFI, $AFC2$, $CC2$ and $CC1$ phases. This is due to the fact that the solid line separating $FC1$ and AFI, $AFC2$, $CC2$ and $CC1$ in fig. 3.1 corresponds to a first order phase transition and the chemical potential cannot be traded by the doping. This region may consist of coexisting domains where the various phases at the boundary are realised (phase separation), in particular AFI and $FC1$ as it has been observed in recent works [3, 4].

As mentioned in section 3.3, the fact that for $t = 0$ we do not permit conductivity restricts the values that chemical potential takes to $y_0 < y_0^{max} = \gamma/2$. By substituting this expression in A we obtain

$$A = \frac{z^{3/2}\,|J_H|M}{15\pi^2(J_{AF}a^3M^2)}\; y_0^{max}. \tag{3.4.11}$$

a curve of validity for our results, that turns out to be a straight line provided that J_H and J_{AF} remain constant as y_0^{max} moves. Only the phase diagram to the left of this curve is trustworthy.

We take a range of values for the coupling constants $t/(J_{AF}a^3M^2) \sim 10 - 20$ and $z|J_H|M/2(J_{AF}a^3M^2) \sim 50 - 200$, which is compatible with the values given in the literature. From these values $A \sim 1-2$ and the two validity straight lines are displayed in fig. 3.1.

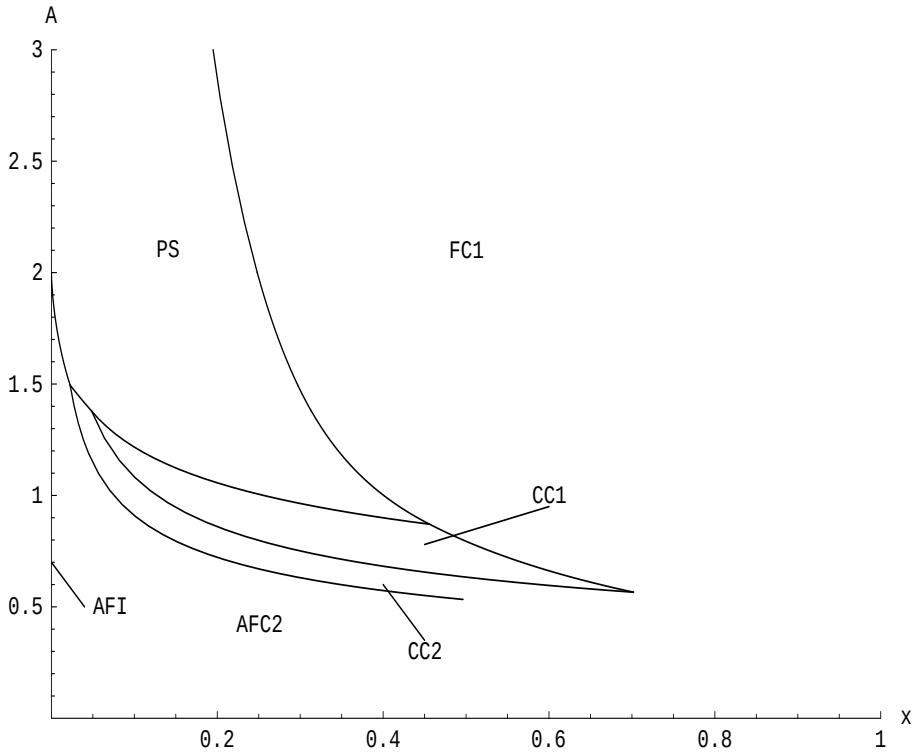

Figure 3.2. Phase diagram in the (x, A) plane. PS indicates the new region where the phases at its boundary may coexist. The $x = 0$ axis corresponds to the AFI phase.

3.5 Conclusions

We have presented a simple model in the continuum which is able to describe the rich phase structure of doped manganites for a wide range of these materials.

We have assumed an underlying cubic crystal for simplicity. Nevertheless, the orthorhombic distortion can be easily accommodated by the following simple changes in the physical parameters: $m^3 \to m_x m_y m_z$, $a^3 \to abc$, $J_{AF} \to J_x + J_y + J_z$ and $t \to t_x + t_y + t_z$. In practice this does not modify our results since it would only lead to a different A, which is anyway a free parameter in our phase diagrams. This fact also suggests that the structural transitions that these materials undergo when increasing the doping [14] are not essential in order to understand the $F - AF$ and $I - C$ transitions.

An important feature of our results is that the two canted phases that we observe are stable against phase separation, unlike in some previous works [3, 4]. We also

observe a region in the phase diagram where phase separation may occur. If we plug realistic values for the physical parameters we find $A \sim 1 - 2$. This means that upon increasing x we may go from the AFI to the $FC1$ phase through the stable canted phases or not depending on the actual values of the parameters, which could explain the controversial results obtained by different authors.

Let us also mention that the two fermion fields $\psi_1(x)$ and $\psi_2(x)$ accommodate the e_g doublet in our model. Indeed in the AF phase the two lower and two higher eigenvalues (3.3.4) are degenerated. In the F and C phases the degeneracy is lifted. This implies that the splitting between the two e_g levels receives a contribution from the dynamics of the conducting fermions in addition to that from the static Jahn-Teller distortion.

The model can be used in the future to study the temperature dependence of the phase diagram. Fluctuations due to spin waves in all the phases (including the canted ones) can also be incorporated [16]. It would also be interesting to see if the model can be generalised to accommodate the Jahn-Teller distorsion dynamically.

3.A ζ-function Techniques

The ζ-function techniques provide a very efficient way to calculate the trace of the logarithm of operators [15]. The ζ-function associated to an operator $\hat{O}$ is defined as

$$\zeta_{\hat{O}}(s) \equiv tr\hat{O}^{-s} = \sum_n \lambda_n^{-s}. \tag{3.A.1}$$

Then

$$\sum_n \log \lambda_n = -\left.\frac{d}{ds}\,\zeta_{\hat{O}}(s)\right|_{s=0}. \tag{3.A.2}$$

Consider the operator $\hat{O}$ in (3.3.2). Once the spin diagonalisation is performed we only have to consider the space-time trace over a generic spin eigenvalue denoted by $\hat{O}_i$. Since the real part of the operator $-i\hat{O}_i$ is positive for positive energies and negative for negative ones, due to the term $i\epsilon\omega$ in (3.3.4), it is convenient to consider the integral form of $\zeta_{\hat{O}}(s)$ over positive and negative energies of separately.

$$tr[(\hat{O}_i\theta(-\omega))^{-s}] = \frac{(-i)^{-s}}{\Gamma(s)}\int_0^\infty d\tau\tau^{s-1}\int_{-\infty}^0 \frac{dw}{2\pi}\frac{d^3\mathbf{k}}{(2\pi)^3}\,e^{-iO_i(q)\tau}\,VT \tag{3.A.3a}$$

$$tr[(\hat{O}_i\theta(\omega))^{-s}] = \frac{i^{-s}}{\Gamma(s)}\int_0^\infty d\tau\tau^{s-1}\int_0^\infty \frac{dw}{2\pi}\frac{d^3\mathbf{k}}{(2\pi)^3}\,e^{iO_i(q)\tau}\,VT. \tag{3.A.3b}$$

After the energy and momentum integration we obtain the expressions

$$tr[(\hat{O}_i\theta(-\omega))^{-s}] = \frac{VT}{16\pi}\left(\frac{2m}{\pi}\right)^{3/2}\frac{\Gamma(s-5/2)}{\Gamma(s)}\,(-i)^{-s-5/2}(-i\Omega_i)^{s+5/2} \tag{3.A.4a}$$

$$tr[(\hat{O}_i\theta(\omega))^{-s}] = -\frac{VT}{16\pi}\left(\frac{2m}{\pi}\right)^{3/2}\frac{\Gamma(s-5/2)}{\Gamma(s)}\,(-i)^{s+5/2}(i\Omega_i)^{-s+5/2}. \tag{3.A.4b}$$

We need the derivative of the above with respect to s at $s=0$. The presence of $1/\Gamma(s)\sim s$ makes the evaluation very easy, giving rise to

$$-\left.\frac{d}{ds}\,\zeta_{\hat{O}}(s)\right|_{s=0} = \frac{VT(2m)^{3/2}}{30\pi^2}\left[i^{5/2}(-i\Omega_i)^{5/2} - (-i)^{5/2}(i\Omega_i)^{5/2}\right]. \tag{3.A.5}$$

The expression between square brackets vanishes when $\Omega_i > 0$, i.e., when the chemical potential is bellow the energy of the i-th state, and is non zero when $\Omega_i < 0$, i.e., when the chemical potential is above the energy of the i-th state. This leads to the effective potential (for $\mu < 0$, $y_0 < y_0^{max} < 1$)

$$V_{eff} = V_0 \left[(2y^2 - 1) - \frac{A}{\gamma^{5/2}} \left[\left(\sqrt{1 + \frac{2\gamma y}{1+\gamma^2}} - \sqrt{1 - \frac{2\gamma y_0}{1+\gamma^2}} \right)^{5/2} \theta(y_0 + y) \right. \right. \quad \text{(3.A.6)}$$
$$\left. \left. + \left(\sqrt{1 - \frac{2\gamma y}{1+\gamma^2}} - \sqrt{1 - \frac{2\gamma y_0}{1+\gamma^2}} \right)^{5/2} \theta(y_0 - y) \right] \right],$$

where $y = cos(\theta/2)$, whereas γ, y_0, and V_0 are defined in (3.3.5), (3.3.6) and (3.3.9) respectively.

$$A = \frac{(2m)^{3/2}}{15\pi^2 J_{AF} M^2} \left(t \sqrt{1+\gamma^2} \right)^{5/2}. \quad \text{(3.A.7)}$$

Eq. (3.3.7) follows from the above by keeping only terms linear in γ.

Bibliography

[1] G. H. Jonker and J. H. Van Santen, *Physica* **50** (1950) 337.

[2] D. P. Arovas and F. Guinea, *"Phase Diagram of Doped Manganates"*, cond-mat/9711145.

[3] D. P. Arovas, G. Gómez-Santos and F. Guinea, *"Phase Separation in Double Exchange Systems"*, cond-mat/9805399.

[4] M. Yu Kagan, D. I. Khomskii and M. Mostovoy, *"Canted Spin or Phase Separation in the Double-Exchange Model"*, cond-mat/9804213.

[5] L.-J. Zou, Q.-Q. Zheng and H. Q. Liu, *Phys. Rev.* **B56** (1997) 13669.

[6] A. J. Millis, P. B. Littlewood and B. I. Shraiman, *Phys. Rev. Lett.* **75** (1995) 5144.

[7] R. Maezono, S. Ishihara and N. Nagaosa, *"Phase Diagram in Manganese Oxides"*, cond-mat/9805267.

[8] D. I. Golosov, M. R. Norman and K. Levin, *"On the Theory of Magnets with Competing Double Exchange and Superexchange Interactions"*, cond-mat/9805238.

[9] S. Yunoki, A. Moreo and E. Dagotto, *"Phase Separation Induced by Orbital Degrees of Freedom in Models for Manganites with Jahn-Teller Phonons"*, cond-mat/9807149.

[10] J. W. Lynn *et al.*, *Phys. Rev. Lett.* **76** (1996) 4046;

Y. Yamada *et al.*, *Phys. Rev. Lett.* **77** (1996) 904;

G. Allodi *et al.*,*Phys. Rev.* **B56** (1997) 6036;

J. M. De Teresa *et al.*, *Phys. Rev.* **B57** (1998) 3305;

M. Hennion *et al.*, cond-mat/9806272;

Wei Bao *et al.*, *Solid State Comm.* **98** (1996) 55.

[11] C. Zener, *Phys. Rev.* **82** (1951) 403.

[12] P. W. Anderson and H. Hasegawa, *Phys. Rev.* **100** (1955) 675.

[13] P. G. De Gennes *Phys. Rev.* **118** (1960) 141.

[14] A. P. Ramirez, *J. Phys.: Cond. Matter* **9** (1997) 8171.

[15] E. Elizalde *et al.*, *"Zeta Regularization Techniques with Applications"*, (World Scientific Cop., Singapore, 1994).

[16] J.M. Román and J. Soto, *"Spin Waves in Canted Phases"*, in preparation, preprint no. UB-ECM-PF 98/19.

Chapter 4

Effective Field Theory Approach to Ferromagnets and Antiferromagnets in Crystalline Solids

In this chapter we present a systematic derivation of effective lagrangians for the low energy and momentum region of ferromagnetic and antiferromagnetic spin waves in crystalline solids. We fully exploit the spontaneous symmetry breaking pattern $SU(2) \to U(1)$, the fact that spin waves are its associated Goldstone modes, the crystallographic space group and time reversal symmetries. We show how to include explicit $SU(2)$ breaking terms due to spin-orbit and magnetic dipole interactions. The coupling to electromagnetic fields is also discussed in detail. For definiteness we work with the crystal point group $\bar{3}m$ and present our results to next to leading order.

4.1 Introduction

Whenever we have a lagrangian (hamiltonian) describing an infinite number of degrees of freedom with a given symmetry group G the ground state of which has a smaller symmetry group H, we say that we are in a situation of spontaneous symmetry breaking (SSB, long range diagonal order). If in addition the symmetry corresponds to a continuous group we have gapless excitations. This is a consequence of the Goldstone's theorem, which was first proven for relativistic quantum field theories in [1], and then extended to nonrelativistic (condensed matter) systems [2, 3, 4]. We shall call Goldstone modes to the lowest lying (gapless) excitations. In particle physics these correspond to massless particles and are known as Goldstone bosons. For instance in strong interaction physics, pions and kaons are the approximate Goldstone bosons of the approximate flavor $G = SU(3)_L \otimes SU(3)_R$ chiral symmetry of the QCD lagrangian which breaks spontaneously down to its vector part $H = SU(3)_V$ [5]. In condensed matter (CM) Goldstone modes appear in a large variety of systems describing quite distinct physics. Among the popular ones, which we shall be concerned with in the rest of the chapter, are the magnons or spin waves in ferromagnets and antiferromagnets. These correspond to a $G = SU(2)$ spin symmetry being broken down to $H = U(1)$. Two more examples are the sound waves in a superfluid which correspond to the spontaneous breaking down of the $G = U(1)$ particle number conservation to $H = Z_1$, and the phonons in a crystal which are the Goldstone modes of the $G = T_3$ continuous translational symmetry to the discrete group H of primitive translations of the crystal [6].

If one probes a physical system in the SSB phase by external sources (e.g. electromagnetic waves) with small energy and momentum at low temperatures, the only relevant degrees of freedom are the Goldstone modes. There is a systematic way to write down an effective lagrangian describing the dynamics of the Goldstone modes which only depends on the symmetry breaking pattern. For relativistic theories this is known from the late 60's [7], but it has only been used extensively to next to leading order for the last ten years [8] (see [9] for a review). It has been pointed out that the same techniques can be applied to condensed matter systems [6], and lagrangians to the lowest order have been provided for the ferromagnetic and antiferromagnetic spin waves, and phonons [10]. In fact for antiferromagnetic spin waves the effective lagrangian at leading and next to leading order has already been used in [11] and [12]

respectively. At the moment it is unclear whether these techniques may help in general to a better understanding of certain CM phenomena, or will be just an innocuous rephrasing of a more conventional CM language. The power of these techniques relies on the fact that one can make a *controlled* expansion for any observable in terms of the typical energy and momentum of the Goldstone modes over the typical energy and momentum of the first gapped excitation. The lagrangian is thus organised in terms of time and space derivatives. For a given precision we only have to take into account derivatives until a given order. Then the lagrangian is a function of a few universal unknown constants which may be obtained from experimental data and be used later on to predict further experimental results. We believe it is worth trying to implement these techniques in realistic CM systems and test whether they allow for an efficient description of interesting phenomena, as it is the case in particle physics, or not.

We shall concentrate on ferromagnetic and antiferromagnetic systems. We wish to illustrate how the effective lagrangian for the spin waves can be built to next to leading order. This order is specially interesting because the symmetries of the crystal start playing an important role. We will also show how the electromagnetic interactions can be included in the effective lagrangian. We will restrict ourselves to the space group $R\bar{3}c$, whose crystallographic point group is $\bar{3}m$, for definiteness, but it will be clear at any stage how to proceed for any other crystallographic group. In the next chapter [13] these results will be applied to calculate the contribution of the spin waves to various (non-linear) electric and magnetic susceptibilities, in particular those leading to non-reciprocal effects in second harmonic generation and gyrotropic birefringence, in the microwave region.

In order to simplify the notation we will take $\hbar = c = 1$ which leads to a relativistic notation. So $x_i = (t, \mathbf{x}_i)$, where subindex i represents a lattice position, subindices $\mu = 0, 1, 2, 3$, where the first one represents the time component. the chapter is distributed as follows. In section 4.2 we describe the basic fields and symmetries. In section 4.3 we explain how to systematically construct the effective lagrangian to a given order of space and time derivatives. In sections 4.4 and 4.5 we present the effective lagrangian to next-to-leading order for the ferromagnet and antiferromagnet respectively. In sections 4.6 and 4.7 we show how to include $SU(2)$ breaking and magnetic dipole interactions respectively. In section 4.8 the coupling to electromagnetic fields is included. Section 4.9 is devoted to a discussion of our results. In appendix 4.A we discuss the effect of non-trivial primitive translations in antiferromagnets. Appendix 4.B

contains technical details. In appendix 4.C we show some particular features for the fundamental representation, $s = 1/2$. Appendix 4.D contains a proof of the equivalence between our formulation and the so-called $O(3)$-*sigma model* as well as a brief comment on the different forms that a certain topological term can be found in the literature. In appendix 4.E we show how constant electric and magnetic fields modify the spin wave dispersion relation.

4.2 Effective Fields and Crystal Symmetries

4.2.1 Internal symmetries

When G is a compact internal symmetry group, namely a compact group disentangled from the space-time symmetry group, a general analysis was provided in ref. [7]. Although the construction of the effective lagrangian was carried out for relativistic theories, it readily applies to non-relativistic theories by just changing the Poincaré group by the relevant space-time group. The outcome of ref. [7] is that the effective lagrangian for the Goldstone modes can always be written in terms of a matrix field $U(x)$ taking values in the coset space G/H, determined by the pattern of symmetry breaking $G \to H$ (recall that H is the internal symmetry group of the ground state). We are searching for an effective lagrangian invariant under $SU(2)$. The field $U(x)$ transforms non-linearly under $SU(2)$ as follows:

$$U(x) \to gU(x)h^\dagger(g,U). \tag{4.2.1}$$

When $g \in H$, the unbroken subgroup, then $h^\dagger = g^\dagger$ and $U(x)$ transforms linearly.

In order to have an intuitive picture of the above mathematical formulation, it is helpful to take the Heisenberg model as a microscopic model,

$$H = \sum_{<i,j>} J_{ij}\mathbf{S}_i\mathbf{S}_j. \tag{4.2.2}$$

Our discussion however is general and holds for more complicated models, like the Hubbard model, $t-J$ model, etc., with the only requirement that they have an $SU(2)$ spin symmetry which breaks spontaneously down to $U(1)$ in the ground state. (4.2.2) can be written in the second quantisation language in terms of the real space creation and annihilation operators, namely, $\psi^\dagger(x)$ and $\psi(x)$,

$$H = \sum_{<i,j>} J_{ij}\left(\psi^\dagger(x_i)\mathbf{S}\psi(x_i)\right)\left(\psi^\dagger(x_j)\mathbf{S}\psi(x_j)\right). \tag{4.2.3}$$

This hamiltonian realises the internal $SU(2)$ symmetry as follows:

$$\psi(x_i) \longrightarrow g\psi(x_i) \quad , \quad g \in SU(2). \tag{4.2.4}$$

As a classical field theory, the ground state configurations $\psi_0(x_i)$ of (4.2.3) are those with a maximum spin in a given direction, say the third direction. For spin 1/2 we have $\psi_0^\dagger(x_i) = (1\ 0)$ for all i in the ferromagnet, whereas in the antiferromagnet half of the is would have the above configuration whereas the remaining half would have $\psi_0^\dagger(x_i) = (0\ 1)$. The symmetry of the ground state configurations is clearly $U(1) = \langle e^{i\theta S^3} \rangle$. We can think of a classical configuration close to the ground state as $\psi(x_i) \sim \tilde{U}(x_i)\psi_0(x_i)$, $\tilde{U}(x_i)$ being slowly varying through the lattice. $\tilde{U}(x_i) \in SU(2)$ admits a unique decomposition $\tilde{U}(x_i) = U(x_i)h(\tilde{U}(x_i))$ where $U(x_i) \in SU(2)/U(1)$ and $h \in U(1)$. Since the ground state configuration is $U(1)$ invariant we can always write $\psi(x_i) \sim U(x_i)\psi_0(x_i)$. Taking into account this relation, (4.2.4) and the $U(1)$ invariance of the ground state configuration, the non-linear transformations (4.2.1) are justified ($h^\dagger(g, U)$ is the suitable factor that left multiplied by gU gives an element of the coset).

If the magnetisation occurs in the third direction then

$$U(x) = exp\left\{ \frac{i\sqrt{2}}{f_\pi} \left[\pi_1(x)S^1 + \pi_2(x)S^2 \right] \right\}, \tag{4.2.5}$$

where S^i, are generators of $SU(2)$ for any representation and $\pi_i(x)$ are the fields describing the spin waves (f_π is a dimensionful factor).

4.2.2 Space-time symmetries

Now that we have our basic field and know what its transformations are under the internal symmetry group, we have to find out how it transforms under the space-time symmetries. The space group and time reversal must be respected by the dynamics. The space-time symmetry will be broken by the ground state configuration. In fact the microscopic hamiltonian presents the symmetry of the paramagnetic fase $\mathcal{S} \otimes T$, i.e., space group and time reversal, which breaks down to the ground state symmetry given by the magnetic space group [14]. As in the case of the internal symmetry we impose our effective lagrangian to be invariant under the unbroken symmetry $\mathcal{S} \otimes T$. For definiteness we will be concerned with the space group $R\bar{3}c$, whose crystallographic point group is $\bar{3}m$, together with time reversal. The $\bar{3}m$ group is generated by a rotation of $2\pi/3$ around the z-axis (C_{3z}^+), the inversion (I) and a reflexion plane perpendicular

to the y-axis (σ_y). The time reversal symmetry just reverses the sign of time. If we introduce holomorphic coordinates $z = x + iy$ and $\bar{z} = x - iy$ these transformations read

$$C_{3z}^{+}: \begin{cases} z & \to & e^{i2\pi/3}z \\ \bar{z} & \to & e^{-i2\pi/3}\bar{z} \\ x^3 & \to & x^3 \end{cases}$$

$$I: \begin{cases} z & \to & -z \\ \bar{z} & \to & -\bar{z} \\ x^3 & \to & -x^3 \end{cases} \tag{4.2.6}$$

$$\sigma_y: \begin{cases} z & \to & \bar{z} \\ \bar{z} & \to & z \\ x^3 & \to & x^3. \end{cases}$$

We will consider $U(x)$ in the continuum, which is always a good approximation for small momentum. Effects due to finite lattice spacing are encoded in higher space derivative terms. In the continuum approach only the crystal point group and the primitive translations (τ) of the full space group are relevant.

The ground state configuration can be arranged ferromagnetically or antiferromagnetically. This leads to different transformations of the $U(x)$ field under the crystal point group and primitive translations.

If the ground state is ferromagnetic the local magnetisation points to the same direction everywhere. This indicates that we have to assign trivial transformation properties to $U(x)$ under both the point group and the primitive translations.

$$\begin{aligned} C_{3z}^{+}: &\ U(x) \to g_3 U(x) h_3^{\dagger} \\ I: &\ U(x) \to U(x) \\ \sigma_y: &\ U(x) \to g_2 U(x) h_2^{\dagger} \end{aligned} \tag{4.2.7}$$

$$\tau: \ U(x) \to U(x),$$

where (g_i, h_i) are the non-linear $SU(2)$ transformations induced by the rotations. Notice that only the rotational part of the roto-translational elements which may exist in the space group is relevant and this is already included in (4.2.7). This is a general feature independent of the particular space group.

On the other hand, if we have an antiferromagnetic ground state the local magnetisation points to opposite directions depending on the point of the space where the magnetic ion is located. This must be reflected in the transformation properties of $U(x)$. Those depend in turn on how the magnetic ions are distributed in the crystal. In order to make it definite, let us consider the Cr_2O_3 crystal, which enjoys the $R\bar{3}c$ space group with $\bar{3}m$ point symmetry group. The rhombohedrical unit cell contains four Cr atoms located along the z-axis which play the role of the magnetic ions, and six oxygen atoms which play no role as far as spin is concerned [15]. However, the presence of oxygen atoms is crucial for the absence of primitive translations which map points with opposite magnetisations. Hence all primitive translations must be implemented trivially. The point group symmetries C_{3z}^{+} and σ_y map points with the same local magnetisation, while the inversion I maps points with opposite local magnetisations. This indicates that we may assign to $U(x)$ the following transformation properties under the $\bar{3}m$ group:

$$\begin{aligned} C_{3z}^{+}: \quad U(x) &\rightarrow g_3 U(x) h_3^{\dagger} \\ I: \quad U(x) &\rightarrow U(x) C h_I^{\dagger} \\ \sigma_y: \quad U(x) &\rightarrow g_2 U(x) h_2^{\dagger} \quad , \quad C = e^{-i\pi S^2}, \\ \\ \tau: \quad U(x) &\rightarrow U(x) \end{aligned} \tag{4.2.8}$$

h_I is a compensating $U(1)$ element that keeps the transformed field in the coset and C turns a spin up into a spin down.

Even though the Cr_2O_3 does not have primitive translations which map points with opposite local magnetisations there are antiferromagnetic materials which do have them. In that case non-trivial transformations should be assigned to $U(x)$. This is discussed in detail in the appendix 4.A.

Notice then, that in the antiferromagnetic case, the transformations of $U(x)$ are dictated not only by the space symmetry group but also by the precise local magnetisation of the points related by the symmetry operation.

Let us finally discuss time-reversal symmetry. This symmetry is spontaneously broken in both ferromagnetic and antiferromagnetic ground states. Time reversal changes the sign of the spin. This transformation is implemented on a wave function by $\psi(x) \rightarrow C\psi^*(x)$ [16], which translates for $U(x)$ field in

$$T: \quad U(x) \rightarrow U(x) C h_t^{\dagger} \quad , \quad C = e^{-i\pi S^2}, \tag{4.2.9}$$

h_t is again a compensating $U(1)$ element that keeps the transformed field in the coset.

It can be shown that when the space-time transformations associated to the magnetic space group, the unbroken subgroup of the space-time group, are considered the transformations of $U(x)$ are linear.

4.3 Construction of the Effective Lagrangian

4.3.1 Building blocks: Internal transformations

After having established the field transformations in the previous section, we shall proceed to construct the effective lagrangian in terms of $U(x)$ and its derivatives. Following [7] we consider $U^\dagger(x) i\partial_\mu U(x)$. This object belongs to the Lie algebra of $SU(2)$ and hence can be decomposed as

$$U^\dagger(x) i\partial_\mu U(x) = a_\mu^-(x) S_+ + a_\mu^+(x) S_- + a_\mu^3(x) S^3, \tag{4.3.1}$$

where we have considered the S_+ and S_- bases for convenience, which verifies

$$\begin{array}{l} S_+ = S^1 + iS^2 \\ S_- = S^1 - iS^2 \end{array} \quad , \quad \begin{array}{l} [S^3, S_+] = S_+ \\ [S^3, S_-] = -S_- \\ [S_+, S_-] = 2S^3. \end{array} \tag{4.3.2}$$

Under the $SU(2)$ transformations

$$U^\dagger i\partial_\mu U \;\rightarrow\; h(U^\dagger i\partial_\mu U)h^\dagger + \partial_\mu \theta S^3 \quad , \quad h = e^{i\theta S^3}, \tag{4.3.3}$$

and hence

$$\begin{array}{rcl} a_\mu^-(x) & \rightarrow & e^{i\theta(x)} a_\mu^-(x) \\ a_\mu^+(x) & \rightarrow & e^{-i\theta(x)} a_\mu^+(x) \\ a_\mu^3(x) & \rightarrow & a_\mu^3(x) + \partial_\mu \theta(x). \end{array} \tag{4.3.4}$$

Namely, $a_\mu^\pm$ transforms covariantly whereas a_μ^3 transforms like a connexion under an effective $U(1)_{local}$ group, associated to the non-linear $SU(2)$ transformations. From now on any reference to the $U(1)_{local}$ transformation must be understood as the effective transformation of the non-linear $SU(2)$ transformation over the fields in (4.3.4). These are taken as the basic building blocks of our construction together with their derivatives. In order to construct the effective lagrangian a covariant derivative over $a_\mu^-(x)$ can be defined as

$$D_\mu \equiv \partial_\mu - i a_\mu^3(x). \tag{4.3.5}$$

Although the connexion does not transform covariantly under $SU(2)$, an invariant field strength can be constructed in the standard way,

$$F_{\mu\nu}(x) \equiv \partial_\mu a^3_\nu(x) - \partial_\nu a^3_\mu(x). \tag{4.3.6}$$

Hence we can in principle construct all invariant terms in the effective lagrangian out of $a^-_\mu(x), a^+_\mu(x), F_{\mu\nu}(x)$ and D_μ. There are however terms which are invariant up to a total derivative which have to be included in the effective lagrangian. These terms are built out of $a^3_\mu(x)$ and are usually called topological. They read

$$\begin{array}{l} a^3_\mu \\ \epsilon^{\mu\nu\rho} a^3_\mu \partial_\nu a^3_\rho. \end{array} \tag{4.3.7}$$

The first term will be important later on. The second term is the well known abelian Chern-Simons form. As we will see our space-time symmetries do not allow this term. However it arises in other condensed matter systems as for instance in quantum Hall ferromagnets [17].

Given the projector P_+ over the higher spin state (see appendix 4.B) the fields in (4.3.1) can be written as

$$\begin{aligned} a^-_\mu(x) &= \frac{1}{2s} tr([U^\dagger i\partial_\mu U, S_-]P_+) \\ a^+_\mu(x) &= -\frac{1}{2s} tr([U^\dagger i\partial_\mu U, S_+]P_+) \\ a^3_\mu(x) &= \frac{1}{s} tr(U^\dagger i\partial_\mu U P_+). \end{aligned} \tag{4.3.8}$$

Once we have an explicit representation for $a^\pm_\mu$ and a^3_μ some relevant properties can be proved, namely, $F_{\mu\nu} \sim (a^+_\mu a^-_\nu - a^+_\nu a^-_\mu)$ and $D_\mu a^-_\nu = D_\nu a^-_\mu$ (see Appendix 4.B). These properties ensure that the invariant terms in the effective lagrangian can be constructed in terms of $a^\pm_\mu$ and symmetrised covariant derivatives acting on them only.

The expert reader may wonder why we do not use the standard $O(3)$-*sigma model* formulation where the effective lagrangian is built out of $n^a(x)$, an $SU(2)$ vector such that $n^a n^a = 1$. The reason is simple: any local invariant that can be constructed in the $O(3)$-*sigma* formulation can be constructed in the formulation above (we prove this in appendix 4.D). However, the opposite is not true. The essential difference comes from topological terms, namely, terms that are invariant up to a total derivative. Those are very elusive in the $O(3)$-*sigma model* formulation but well under control in our formulation, as it should be clear from (4.3.7).

4.3.2 Building blocks: Space-time transformations

The most efficient procedure to construct the effective lagrangian is the following:

1. First we construct all the $SU(2)$ invariants under the transformations (4.3.4), order by order in the derivative expansion.

2. After that we search for invariants under the space-time transformations (4.2.7)-(4.2.9) among those terms.

This procedure allows us to ignore the $SU(2)$ spin transformations induced by the space-time transformations in (4.2.7)-(4.2.9). Hence, the effective space transformations for the ferromagnetic systems read

$$\xi : \{C^+_{3z}, I, \sigma_y\} : \quad \left\{ \begin{array}{lcl} a^-_\mu & \to & a^-_{\xi\mu} \\ a^3_\mu & \to & a^3_{\xi\mu}, \end{array} \right. \tag{4.3.9}$$

where the symbol $\xi\mu$ stands for the transformed index μ under the space transformation ξ together with the appropriate coefficient in each case. Recall that the subindex μ corresponds to a derivative, which transforms with the inverse representation of the space points given in (4.2.6). Whereas for the antiferromagnetic systems they become

$$\xi : \{C^+_{3z}, \sigma_y\} : \quad \left\{ \begin{array}{lcl} a^-_\mu & \to & a^-_{\xi\mu} \\ a^3_\mu & \to & a^3_{\xi\mu} \end{array} \right. \tag{4.3.10a}$$

$$\xi : \{I\} : \quad \left\{ \begin{array}{lcl} a^-_\mu & \to & -a^+_{\xi\mu} \\ a^3_\mu & \to & -a^3_{\xi\mu}. \end{array} \right. \tag{4.3.10b}$$

The effective time reversal transformation for both ferromagnet and antiferromagnet reads

$$T : \quad \left\{ \begin{array}{lcl} a^-_\mu & \to & -a^+_{t\mu} \\ a^3_\mu & \to & -a^3_{t\mu}, \end{array} \right. \tag{4.3.11}$$

again $t\mu$ represents the transformation of the index μ under time reversal symmetry T. Let us remark at this point that because of the different transformation properties under the space symmetries the effective lagrangians for the ferromagnetic and antiferromagnetic spin waves will be different. This is in fact not surprising since it is well known that the low momentum dispersion relation of the spin waves is quadratic for the ferromagnet but linear for the antiferromagnet. We shall obtain this result from symmetry considerations only. The difference arises from the different transformations given by

(4.3.9) for the ferromagnet and by (4.3.10) for the antiferromagnet. In fact only the terms with an odd number of time derivatives lead eventually to the above mentioned differences. In order to prove this let us consider the set of generators $\{C_{3z}^{+}, \sigma_y, I, T\}$, as displayed in (4.3.9) and (4.3.11), for the ferromagnet and $\{C_{3z}^{+}, \sigma_y, TI, T\}$ for the antiferromagnet, where we choose TI instead of I in (4.3.10b) as a generator. Notice that $\{C_{3z}^{+}, \sigma_y, T\}$ act identically in the ferromagnetic and antiferromagnetic case, and hence the only differences may arise due to action of I or TI. Consider next TI on the space derivatives $p = z, \bar{z}, 3$ for the antiferromagnetic case,

$$T\xi : \{TI\} : \quad \begin{cases} a_p^- & \rightarrow & a_{\xi p}^- \\ a_p^3 & \rightarrow & a_{\xi p}^3, \end{cases} \tag{4.3.12}$$

and notice that these transformations are identical to those of I on space derivatives for the ferromagnetic case (4.3.9). Finally the action of TI on time derivatives for the antiferromagnet reads

$$T\xi : \{TI\} : \quad \begin{cases} a_0^- & \rightarrow & -a_0^- \\ a_0^3 & \rightarrow & -a_0^3. \end{cases} \tag{4.3.13}$$

which only differs by a sign from the action of I on time derivatives for ferromagnets (4.3.11). Therefore the invariants with an even number of time derivatives are the same for both ferromagnetic and antiferromagnetic spin waves. Notice that the proof which we carried out is independent of the particular point group we choose; the only thing we have to do is to substitute the space transformation ξ which maps points with opposite magnetisation (in our case the inversion I) by itself followed by the time reversal transformation $T\xi$.

It is worth mentioning at this point that if primitive translations which map points with opposite magnetisation existed, terms with an odd number of time derivatives would not be allowed (see appendix 4.A). Only in this case the ground state of the antiferromagnet appears to be time reversal invariant at macroscopic scales, which enforces the above restriction on the effective lagrangian [18]. However, as it should be clear from the above, this is not the most general situation, although it is the most usual one.

4.3.3 Derivative expansion: Power counting

The organisation of the effective lagrangian in terms of derivatives is easier in relativistic theories than in non-relativistic ones. Energy and momentum are universally

related in the former, which allows to control the derivative expansion by means of a single dimensionful parameter. This parameter may be thought of as the energy of the first massive excitation. For non-relativistic theories, energy and momentum need not fit in any precisely given form, so we may expect the derivative expansion to be controled by at least two independent parameters: one with dimensions of energy for the time derivatives and one with dimensions of momentum for the space derivatives. We may identify the former as the energy of the first gapped excitation J and the latter as the typical inverts lattice spacing $1/a$. A natural way to relate the time derivative expansion to the space derivative expansion arises once the lowest order terms are written down. It consist of counting the lowest order in time derivatives as being equally important as the lowest order in space derivatives, no matter how many derivatives are in either. This procedure enforces that time and space derivatives are related in the same fashion as energy and momentum in the dispersion relation. This is the right way to proceed as far as there is no external source probing the system (for instance if we wish to calculate the magnetic susceptibility) or the external source has a typical energy and momentum compatible with the dispersion relation. Otherwise the counting should be rearranged according to the the typical energy and momentum of the external source (this will be the case when probing the system by electromagnetic radiation). The latter situation never occurs in relativistic theories because, as mention before, energy and momentum are universally related.

4.4 Effective Lagrangian for the Ferromagnet

As we mention in the introduction the effective lagrangian for the Goldstone modes must be constructed order by order in space and time derivatives.

The lowest order terms in space derivatives being invariant both under $SU(2)$ and the space-time symmetries read

$$\begin{array}{l} a_z^+ a_{\bar{z}}^- + a_z^- a_{\bar{z}}^+ \\ a_3^+ a_3^- . \end{array} \tag{4.4.1}$$

We call these terms $O(p^2)$. It is very easy to convince oneself that there are no $O(p^1)$ terms (i.e., with a single space derivative) which are invariant. However, (4.3.7) provides a term which is invariant up to a total time derivative. It reads

$$a_0^3. \tag{4.4.2}$$

This term appears in the literature [10, 19, 20] in a variety of forms, none of which being local as above, which we will show to be equivalent to (4.4.2) in the appendix 4.D. There, we also discuss its relation to certain topological objects.

Equations (4.4.1) and (4.4.2) indicate how time derivatives must be counted in relation to space derivatives. A time derivative must be counted as $O(p^2)$. Let us at this point elaborate a bit on the lowest order lagrangian in order to see how it produces the usual dispersion relation for ferromagnetic spin waves together with their interaction. We write

$$\mathcal{L}(x) = f_\pi^2 \left[\frac{1}{2} a_0^3 - \frac{1}{m}(a_z^+ a_{\bar{z}}^- + a_z^- a_{\bar{z}}^+) - \frac{1}{2\gamma m} a_3^+ a_3^- \right], \tag{4.4.3}$$

where f_π, m and γ are free parameters. The connexion $U^\dagger i\partial_\mu U$ is expanded in terms of the Goldstone modes field,

$$U^\dagger i\partial_\mu U = -\frac{1}{f_\pi^2}\left[(f_\pi \partial_\mu \pi^- + \cdots) S_+ + (f_\pi \partial_\mu \pi^+ + \cdots) S_- + (i(\pi^+ \partial_\mu \pi^- - \pi^- \partial_\mu \pi^+) + \cdots) S^3 \right], \tag{4.4.4}$$

where $\pi^\pm = (\pi^1 \pm i\pi^2)/\sqrt{2}$, giving rise to

$$\mathcal{L}(x) = \pi^- i\partial_0 \pi^+ - \frac{1}{2m}\partial_i \pi^- \partial_i \pi^+ - \frac{1}{2\gamma m}\partial_3 \pi^- \partial_3 \pi^+, \tag{4.4.5}$$

up to quadratic order in the spin wave fields. From (4.4.5) we see clearly that a time derivative must be counted as $1/2m$ two space derivatives. Observe that because (4.4.5) is first order in time derivatives, the remaining $U(1)$ spin symmetry implies that the number of ferromagnetic spin waves is conserved. It is also remarkable that the interaction of any number of spin waves at this order, which is obtained by keeping more terms of the expansion (4.4.4) in (4.4.5), is given by just three constants, namely f_π, m and γ.

The order of magnitude of the constants above follows from the fact that the effective lagrangian is an expansion for low energy and momentum controlled by the parameters J and $1/a$, namely the energy of the first gapped excitation and the typical lattice spacing respectively. J suppresses the time derivatives and $1/a$ the space ones. Since the lagrangian density has dimensions of $(energy) \times (momentum)^3$ we can estimate the size of each term by writing $\mathcal{L}(x) \sim J/a^3 \times (dimensionless\ quantities)$ and taking into account that the dimensionless quantities are built out of time derivatives over J and space derivatives over $1/a$. We obtain $f_\pi^2 \sim 1/a^3$ and $1/m \sim Ja^2$, in accordance with standard microscopic calculations in the Heisenberg model.

The following non-trivial order is $O(p^4)$, which gives rise to the terms below:

$$\begin{array}{l} a_0^+ a_0^- \\ i(D_0 a_3^+ a_3^- - D_0 a_3^- a_3^+) \\ i[(D_0 a_z^+ a_{\bar{z}}^- - D_0 a_z^- a_{\bar{z}}^+) - (D_0 a_{\bar{z}}^- a_z^+ - D_0 a_{\bar{z}}^+ a_z^-)] \end{array} \tag{4.4.6}$$

$$\begin{array}{l} a_3^+ a_3^- a_3^+ a_3^- \\ a_3^+ a_3^- (a_z^+ a_{\bar{z}}^- + a_z^- a_{\bar{z}}^+) \\ a_3^+ a_z^- a_3^+ a_{\bar{z}}^- + a_3^- a_{\bar{z}}^+ a_3^- a_z^+ \\ a_z^+ a_z^- (a_3^+ a_z^- + a_3^- a_z^+) + a_{\bar{z}}^- a_{\bar{z}}^+ (a_3^- a_{\bar{z}}^+ + a_3^+ a_{\bar{z}}^-) \\ a_z^+ a_{\bar{z}}^- a_z^+ a_{\bar{z}}^- + a_z^- a_{\bar{z}}^+ a_z^- a_{\bar{z}}^+ \\ a_z^+ a_{\bar{z}}^- a_{\bar{z}}^+ a_z^- \\ D_3 a_3^+ D_3 a_3^- \\ D_3 a_z^+ D_3 a_{\bar{z}}^- + D_3 a_z^- D_3 a_{\bar{z}}^+ \\ (D_3 a_z^+ D_z a_z^- + D_3 a_z^- D_z a_z^+) + (D_3 a_{\bar{z}}^- D_{\bar{z}} a_{\bar{z}}^+ + D_3 a_{\bar{z}}^+ D_{\bar{z}} a_{\bar{z}}^-) \\ D_z a_{\bar{z}}^+ D_z a_{\bar{z}}^- + D_{\bar{z}} a_z^- D_{\bar{z}} a_z^+ . \end{array} \tag{4.4.7}$$

4.5 Effective Lagrangian for the Antiferromagnet

In this section we follow exactly the same logical steps as in the ferromagnetic case, but taking into account that the transformation properties of $U(x)$ under the point group are different.

The lowest order terms in space derivatives are exactly the same as in (4.4.1). Namely,

$$\begin{array}{l} a_z^+ a_{\bar{z}}^- + a_z^- a_{\bar{z}}^+ \\ a_3^+ a_3^- . \end{array} \tag{4.5.1}$$

The lowest order term in time derivatives is not (4.4.2) anymore. Indeed, the transformation properties under I now forbid this term. Therefore as it was pointed out in section 4.3 the difference between ferromagnetic and antiferromagnetic spin waves arises from terms containing an odd number of time derivatives. Then the lowest order term in time derivatives is in this case

$$a_0^+ a_0^- . \tag{4.5.2}$$

Hence the effective lagrangian to lowest order reads

$$\mathcal{L}(x) = f_\pi^2 \left[a_0^+ a_0^- - 2v^2 (a_z^+ a_{\bar{z}}^- + a_z^- a_{\bar{z}}^+) - (\gamma v)^2 a_3^+ a_3^- \right], \tag{4.5.3}$$

where f_π is the spin stiffness, v the spin wave velocity in $x-y$ plain and γv the spin wave velocity in the z direction. In terms of the spin wave fields (4.4.4), the lagrangian above reads

$$\mathcal{L}(x) = \partial_0 \pi^+ \partial_0 \pi^- - v^2 \partial_i \pi^+ \partial_i \pi^- - (\gamma v)^2 \partial_3 \pi^+ \partial_3 \pi^-, \tag{4.5.4}$$

where it is apparent that now we have a linear dispersion relation. It also becomes apparent that the time derivatives must be counted as v times a space derivative. Observe that because (4.5.4) is second order in derivatives it describes two degrees of freedom. The remaining $U(1)$ spin symmetry tells us that antiferromagnetic spin waves can only be produced (or annihilated) in pairs. This is completely analogous to a relativistic theory: one of the spin waves plays the role of a (massless) particle and the other of an antiparticle. The total number of particles plus antiparticles is conserved due to the $U(1)$ symmetry. It is again remarkable that the interaction between spin waves at this order, which we would obtain by keeping further terms in the expansion (4.4.4), is given in terms of three parameters only, namely f_π, v and γ [12].

The order of magnitude of the constants above is estimated as in the ferromagnetic case. Now we obtain $f_\pi^2 \sim 1/Ja^3$ and $v \sim Ja$, which is again in accordance with microscopic calculations in the Heisenberg model.

It is worth mentioning that the following extra term appears at the lowest order

$$F_{03} \sim (a_0^+ a_3^- - a_0^- a_3^+). \tag{4.5.5}$$

This term is a total derivative and will be dropped. This is fine as far as we stay within a perturbative approach. However, since it is a total derivative of an object which is not $SU(2)$ invariant, it may become relevant if a non-perturbative analysis is attempted.

The next to leading non-trivial order is $O(p^4)$, which reads

$$\begin{aligned}
&a_0^+ a_0^- a_0^+ a_0^- \\
&i a_0^+ a_0^- (a_0^+ a_3^- - a_0^- a_3^+) \\
&a_0^+ a_0^- a_3^+ a_3^- \\
&a_0^+ a_3^- a_0^+ a_3^- + a_0^- a_3^+ a_0^- a_3^+ \\
&i(a_0^+ a_3^- - a_0^- a_3^+) a_3^+ a_3^- \\
&a_0^+ a_0^- (a_z^+ a_{\bar{z}}^- + a_z^- a_{\bar{z}}^+) \\
&a_0^+ a_z^- a_0^+ a_{\bar{z}}^- + a_0^- a_{\bar{z}}^+ a_0^- a_z^+ \\
&i(a_0^+ a_3^- - a_0^- a_3^+)(a_z^+ a_{\bar{z}}^- + a_z^- a_{\bar{z}}^+) \\
&i(a_0^+ a_z^- a_3^+ a_{\bar{z}}^- - a_0^- a_{\bar{z}}^+ a_3^- a_z^+) \\
&i[a_z^+ a_z^- (a_0^+ a_z^- - a_0^- a_z^+) - a_{\bar{z}}^- a_{\bar{z}}^+ (a_0^- a_{\bar{z}}^+ - a_0^+ a_{\bar{z}}^-)] \\
&D_0 a_0^+ D_0 a_0^- \\
&D_0 a_3^+ D_0 a_3^- \\
&D_0 a_z^+ D_0 a_{\bar{z}}^- + D_0 a_z^- D_0 a_{\bar{z}}^+ \\
&i[D_0 a_3^+ (D_z a_{\bar{z}}^- + D_{\bar{z}} a_z^-) - D_0 a_3^- (D_{\bar{z}} a_z^+ + D_z a_{\bar{z}}^+)]
\end{aligned} \tag{4.5.6}$$

together with the space derivatives terms given in (4.4.7). Notice that the above terms with an odd number of time derivatives would not appear if a primitive translation mapping points with opposite magnetisations existed in the Cr_2O_3 (see appendix 4.A).

4.6 Spin-orbit Corrections

The spin-orbit coupling of the electrons in the magnetic ions is usually the main source of explicit $SU(2)$ breaking. This explicit breaking can be taken into account in Heisenberg-type models by the inclusion of two new terms in the hamiltonian [21]

$$H = \sum_{<i,j>} J_{ij} \mathbf{S}_i \mathbf{S}_j + \sum_{<i,j>} \mathbf{D}_{ij} (\mathbf{S}_i \times \mathbf{S}_j) + \sum_{<i,j>} M_{ij}^{ab} S_i^a S_j^b, \tag{4.6.1}$$

where $D^a \sim (\Delta g/g) J$ and $M^{ab} \sim (\Delta g/g)^2 J$ are the antisymmetric and symmetric anysotropies respectively (M^{ab} is symmetric with respect the spin indices). These are related to the (super)exchange coupling through the change in the effective gyromagnetic factor due to the spin-orbit interaction. Typically $\Delta g \sim 10^{-2} g$ [22].

In order to incorporate the effects of (4.6.1) in the effective theory we promote $\mathbf{D}_{ij}$ and M_{ij}^{ab} to source fields $D^a(\mathbf{x}_i, \mathbf{x}_j)$ and $M^{ab}(\mathbf{x}_i, \mathbf{x}_j)$ and assign transformation

properties to them such that (4.6.1) becomes $SU(2)$ invariant,

$$\begin{array}{rcl} D^a(\mathbf{x}_i,\mathbf{x}_j) & \to & R^a{}_b D^b(\mathbf{x}_i,\mathbf{x}_j) \\ M^{ab}(\mathbf{x}_i,\mathbf{x}_j) & \to & R^a{}_c R^b{}_d M^{cd}(\mathbf{x}_i,\mathbf{x}_j). \end{array} \tag{4.6.2}$$

Now, if we could derive our effective lagrangian for the spin waves from the microscopic model it would be a functional of $U(x)$, D^a and M^{ab} invariant under $SU(2)$ transformations. Once we particularise the sources to reproduce the anisotropic spin-orbit tensors we automatically obtain the effects of the latter in the effective theory.

Since the spin-orbit corrections lead to short range interactions in (4.6.1), the local limit of the sources will be taken. In this limit the leading contribution compatible with the crystal symmetries of the antisymmetric anisotropy is represented by a tensor with one $SU(2)$ and two symmetric space indices, D^a_{pq}, where $p,q = z,\bar{z},3$ (these indices transform with the inverse representation of the space points (4.2.6)). The symmetric tensor is represented by a second order tensor of $SU(2)$ with no space indices, M^{ab}.

Let us next consider the following objects which transform covariantly under $SU(2)$,

$$\begin{array}{rcl} D_{pq} \equiv D^a_{pq} S^a & \to & g D_{pq} g^\dagger \\ M \equiv M^{ab}(S^a \otimes S^b + S^b \otimes S^a) & \to & (g \otimes g) M (g^\dagger \otimes g^\dagger). \end{array} \tag{4.6.3}$$

When these sources are set to their most general form compatible with the crystal symmetries only a few non-vanishing terms remain. Namely,

$$\begin{array}{ll} D_{zz} = D^-_{zz} S_+ & D^-_{zz} = -D^+_{\bar{z}\bar{z}} \\ D_{\bar{z}\bar{z}} = D^+_{\bar{z}\bar{z}} S_- & \\ & \\ D_{3z} = D^+_{3z} S_- & D^+_{3z} = -D^-_{3\bar{z}} \\ D_{3\bar{z}} = D^-_{3\bar{z}} S_+ & \end{array} \tag{4.6.4}$$

$$M = M^{-+}(S_+ \otimes S_- + S_- \otimes S_+) + M^{33}(S^3 \otimes S^3),$$

where $D^+_{\bar{z}\bar{z}}$, D^+_{3z}, M^{-+} and M^{33} are free parameters.

4.6.1 Spin-orbit sources: Internal transformations

Since our basic building blocks transform in a simple way under the $U(1)_{local}$ in the $SU(2)$ non-linear realisation, it is convenient to introduce new sources with simple

transformation properties under $U(1)_{local}$ in the following way:

$$U^{\dagger}(x)D_{pq}U(x) = d^{-}_{pq}(x)S_{+} + d^{+}_{pq}(x)S_{-} + d^{3}_{pq}(x)S^{3}. \tag{4.6.5}$$

These new sources transform as

$$\begin{aligned} d^{-}_{pq}(x) &\rightarrow e^{i\theta(x)}d^{-}_{pq}(x) \\ d^{+}_{pq}(x) &\rightarrow e^{-i\theta(x)}d^{+}_{pq}(x) \\ d^{3}_{pq}(x) &\rightarrow d^{3}_{pq}(x). \end{aligned} \tag{4.6.6}$$

The same can be done for the symmetric source,

$$\begin{aligned} \Big(U^{\dagger}(x)\otimes U^{\dagger}(x)\Big)\, M\Big(U(x)\otimes U(x)\Big) = {} & m^{--}(x)(S_{+}\otimes S_{+}) \\ & + m^{++}(x)(S_{-}\otimes S_{-}) \\ & + m^{33}(x)(S^{3}\otimes S^{3}) \\ & + m^{-+}(x)(S_{+}\otimes S_{-} + S_{-}\otimes S_{+}) \\ & + m^{-3}(x)(S_{+}\otimes S^{3} + S^{3}\otimes S_{+}) \\ & + m^{+3}(x)(S_{-}\otimes S^{3} + S^{3}\otimes S_{-}). \end{aligned} \tag{4.6.7}$$

The transformation properties for these components are

$$\begin{aligned} m^{--}(x) &\rightarrow e^{2i\theta(x)}m^{--}(x) \\ m^{++}(x) &\rightarrow e^{-2i\theta(x)}m^{++}(x) \\ m^{-3}(x) &\rightarrow e^{i\theta(x)}m^{-3}(x) \\ m^{+3}(x) &\rightarrow e^{-i\theta(x)}m^{+3}(x) \\ m^{-+}(x) &\rightarrow m^{-+}(x) \\ m^{33}(x) &\rightarrow m^{33}(x). \end{aligned} \tag{4.6.8}$$

An explicit representation for the sources $d^{a}_{pq}(x)$ introduced in (4.6.5) is given by

$$\begin{aligned} d^{-}_{pq}(x) &= \frac{1}{2s}tr([U^{\dagger}D_{pq}U, S_{-}]P_{+}) \\ d^{+}_{pq}(x) &= -\frac{1}{2s}tr([U^{\dagger}D_{pq}U, S_{+}]P_{+}) \\ d^{3}_{pq}(x) &= \frac{1}{s}tr(U^{\dagger}D_{pq}UP_{+}), \end{aligned} \tag{4.6.9}$$

and a similar but lengthier expression can be given for $m^{ab}(x)$ in (4.6.7). From the explicit representation (4.6.9) for the sources d^a_{pq} together with (4.6.4) it is obvious that $d^a_{zz}d^b_{3\bar{z}} = d^b_{zz}d^a_{3\bar{z}}$, $d^a_{\bar{z}\bar{z}}d^b_{3z} = d^b_{\bar{z}\bar{z}}d^a_{3z}$ and $d^a_{zz}d^b_{3z} = d^b_{\bar{z}\bar{z}}d^a_{3\bar{z}}$. Moreover one can easily prove that derivatives over these sources can be written as the source itself multiplied by $a^{\pm}_{\mu}(x)$ or $a^3_{\mu}(x)$. Therefore only $d^a_{pq}(x)$ and $m^{ab}(x)$ and not their derivatives have to be used in addition to our basic building blocks (4.3.1) to construct the effective lagrangian.

4.6.2 Spin-orbit sources: Space-time transformations

Let us next see how these sources transform under the space-time symmetries. Recall first that a space transformation induces a $SU(2)$ spin transformation also in the sources. However, as it was pointed out in section 4.3, the $SU(2)$ transformations induced by space-time transformations can be ignored because the lagrangian is first constructed to be $SU(2)$ invariant.

For the ferromagnet the effective $\bar{3}m$ transformations are given by

$$\xi : \{C^+_{3z}, I, \sigma_y\} : \quad \left\{ \begin{array}{lcl} d^-_{pq} & \to & d^-_{\xi p \xi q} \\ d^3_{pq} & \to & d^3_{\xi p \xi q} \\ m^{ab} & \to & m^{ab}, \end{array} \right. \tag{4.6.10}$$

and for the antiferromagnet

$$\xi : \{C^+_{3z}, \sigma_y\} : \quad \left\{ \begin{array}{lcl} d^-_{pq} & \to & d^-_{\xi p \xi q} \\ d^3_{pq} & \to & d^3_{\xi p \xi q} \\ m^{ab} & \to & m^{ab} \end{array} \right. \tag{4.6.11a}$$

$$\xi : \{I\} : \quad \left\{ \begin{array}{lcl} d^-_{pq} & \to & -d^+_{\xi p \xi q} \\ d^3_{pq} & \to & -d^3_{\xi p \xi q} \\ m^{--} & \to & m^{++} \\ m^{-+} & \to & m^{-+} \\ m^{-3} & \to & m^{+3} \\ m^{33} & \to & m^{33}. \end{array} \right. \tag{4.6.11b}$$

Time reversal, like in (4.3.11), gives the same transformations both for the ferromagnet and the antiferromagnet,

$$T: \left\{ \begin{array}{lcl} d^-_{pq} & \to & -d^+_{pq} \\ d^3_{pq} & \to & -d^3_{pq} \\ m^{--} & \to & m^{++} \\ m^{-+} & \to & m^{-+} \\ m^{-3} & \to & m^{+3} \\ m^{33} & \to & m^{33}. \end{array} \right. \tag{4.6.12}$$

Again, as in section 4.3, it is easy to prove that the transformations (4.6.10) and (4.6.12) give the same invariants as (4.6.11) and (4.6.12). Consider instead of (4.6.11b) the transformation given by $T\xi$,

$$T\xi : \{TI\} : \left\{ \begin{array}{lcl} d^-_{pq} & \to & d^-_{\xi p \xi q} \\ d^3_{pq} & \to & d^3_{\xi p \xi q} \\ m^{ab} & \to & m^{ab}. \end{array} \right. \tag{4.6.13}$$

Therefore all the invariants constructed out of ds, ms and as with an arbitrary number of space derivatives and an even number of time derivatives are the same for ferromagnetic and antiferromagnetic spin waves.

4.6.3 Invariant terms

The previous transformation properties lead to the following invariants at leading order in terms of ds and ms,

$$\begin{array}{l} d^+_{zz} d^-_{\bar{z}\bar{z}} + d^-_{zz} d^+_{\bar{z}\bar{z}} \\ (d^+_{3z} d^-_{zz} + d^-_{3z} d^+_{zz}) + (d^-_{3\bar{z}} d^+_{\bar{z}\bar{z}} + d^+_{3\bar{z}} d^-_{\bar{z}\bar{z}}) \\ d^+_{3z} d^-_{3\bar{z}} + d^-_{3z} d^+_{3\bar{z}} \\ d^3_{zz} d^3_{\bar{z}\bar{z}} \\ d^3_{3z} d^3_{zz} + d^3_{3\bar{z}} d^3_{\bar{z}\bar{z}} \\ d^3_{3z} d^3_{3\bar{z}} \end{array} \tag{4.6.14}$$

$$\begin{array}{l} m^{-+} \\ m^{33}. \end{array}$$

If we expand the ds and ms sources in terms of the spin wave fields we obtain

$$\begin{aligned} U^\dagger D_{pq} U &= \left[D^-_{pq} + \frac{1}{f_\pi^2}(D^+_{pq}\pi^-\pi^+ - D^-_{pq}\pi^+\pi^-) + \cdots \right] S_+ \\ &+ \left[D^+_{pq} + \frac{1}{f_\pi^2}(D^-_{pq}\pi^+\pi^+ - D^+_{pq}\pi^+\pi^-) + \cdots \right] S_- \\ &+ \left[-\frac{2i}{f_\pi}(D^+_{pq}\pi^- - D^-_{pq}\pi^+) + \cdots \right] S^3, \end{aligned} \tag{4.6.15}$$

$$\begin{aligned} (U^\dagger \otimes U^\dagger) M (U \otimes U) = {} & [(2M^{-+} - M^{33})\pi^-\pi^- + \cdots](S_+ \otimes S_+) \\ & + [(2M^{-+} - M^{33})\pi^+\pi^+ + \cdots](S_- \otimes S_-) \\ & + [M^{-+} - 2(2M^{-+} - M^{33})\pi^+\pi^- + \cdots](S_+ \otimes S_- + S_- \otimes S_+) \\ & + [-i(2M^{-+} - M^{33})\pi^- + \cdots](S_+ \otimes S^3 + S^3 \otimes S_+) \\ & + [i(2M^{-+} - M^{33})\pi^+ + \cdots](S_- \otimes S^3 + S^3 \otimes S_-) \\ & + [2(2M^{-+} - M^{33})\pi^+\pi^- + M^{33} + \cdots](S^3 \otimes S^3). \end{aligned} \tag{4.6.16}$$

From these two expansions we can easily see that the terms (4.6.14) at quadratic order in the spin waves fields produce a gap in the dispersion relation. Notice however that the energy gap for the spin waves is $\sim d^2$ for the ferromagnet, since its spin waves verify a Schrödinger like equation, whereas it is $\sim d$ for the antiferromagnet, since its spin waves verify a Klein-Gordon type equation.

Notice also that the terms in (4.6.14) contribute to the ground state energy and force the (staggered) magnetisation to be along the third direction. This is why we took the direction of the spontaneously symmetry breaking along the third axes in (4.2.5). Otherwise terms with a single spin wave field would appear in the expansion of (4.6.14) indicating us that we chose a wrong direction for the (staggered) magnetisation.

The above considerations allow us to decide how to take the relative order of magnitude for the derivatives and the anisotropy tensors. If we consider, for instance, the typical energy of the spin waves of the order of their energy gap, the counting for the ferromagnet becomes $a_0 \sim a_i^2 \sim d^2 \sim m$, which leads to the following $O(p^3)$ terms:

$$\begin{aligned} & i[d^3_{\bar z\bar z}(a^+_{\bar z}a^-_3 - a^-_{\bar z}a^+_3) - d^3_{zz}(a^-_z a^+_3 - a^+_z a^-_3)] \\ & i[d^3_{3z}(a^+_{\bar z}a^-_3 - a^-_{\bar z}a^+_3) - d^3_{3\bar z}(a^-_z a^+_3 - a^+_z a^-_3)], \end{aligned} \tag{4.6.17}$$

whereas for the antiferromagnet an analogous counting implies $a_0^2 \sim a_i^2 \sim d^2 \sim m$,

which in addition to the previous (4.6.17) terms leads to new $O(p^3)$ terms:

$$\begin{array}{l} d^3_{\bar{z}\bar{z}}(a^+_{\bar{z}}a^-_0 + a^-_{\bar{z}}a^+_0) + d^3_{zz}(a^-_z a^+_0 + a^+_z a^-_0) \\ d^3_{3z}(a^+_{\bar{z}}a^-_0 + a^-_{\bar{z}}a^+_0) + d^3_{3\bar{z}}(a^-_z a^+_0 + a^+_z a^-_0). \end{array} \tag{4.6.18}$$

Notice again that if primitive translations which map points with opposite magnetisations existed these terms would be forbidden.

4.7 Magnetic Dipole Corrections

A second source of explicit $SU(2)$ breaking are the magnetic dipole interactions. They have the form [22]

$$H = \mu^2 \sum_{i \neq j} \left(\frac{\mathbf{S}_i \mathbf{S}_j}{|\mathbf{x}_i - \mathbf{x}_j|^3} - \frac{(\mathbf{S}_i \hat{\mathbf{x}}_i)(\mathbf{S}_j \hat{\mathbf{x}}_j)}{|\mathbf{x}_i - \mathbf{x}_j|^3} \right). \tag{4.7.1}$$

The first term is $SU(2)$ invariant, and has the form of the (super)exchange parameter in the Heisenberg model, while the second term has the form of the symmetric anisotropy in (4.6.1),

$$\frac{1}{|\mathbf{x}_i - \mathbf{x}_j|^3} \sim J_{ij} \qquad , \qquad \frac{\hat{x}^a_i \hat{x}^b_j}{|\mathbf{x}_i - \mathbf{x}_j|^3} \sim M^{ab}_{ij}, \tag{4.7.2}$$

Let us point out however that whereas the superexchange and anisotropic terms lead to short range interactions the terms above lead to long range interactions. In spite of this, the local limit will be taken since the strength of the interactions decays like the third power of the distance between the magnetic dipoles and furthermore it is usually very small compared to the spin-orbit terms. In fact this long range interaction starts playing a crucial role at very long distance phenomena, like in the formation of domain walls in ferromagnets [22], which lie beyond the scope of this work. If we restrict ourselves to the local limit, then both terms have been already taken into account in the $SU(2)$ invariant structure (J_{ij}) and in the explicit symmetry breaking source (M^{ab}).

4.8 The Coupling to Electromagnetic Fields

If we probe our ferromagnet or antiferromagnet by electromagnetic waves the energy of which is much smaller than the energy of the first gaped excitation, the only relevant

magnetic degrees of freedom are the spin waves. It is then relevant how to include the electromagnetic fields in the effective lagrangians built in the previous sections.

When the electromagnetic fields enter the game the $U(1)_{em}$ local gauge invariance is the additional symmetry that we have to take into account. Since the fields $U(x)$ have trivial transformation properties under the $U(1)_{em}$ (spin waves have no electric charge) we may naïvely expect non-minimal couplings (couplings to the field strength tensor) only. However, the Pauli term which arises in any microscopic model when a magnetic field is present breaks explicitly the $SU(2)$ spin symmetry in a very particular way. We shall first address how to introduce in the effective lagrangian the effects of the microscopic Pauli term.

4.8.1 Pauli coupling

For definiteness we may have in mind the Heisenberg model, but the argument we present goes through for more complicated models like the t-J model, Hubbard model, etc.. For any microscopic model we can think of the hamiltonian in the presence of a magnetic field will be augmented, at least, by the Pauli term, which explicitly breaks the $SU(2)$ spin symmetry,

$$H = \sum_{<i,j>} J_{ij}\mathbf{S}_i\mathbf{S}_j - \mu \sum_i \mathbf{S}_i\mathbf{B}. \tag{4.8.1}$$

Let us assume that the remaining part of the hamiltonian is invariant under the original $SU(2)$ symmetry, as in (4.8.1), even when the electromagnetic fields are switched on. Then the only term which breaks this symmetry is the Pauli term. Let us then write the lagrangian in the second quantisation formalism,

$$L = \sum_i \psi^\dagger(x_i) i\partial_0 \psi(x_i) + \mu \sum_i \left(\psi^\dagger(x_i)\mathbf{S}\psi(x_i)\right)\mathbf{B}(x_i) + \cdots. \tag{4.8.2}$$

This lagrangian can be rewritten in a form that the Pauli term is associated to the time derivative,

$$L = \sum_i \psi^\dagger(x_i) i\left(\partial_0 - i\mu\mathbf{S}\mathbf{B}(x_i)\right)\psi(x_i) + \cdots. \tag{4.8.3}$$

Written in this way the term inside the parenthesis has the form of a covariant derivative for time dependent $SU(2)$ transformations. Then if we promote the Pauli term to a new source, $A_0(x) \sim \mu\mathbf{S}\mathbf{B}(x)$ such that it transforms like a connexion under time dependent $SU(2)$ transformations,

$$A_0(x) \to g(t)A_0(x)g^\dagger(t) + ig(t)\partial_0 g^\dagger(t), \tag{4.8.4}$$

the microscopic lagrangian becomes invariant under time dependent $SU(2)$ spin transformations. Now we can construct the effective theory with this source, and finally set it to its actual value. This is completely analogous to the procedure carried out in section 4.6 for the spin-orbit breaking terms. The effective theory derived from the microscopic level would be a functional of the $U(x)$ and the connexion $A_0(x)$ invariant under time dependent $SU(2)$ transformations. This is easily achieved by replacing the time derivatives acting on U by covariant time derivatives. Namely,

$$\partial_0 \to D_0 \equiv \partial_0 - iA_0(x). \tag{4.8.5}$$

When we particularise the $A_0(x)$ to reproduce the Pauli term we obtain its effects in the effective theory. From now on we will have to write $a_0^{\pm}$ and a_0^3 as

$$\begin{aligned} U^{\dagger} i D_0 U = -\frac{1}{f_\pi^2} \Bigg\{ & \left[f_\pi \partial_0 \pi^- - \mu \left(\frac{1}{2}(f_\pi^2 - \pi^+\pi^-) B^{\bar{z}} + \frac{1}{2}\pi^-\pi^- B^z + i f_\pi \pi^- B^3 \right) + \cdots \right] S_+ \\ & + \left[f_\pi \partial_0 \pi^+ - \mu \left(\frac{1}{2}\pi^+\pi^+ B^{\bar{z}} + \frac{1}{2}(f_\pi^2 - \pi^+\pi^-) B^z - i f_\pi \pi^+ B^3 \right) + \cdots \right] S_- \\ & + \left[i(\pi^+ \partial_0 \pi^- - \pi^- \partial_0 \pi^+) - \mu \left(i f_\pi \pi^+ B^{\bar{z}} - i f_\pi \pi^- B^z + (f_\pi^2 - 2\pi^+\pi^-) B^3 \right) + \cdots \right] S^3 \Bigg\}, \end{aligned} \tag{4.8.6}$$

whereas $a_i^{\pm}$ and a_i^3 are still given by (4.4.4).

It is important to realise that we do not have to introduce any additional unknown constant, but the effective gyromagnetic factor of the spin degrees of freedom in the microscopic theory in the above terms. Notice, however, that space derivatives on $A_0(x)$ transform covariantly under time dependent $SU(2)$ transformations. Hence they may be used to construct further invariants in analogy to the ds in (4.6.5) and (4.6.9). We will not present these invariants explicitly since, as we will see later on, they are very suppressed in realistic situations.

4.8.2 Non-minimal couplings

Let us next discuss the non-minimal couplings. This is the only way the electromagnetic field can couple to non charged excitations like the spin waves, namely, by means of the field strength tensor, i.e., electric field, **E**, and magnetic field, **B**. The transformation properties associated to the electromagnetic fields are the following:

1. they both are scalars under $SU(2)$ spin transformations,

2. the electric field transforms like a vector under $\bar{3}m$,

3. the magnetic field transforms like a pseudovector under $\bar{3}m$, and

4. they both are scalars under under primitive translations,

5. under the time reversal they transform as

$$T: \begin{cases} E^a & \to & E^a \\ B^a & \to & -B^a. \end{cases} \tag{4.8.7}$$

4.8.3 Power counting

Once we have the transformation properties for the electromagnetic fields let us consider their relative size in order to write the derivative expansion in the effective theory.

The expression (4.8.5) indicates us that the Pauliterm, $\mu\mathbf{B}$, has to be suppressed by the first gapped excitation, J. Consider next the electromagnetic fields in terms which are $SU(2)$ invariant. They may arise from a microscopic model in two ways: (i) originated by minimal couplings of the electromagnetic potentials or (ii) by explicit non-minimal couplings in the microscopic model, which may arise when integrating out even higher scales of energy and momentum. The second kind of terms are suppressed by a higher energy and momentum scale and will be ignored as far as estimates are concerned. They would slightly modify the values of the parameters in the effective lagrangian, which are anyway unknown. The relative suppression of the terms originated by minimal coupling are simple to estimate: the scalar potential goes always accompanying a time derivative and hence it will be suppressed by J, whereas the vector potential is associated to a link variable (in a lattice model) and hence suppressed by $1/a$ (in the continuum limit the space derivative is associated to the link and therefore the vector potential is associated to the space derivative). Consequently the electric fields are suppressed by J/ea whereas the magnetic fields by $1/ea^2$, where e is the electron charge.

When the electromagnetic field enters the system it fixes the relevant scales of energy and momentum. For the effective theory to make sense these must be much smaller than J and $1/a$ respectively. The amplitude of the electromagnetic field is also constrained so that we can organise our effective lagrangian in increasing powers of E and B as well as derivatives. This requires $\mu B/J$, eaE/J and ea^2B be much smaller than 1.

Nothing else can be said in general about the organisation of the effective lagrangian. Let us at this point introduce $v = Ja$ which combines the energy and momentum scales in a single parameter. This parameter allows us to write our theory in terms of a single scale, namely, J. For the antiferromagnetic spin waves v has a precise meaning: it is the velocity of propagation of the spin waves, whereas for the ferromagnetic spin waves it does not have any particular meaning. Given typical values for $J \sim 10meV$ and $a \sim 10\text{Å}$[22], then $v \sim 10^{-4}$ (Recall that we have taken $c = 1$, therefore v has to be thought as v/c).

In order to further illuminate the construction of the effective lagrangian, let us consider the interaction with a classical monochromatic electromagnetic wave of energy ω. In this case the amplitude of the electric and magnetic fields is the same. Let us choose $\omega \sim 10^{-1}J$, which tells us that we must count ∂_0 as $10^{-1}J$. The momentum of the electromagnetic field is in this case ω, which tells us that for typical lattice spacings we must count $v\partial_i \sim 10^{-4}\partial_0$. Notice that the counting is very different in the absence of electromagnetic field. We still have to fix the amplitude of the electromagnetic field. For simplicity let us choose $eaE \sim 10^{-1}J$. Then the following relative suppressions hold:

$$\begin{array}{rcl} \partial_0, eaE & \sim & 10^{-1}J \\ d & \sim & 10^{-2}J \\ \mu B, m & \sim & 10^{-4}J \\ v\partial_i, eavB & \sim & 10^{-5}J. \end{array} \tag{4.8.8}$$

where a typical value for the gyromagnetic factor $\mu \sim \mu_B = 9.27\,10^{-24}J/T$ has been taken. With the counting above the following terms are obtained for the ferromagnetic systems:

First order $O(p^1)$:

$$a_0^3. \tag{4.8.9}$$

Second order $O(p^2)$:

$$\begin{array}{l} a_0^+ a_0^- \\ E^z E^{\bar{z}} \\ E^3 E^3. \end{array} \tag{4.8.10}$$

Fourth order $O(p^4)$:

$$
\begin{array}{l}
a_0^+ a_0^- a_0^+ a_0^- \\
\\
E^z E^{\bar{z}} E^z E^{\bar{z}} \\
E^z E^{\bar{z}} E^3 E^3 \\
E^3 E^3 E^3 E^3 \\
\\
\partial_0 E^z \partial_0 E^{\bar{z}} \\
\partial_0 E^3 \partial_0 E^3 \\
\\
a_0^+ a_0^- E^z E^{\bar{z}} \\
a_0^+ a_0^- E^3 E^3 \\
\\
d_{zz}^+ d_{\bar{z}\bar{z}}^- + d_{zz}^- d_{\bar{z}\bar{z}}^+ \\
(d_{3z}^+ d_{zz}^- + d_{3z}^- d_{zz}^+) + (d_{3\bar{z}}^- d_{\bar{z}\bar{z}}^+ + d_{3\bar{z}}^+ d_{\bar{z}\bar{z}}^-) \\
d_{3z}^+ d_{3\bar{z}}^- + d_{3z}^- d_{3\bar{z}}^+ \\
d_{zz}^3 d_{\bar{z}\bar{z}}^3 \\
d_{3z}^3 d_{zz}^3 + d_{3\bar{z}}^3 d_{\bar{z}\bar{z}}^3 \\
d_{3z}^3 d_{3\bar{z}}^3 \\
\\
m^{-+} \\
m^{33}.
\end{array}
\tag{4.8.11}
$$

Notice that it is not up to fourth order that we obtain a coupling of the electric field to the spin waves. The Pauli coupling is encoded in the a_0 blocks as given in (4.8.6). At $O(p^4)$ there is only a contribution arising from (4.8.9) when we substitute the time derivative by the covariant derivative (4.8.5).

For the antiferromagnet there is no invariant at $O(p^1)$. Second order ($O(p^2)$) invariants are the same as those for the ferromagnet in (4.8.10). At fourth order ($O(p^4)$) in addition to the terms given in (4.8.11) we have two new terms,

$$
\begin{array}{l}
i[(d_{\bar{z}\bar{z}}^+ a_0^- - d_{\bar{z}\bar{z}}^- a_0^+) E^z - (d_{zz}^- a_0^+ - d_{zz}^+ a_0^-) E^{\bar{z}}] \\
i[(d_{3z}^+ a_0^- - d_{3z}^- a_0^+) E^z - (d_{3\bar{z}}^- a_0^+ - d_{3\bar{z}}^+ a_0^-) E^{\bar{z}}].
\end{array}
\tag{4.8.12}
$$

Notice that these new terms which appear in the antiferromagnetic case at $O(p^4)$ contain time derivatives and the spin-orbit tensor which breaks explicitly the $SU(2)$

spin symmetry, which give rise to an electromagnetic coupling mediated by the spin-orbit interaction. These terms would be forbidden if a primitive translation mapping points with opposite magnetisations existed.

4.9 Summary and Discussion

We have provided a systematic way to write down effective lagrangians for spin waves in ferromagnetic and antiferromagmetic crystalline solids. We have done so at next to leading order. This is achieved by fully exploiting the internal symmetry breaking pattern $SU(2) \to U(1)$ as well as the space symmetries and time reversal. We have shown how to introduce explicit symmetry breaking terms, as those induced by atomic spin-orbit couplings and magnetic dipole interactions. We have also shown how to introduce couplings to electromagnetic fields.

The alert reader may wonder about the role that the magnetic group plays in our construction. In fact, it does not play any role else that indicating us the symmetry group of the ground state configuration. Notice that when we have spontaneous symmetry breaking the magnetic group should not be important since in a first approximation the local magnetisation direction is arbitrary, and each direction corresponds to a different magnetic group. It is only after introducing explicit $SU(2)$ breaking corrections, like those induced by the spin-orbit interactions, that the local magnetisations take the direction of a crystal symmetry axis, giving rise to a non-trivial magnetic group. If we introduce a constant magnetic field in an arbitrary direction whose contribution is larger than that of the spin-orbit interactions the local magnetisations will point to the direction of the magnetic field. Then the magnetic group will be trivial again. Within our formalism all the possible situations are taken into account once we have assign the proper space-time transformations to the field $U(x)$ in (4.2.6)-(4.2.8).

A word of caution is needed when using the effective lagrangians to higher orders: quantum (loop) corrections to lower order terms give in general contributions of some higher order. Then in order to make a consistent calculation to a given higher order, in general a loop calculation at lower order is necessary. For the antiferromagnet the kind of loop calculations to be carried out is completely analogous to calculations in relativistic theories, for which there is abundant experience [8, 12]. Typically a one loop calculation at $O(p^2)$ gives $O(p^4)$, a two loop one $O(p^6)$, etc. For the ferromagnet, there are no explicit loop calculations in the literature to our knowledge. On general

grounds, we expect a similar pattern though the exact way in which lower order loop contributions combine into higher orders might be different[1].

We would like to point out a few issues in our work that we find particularly relevant.

(i) Our formulation easily keeps track of elusive topological terms.

(ii) We find the remarkable differences between the ferromagnetic and antiferromagnetic spin wave effective lagrangian by the only use of symmetry properties.

(iii) Within the antiferromagnetic case, we point out that the existence of primitive translations which map points with opposite magnetisations has non-trivial consequences in the effective lagrangian.

(iv) We easily see that the Pauli term does not introduce any new parameter in the effective lagrangian.

In view of the relative large number of terms that arise at next to leading order in our lagrangians one may wonder if they may be of any use at all. We propose to use it as a guideline on possible interesting phenomena due to spin waves. If one suspects that a given material may have exciting magnetic properties in the spin wave region, one need not carry out a microscopic calculation to check so. By writing down the effective lagrangian one can most easily check if the expected phenomenon may occur or not. To do this one has to input realistic numbers for the J and a parameters according to the given material, changing the counting (4.8.8) if necessary, and proceed as above. In case it is feasible a microscopic calculation may be supplemented to fix the unknown parameters. A non-trivial application of these techniques is presented in the following chapter [13].

[1] A recent non-trivial loop calculation can be found in [23]

4.A Primitive Translation Effects in Antiferromagnetic Spin Waves

In this appendix we discuss the important consequences that primitive translations which map points with opposite magnetisations have in the effective lagrangian for antiferromagnets. Let us call τ to one such translations. According to the procedure in section 2, τ may be implemented by

$$\tau : \quad U(x) \quad \rightarrow \quad U(x)Ch_{\tau}^{\dagger}, \tag{4.A.1}$$

where h_τ is a compensating $U(1)$ element that keeps the transformed field in the coset. This implies

$$\tau : \quad \begin{cases} a_{\mu}^{-} & \rightarrow & -a_{\mu}^{-} \\ a_{\mu}^{3} & \rightarrow & -a_{\mu}^{3}. \end{cases} \tag{4.A.2}$$

This transformation differs from T in (4.3.11) only in terms with time derivatives. If we consider τT instead of τ as an independent generator, we have

$$\tau T : \begin{cases} a_{\mu}^{-} & \rightarrow & a_{t\mu}^{-} \\ a_{\mu}^{3} & \rightarrow & a_{t\mu}^{3}. \end{cases} \tag{4.A.3}$$

Consequently, terms with an odd number of time derivatives are forbidden. Moreover, it is worth mentioning that the remaining terms for the antiferromagnetic effective lagrangian are the same as those for the ferromagnetic one. This statement holds from considering $\tau\xi$,

$$\tau\xi : \begin{cases} a_{\mu}^{-} & \rightarrow & a_{\xi\mu}^{-} \\ a_{\mu}^{3} & \rightarrow & a_{\xi\mu}^{3}, \end{cases} \tag{4.A.4}$$

where ξ stands for elements of the point group which map points with opposite magnetisations, like that in (4.3.10b), together with T and τT as the symmetry generators.

The transformations $\tau\xi$ and τT, given by (4.A.4) and (4.A.3) respectively, where proposed in [18] as the macroscopic transformation for the antiferromagnetic spin waves. Notice that these transformations are slightly less restrictive than the ones we have, namely, $\tau\xi$, T and τT.

The introduction of the spin-orbit interaction does not invalidate the previous statements. Indeed, as mention before the differences between T and τ come from the time indices. However, spin-orbit sources have no time indices and, therefore, they transform trivially under τT.

Nevertheless, the statements above must be generalised in the presence of electromagnetic fields. The electromagnetic fields transform trivially under τ, and therefore, under τT the magnetic field, $\mathbf{B}$, changes sign. This implies that the invariants with an odd number of time derivatives plus magnetic fields are not allowed in the effective lagrangian for the antiferromagnetic spin waves. The remaining terms in the effective lagrangian are the same as the ones for the ferromagnetic spin waves.

4.B Mathematical Properties

In this appendix we discuss a few important technicalities which have been used through the chapter.

The projectors $P_\pm$ are introduced in sect. 4.2 in order to single out the magnetisation direction. They are given by

$$P_+ = \begin{pmatrix} 1 & & & \\ & 0 & & \\ & & \ddots & \\ & & & 0 \end{pmatrix} \quad , \qquad P_- = \begin{pmatrix} 0 & & & \\ & 0 & & \\ & & \ddots & \\ & & & 1 \end{pmatrix}, \tag{4.B.1}$$

and verify

$$tr(P_\pm S^a) = \pm s\delta^{a3}. \tag{4.B.2}$$

When two of these projectors are in a trace, we can split it in two pieces

$$tr\Big(P_\pm(\cdots)P_\pm(\cdots)\Big) = tr\Big(P_\pm(\cdots)\Big)tr\Big(P_\pm(\cdots)\Big). \tag{4.B.3}$$

This is immediate because the only non-zero element in the matrix $P_+(\cdots)P_+$ is the $(\cdots)_{11}$, or $(\cdots)_{(2s+1)\,(2s+1)}$ for the P_- case.

Another important property is that in any product of generators between two P_+ where at most two of them are different from S^3 the following substitution can be performed:

$$\begin{aligned} S^\alpha &\rightarrow \frac{\sqrt{2s}}{2}\,(\sigma^\alpha \oplus 0) \qquad\qquad (\alpha = 1,2) \\ S^3 &\rightarrow (s-1)\,(\mathbf{1}\oplus 0) + P_+, \end{aligned} \tag{4.B.4}$$

since in this case only the upper-left 2×2 matrix contributes to the trace. An analogous property holds for P_-.

In addition in section 4.2 the matrix $C = e^{-i\pi S^2}$ is introduced to implement the space and time inversions. Below we give some relevant properties of this matrix.

The time inversion implies [16]

$$C^\dagger S^a C = -(S^a)^T. \tag{4.B.5}$$

The action of C over the projectors is given by

$$C^\dagger P_+ C = P_-, \tag{4.B.6}$$

which follows from the fact that $P_\pm$ belong to the subspace spanned by arbitrary powers of S^3. We also have that

$$tr(P_+ S^{a_1} \cdots S^{a_n} P_+) \;\; = \;\; (-)^n tr(P_- S^{a_n} \cdots S^{a_1} P_-), \tag{4.B.7}$$

which follows immediately by inserting $C^\dagger C$ between the elements on the l.h.s. and using the properties above.

By using this property together with the clausure relations for the Pauli matrices,

$$\frac{1}{2}(\sigma_+)_{\alpha\beta}(\sigma_-)_{\gamma\delta} + \frac{1}{2}(\sigma_-)_{\alpha\beta}(\sigma_+)_{\gamma\delta} = -\delta_{\alpha\beta}\delta_{\gamma\delta} - \sigma^3_{\alpha\beta}\sigma^3_{\gamma\delta} + 2\delta_{\alpha\delta}\delta_{\gamma\beta}, \tag{4.B.8}$$

the relations $F_{\mu\nu} \sim a^+_\mu a^-_\nu - a^+_\nu a^-_\mu$ and $D_\mu a^-_\nu = D_\nu a^-_\mu$ mentioned in section 4.2 can be proved from the explicit representation (4.3.8).

4.C Fundamental Representation Formulation

In this appendix we point out the simplifications that occur for $s = 1/2$ which follow from the properties of the appendix 4.B.

All the invariants can be constructed in terms of

$$T(x) = U(x)\sigma^3 U^\dagger(x), \tag{4.C.1}$$

which transforms covariantly under $SU(2)$, their derivatives and topological terms, which are built out of a^3_μ alone. Notice that

$$a^3_\mu = tr(U^\dagger i\partial_\mu U \sigma^3). \tag{4.C.2}$$

Recall that T verifies

$$T^2 = 1 \qquad , \qquad trT = 0. \tag{4.C.3}$$

In the fundamental representation $P_+ = (\mathbf{1} + \sigma^3)/2$ and the building blocks are:

$$a_\mu^-(x) = \frac{1}{4} tr\left([U^\dagger i\partial_\mu U, \sigma_-]\sigma^3\right) = -\frac{i}{4} tr(U^\dagger \partial_\mu T U \sigma_-). \tag{4.C.4}$$

Let us consider the covariant derivative $D_\nu = \partial_\nu - i a_\nu^3$ on terms of the form (4.C.4),

$$tr(U^\dagger A U \sigma_-) \qquad , \qquad A \to g A g^\dagger \in \mathcal{L}(SU(2)), \tag{4.C.5}$$

where A transforms covariantly under $SU(2)$ and is in the Lie algebra. The result of the covariant derivative is

$$D_\nu tr(U^\dagger A U \sigma_-) = tr(U^\dagger \partial_\nu A U \sigma_-) - \frac{1}{2} tr(AT) tr(U^\dagger \partial_\nu T U \sigma_-). \tag{4.C.6}$$

Since all the terms can be derived from (4.C.4) the most general form of A is

$$A = \partial_{\mu_1} \cdots \partial_{\mu_n} T, \tag{4.C.7}$$

which leads us to write for the Ts

$$\begin{aligned} D_\nu tr(U^\dagger \partial_{\mu_1} \cdots \partial_{\mu_n} T U \sigma_-) &= tr(U^\dagger \partial_\nu \partial_{\mu_1} \cdots \partial_{\mu_n} T U \sigma_-) \\ &\quad - \frac{1}{2} tr(\partial_{\mu_1} \cdots \partial_{\mu_n} T T) tr(U^\dagger \partial_\nu T U \sigma_-). \end{aligned} \tag{4.C.8}$$

In order to get $SU(2)$ invariants we will have products of the form

$$\begin{aligned} &tr(U^\dagger A U \sigma_+) tr(U^\dagger B U \sigma_-) = \\ &\qquad \frac{1}{2}\left[tr(U^\dagger A U \sigma_+) tr(U^\dagger B U \sigma_-) + tr(U^\dagger A U \sigma_-) tr(U^\dagger B U \sigma_+)\right] \\ &\quad + \frac{1}{2}\left[tr(U^\dagger A U \sigma_+) tr(U^\dagger B U \sigma_-) - tr(U^\dagger A U \sigma_-) tr(U^\dagger B U \sigma_+)\right], \end{aligned} \tag{4.C.9}$$

which have been written as the sum of its symmetric and antisymmetric parts

Now the Pauli matrices $\sigma_\pm$ can be eliminated with the aid of the clausure relation (4.B.8). For the symmetric part it is immediate, leading to

$$-tr(AT) tr(BT) + 2tr(AB), \tag{4.C.10}$$

while for the antisymmetric part a little trick has to be used in order to be able to use the clausure relation: we perform in the first factor of each term the substitution $[\sigma^3, \sigma_\pm] = \pm 2\sigma_\pm$, and we obtain

$$\left[tr(U^\dagger A U [\sigma^3, \sigma_+]) tr(U^\dagger B U \sigma_-) + tr(U^\dagger A U [\sigma^3, \sigma_-]) tr(U^\dagger B U \sigma_+)\right] = -4tr([A, B]T). \tag{4.C.11}$$

Hence we conclude that for the $s = 1/2$ case all the invariants can be constructed from products of the following traces:

$$\begin{array}{l} tr\,(\partial_{\mu_1}\cdots\partial_{\mu_n}T\partial_{\nu_1}\cdots\partial_{\nu_m}T) \\ tr\,([\partial_{\mu_1}\cdots\partial_{\mu_n}T,\partial_{\nu_1}\cdots\partial_{\nu_m}T]T) \end{array} \qquad (n,m=0,1,2,\ldots), \tag{4.C.12}$$

which correspond to take into account the symmetric and antisymmetric parts of the product $\partial_{\mu_1}\cdots\partial_{\mu_n}T\partial_{\nu_1}\cdots\partial_{\nu_m}T$ respectively.

4.D Equivalence with the $O(3)$-*sigma model*

Let us next make contact with the so called $O(3)$-*sigma model* formulation, which uses a unitary vector $n^a(x)$ as the basic building block of the effective lagrangian. Recall first that a formula like (4.C.4) exist for any representation,

$$a_\mu^-(x) = \frac{1}{2s}tr\left([U^\dagger i\partial_\mu U, S_-]P_+\right) = -\frac{i}{2s}tr(U^\dagger\partial_\mu T_+ U S_-) \quad , \quad T_+ = UP_+U^\dagger. \tag{4.D.1}$$

We can relate our notation with the standard one of the unitary vector $n^a(x)$ by noting that

$$T(x) = U(x)S^3U^\dagger(x) = n^a(x)S^a. \tag{4.D.2}$$

It is easy to check that $\mathbf{n}^2 = 1$ and clearly n^a transforms like a vector. Recall next that P_+ can be written as

$$P_+ = \sum_{n=0}^{2s} a_n (S^3)^n \tag{4.D.3}$$

since $\{(S^3)^n\}$ is a bases of the subspace of diagonal matrices. Hence

$$T_+ = \sum_{n=0}^{2s} a_n (US^3U^\dagger)^n = \sum_{n=0}^{2s} a_n T^n. \tag{4.D.4}$$

For an arbitrary representation the covariant derivative (4.3.5) on a term like (4.D.1) yields a formula similar to that in (4.C.6),

$$D_\nu tr(U^\dagger AUS_-) = tr(U^\dagger\partial_\nu AUS_-) - \frac{1}{s}tr(AT)tr(U^\dagger\partial_\nu T_+ US_-), \tag{4.D.5}$$

where A is made of an arbitrary number of derivatives on T_+. The possible invariants will be made out of products of the form

$$\begin{aligned} tr(U^\dagger AUS_+)tr(U^\dagger BUS_-) = & \\ & \frac{1}{2}\left[tr(U^\dagger AUS_+)tr(U^\dagger BUS_-) + tr(U^\dagger AUS_-)tr(U^\dagger BUS_+)\right] \\ & + \frac{1}{2}\left[tr(U^\dagger AUS_+)tr(U^\dagger BUS_-) - tr(U^\dagger AUS_-)tr(U^\dagger BUS_+)\right]. \end{aligned} \tag{4.D.6}$$

Taking into account that $U \in SU(2)$ the property below follows:

$$(US^aU^\dagger)(US^aU^\dagger) = (S^a)(S^a), \tag{4.D.7}$$

which can be rewritten as

$$\frac{1}{2}\Big[(US_+U^\dagger)(US_-U^\dagger) + (US_-U^\dagger)(US_+U^\dagger)\Big] = -(T)(T) + \frac{1}{2}\Big[(S_+)(S_-) + (S_-)(S_+)\Big] + (S^3)(S^3). \tag{4.D.8}$$

Using (4.D.8) the symmetric part of (4.D.6) is

$$-tr(AT)tr(BT) + \frac{1}{2}\Big[tr(AS_+)tr(BS_-) + tr(AS_-)tr(BS_+)\Big] + tr(AS^3)tr(BS^3), \tag{4.D.9}$$

whereas for the antisymmetric part the same trick as in appendix 4.C has to be used, i.e., change $S_\pm = \pm[S^3, S_\pm]$ in the first factor of each term. We obtain

$$\frac{1}{2}\Big[tr(U^\dagger AU[S^3, S_+])tr(U^\dagger BUS_-) + tr(U^\dagger AU[S^3, S_-])tr(U^\dagger BUS_+)\Big] = \frac{1}{2}\Big[tr([A,T]S_+)tr(BS_-) + tr([A,T]S_-)tr(BS_+)\Big] + tr([A,T]S^3)tr(BS^3). \tag{4.D.10}$$

Finally it has been shown that all the invariants can be written in terms of T and therefore in terms of $n^a(x)$. The reverse is also true. Suppose we have written our effective lagrangian in terms of derivatives of n^a. From (4.D.2)

$$n^a = \frac{3}{s(s+1)(2s+1)} tr(S^3U^\dagger S^aU). \tag{4.D.11}$$

Consider a vector of the form

$$v^a = tr(AU^\dagger S^aU) \qquad , \qquad A \in \mathcal{L}(SU(2)), \tag{4.D.12}$$

$$\partial_\mu v^a = tr(\partial_\mu AU^\dagger S^aU) + tr([U^\dagger \partial_\mu U, A]U^\dagger S^aU). \tag{4.D.13}$$

Since any vector will be obtained by applying several derivatives on n^a, A in (4.D.12) will only contain $U^\dagger\partial_\mu U$ and its derivatives, which can be written in terms of our basic fields $a^\pm_\mu, a^3_\mu$. The remaining dependence on U is through $U^\dagger S^aU$ only which will cancel out upon contraction with other vectors, according to (4.D.7), in order to build a scalar lagrangian.

So far we have been talking about invariant terms in the effective lagrangian. It is not true however that terms which are invariant up to a total derivative, like a^3_μ, can

be written in terms of n^a in a local form. However, we can write them locally in T_+ or n^a if we introduce an extra dimension in the following way. We interpolate smoothly the Goldstone fields $\pi^\alpha(x) \to \pi^\alpha(x,\lambda)$, $\lambda \in [0,1]$ in such a way that $\pi^\alpha(x,1) = \pi^\alpha(x)$ and $\pi^\alpha(x,0) = 0$. Let us concentrate on a_0^3 which is the only one which arises in our effective lagrangian. It is very easy to check that

$$a_0^3 = \frac{1}{s}\int_0^1 d\lambda \epsilon^{\alpha\beta} tr(T_+ \partial_\alpha T_+ \partial_\beta T_+) \sim \int_0^1 d\lambda \epsilon^{\alpha\beta}\epsilon_{abc} n^a \partial_\alpha n^b \partial_\beta n^c, \tag{4.D.14}$$

$(\alpha, \beta = 0, \lambda)$. The second equality follows upon using (4.D.2) and performing the trace. The final result must be a scalar function of n^a, $\partial_\alpha n^b$ and $\partial_\beta n^c$ antisymmetric under the exchange of α and β, being (4.D.14) the only possibility. To our knowledge this term was first written in the last form in [19] (see also [6]), whereas we have not been able to locate the two previous forms in the literature. We stress again that only the form that we use in our effective lagrangian is local. It is usual however to find (4.D.14) with a rather different aspect, namely,

$$a_0^3 \sim A^a(n)\partial_0 n^a \qquad , \qquad n^a = \epsilon_{abc}\frac{\partial A^b}{\partial n^c}, \tag{4.D.15}$$

where the second equation gives A^a as an implicit function of n^b [20, 24]. It is easy to check that the last expression of (4.D.14) and (4.D.15) give rise to the same equations of motion.

4.E Coupling to Constant Electric and Magnetic Fields

In this appendix we present a further example on how the effective lagrangian for spin waves coupled to electromagnetism can be used to obtain qualitative information on the system.

Let us suppose that the system is exposed to constant electric and magnetic fields and address the question on how the low momentum dispersion relations of the spin waves change in the ferromagnetic and antiferromagnetic case. For simplicity we assume that the magnetic field is on the third direction and the electric field in the $z - \bar{z}$ plane, and fix their relative size, which is now arbitrary, as $eaE/J \sim ea^2B$. Recall that the Pauli term must be counted as $\mu B/J \sim 10ea^2B$. We also neglect terms induced by spin-orbit or magnetic dipole interactions which explicitly break the $SU(2)$ symmetry

since it is straightforward to take them into account if desired. We shall focus in the leading effects due to higher order terms, since those due to the lowest order terms are well known and will be easily reproduced.

For the ferromagnetic case the leading corrections due to higher order terms arise from

$$\begin{array}{l}(a_z^+ a_{\bar{z}}^- + a_z^- a_{\bar{z}}^+) E^z E^{\bar{z}} \\ a_3^+ a_3^- E^z E^{\bar{z}} \\ a_z^+ a_z^- E^z E^z + a_{\bar{z}}^- a_{\bar{z}}^+ E^{\bar{z}} E^{\bar{z}} \\ (a_z^+ a_3^- + a_z^- a_3^+) E^{\bar{z}} E^{\bar{z}} + (a_{\bar{z}}^- a_3^+ + a_{\bar{z}}^+ a_3^-) E^z E^z \\ (a_z^+ a_{\bar{z}}^- + a_z^- a_{\bar{z}}^+) B^3 B^3 \\ a_3^+ a_3^- B^3 B^3,\end{array} \tag{4.E.1}$$

which together with the contributions of the leading order lagrangian in (4.4.3) lead to

$$\begin{aligned}\omega \;=\; & \mu B^3 + \frac{2}{m}[1 + \epsilon_1 E^z E^{\bar{z}} + \beta_1 B^3 B^3] k^z k^{\bar{z}} \\ & + \frac{1}{2\gamma m}[1 + \epsilon_2 E^z E^{\bar{z}} + \beta_2 B^3 B^3](k^3)^2 \\ & + \epsilon_3[(E^z k^{\bar{z}})^2 + (E^{\bar{z}} k^z)^2] \\ & + 2\epsilon_4[(E^z E^z k^z) + (E^{\bar{z}} E^{\bar{z}} k^{\bar{z}})] k^3.\end{aligned} \tag{4.E.2}$$

The effect of our particular constant electric and magnetic fields is, apart from creating the well known energy gap proportional to the magnetic field, (i) renormalising $1/m$ and γ and (ii) producing further anisotropies in the dispersion relation (due to ϵ_3 and ϵ_4), which vanish if the electric field vanishes.

For the antiferromagnetic case the leading corrections due to higher order terms arise from the same terms as in the ferromagnetic case (4.E.1) plus the following extra terms,

$$\begin{array}{l}a_0^+ a_0^- E^z E^{\bar{z}} \\ a_0^+ a_0^- B^3 B^3 \\ i[(a_0^+ a_z^- + a_0^- a_z^+) E^z B^3 - (a_0^- a_{\bar{z}}^+ + a_0^+ a_{\bar{z}}^-) E^{\bar{z}} B^3,\end{array} \tag{4.E.3}$$

which together with the contributions of the leading order lagrangian (4.5.3) lead to

$$\begin{aligned}\omega_{\pm} &= \pm\mu B^3 \pm i\eta[(E^z k^{\bar{z}}) - (E^{\bar{z}} k^z)]B^3 \\ &\quad + \Big[4v^2[1 + \epsilon_1 E^z E^{\bar{z}} + \beta_1 B^3 B^3]k^z k^{\bar{z}} \\ &\quad + (\gamma v)^2[1 + \epsilon_2 E^z E^{\bar{z}} + \beta_2 B^3 B^3](k^3)^2 \\ &\quad + \epsilon_3[(E^z k^{\bar{z}})^2 + (E^{\bar{z}} k^z)^2] \\ &\quad + 2\epsilon_4[(E^z E^z k^z) + (E^{\bar{z}} E^{\bar{z}} k^{\bar{z}})]k^3\Big]^{1/2}.\end{aligned} \tag{4.E.4}$$

The effect of our particular constant electric and magnetic fields is, apart from providing the well known "chemical potential" term proportional to the magnetic field, (i) renormalising v and γ, (ii) producing further anisotropies in the dispersion relation (due to ϵ_3 and ϵ_4), which vanish if the electric field vanishes, and (iii) producing a momentum dependent distinction between the two components of the spin wave (due to η). We find the latter effect particularly interesting. Notice that it requires both the electric and magnetic fields be differnt from zero.

Bibliography

[1] J. Goldstone, *Nuovo Cim.* **19** (1961) 145.

[2] G. S. Guralnik, C. R. Hagen and T. W. B. Kibble, *"Advances in Particle Physics"*, Vol.2, p.567, ed. R. L. Cool and R. E. Marshak (Willey, New York, 1968).

[3] H. B. Nielsen and S. Chada, *Nucl. Phys.* **B105** (1976) 445.

[4] P. W. Anderson, *"Basic Notions of Condensed Matter Physics"* (Benjamin, Menlo Park, 1984).

[5] S. Weinberg, *Phys. Rev.* **166** (1968) 1568;

S. Weinberg, *Physica* **A96** (1979) 327.

[6] H. Leutwyler, *Phys. Rev.* **D49** (1994) 3033.

[7] S. Coleman, J. Wess and B. Zumino, *Phys. Rev.* **177** (1969) 2239;

C. Callan, S. Coleman, J. Wess and B. Zumino, *Phys. Rev.* **177** (1969) 2247.

[8] J. Gasser and H. Leutwyler, *Ann. Phys. (N.Y.)* **158** (1984) 142.

[9] H. Leutwyler, TASI **91**, 97-138.

[10] H. Leutwyler, *Helv. Phys. Acta* **70** (1997) 275.

[11] S. Chakravarty, B. I. Halperin and D. R. Nelson, *Phys. Rev.* **B39** (1989) 2344.

[12] P. Hasenfratz and F. Niedermayer, *Z. Physik* **B92** (1993) 91;

P.Hasenfratz and H. Leutwyler, *Nucl. Phys.* **B343** (1990) 241.

[13] J. M. Román and J. Soto, *"Spin Wave Mediated Non-reciprocal Effects in Antiferromagnets"*, Univ. of Barcelona, preprint no. UB-ECM-PF 97/24, cond-mat/9709299.

[14] R. R. Birss, *"Symmetry and Magnetims"* (North Holland, Amsterdam, 1964).

[15] Landolt-Börnstein, New Series III/27f3 p.128.

[16] A. Galindo and P. Pascual, *"Quantum Mechanics"* (Springer, Berlin, 1990).

[17] W. Apel and Yu. A. Bychkov, *Phys. Rev. Lett.* **79** (1997) 3792 .

R. Ray and J. Soto, *"Field Theoretical Approach to Quantum Hall Ferromagnets"*, cond-mat/9708067.

[18] C. P. Burgess, *"An Introduction to Effective Lagrangians and their Applications"* (Course given in Lausanne, Switzerland, June 1995).

[19] G. E. Volovik, *J. Phys.* **C20** (1987) L83.

[20] K. Moon *et al.*, *Phys. Rev.* **B51** (1995) 5138.

[21] T. Moriya, *Phys. Rev.* **120** (1960) 91.

[22] N. W. Ashcroft and N. D. Mermin, *"Solid State Physics"* (Saunders College Publishing, Forth Worth, 1976);

C. Kittel, *"Introduction to Solid State Physics"* (John Wiley & Sons, Inc., New York, 1971);

G. Burns, *"Solid State Physics"* (Academic Press, Inc., San Diego, 1985).

[23] C. P. Hofmann, *"Thermodynamic Behavior of the $O(3)$ Ferromagnet"*, Universität Bern, prepint no. BUTP-97/31.

[24] E. Fradkin, *"Field Theories of Condensed Matter Systems"* (Addison-Wesley, Reading, MA, 1990).

Chapter 5

Spin Wave Mediated Non-reciprocal Effects in Antiferromagnets

By using an effective field theory for the electromagnetic interaction of spin waves, we show in this chapter that, in certain antiferromagnets, the latter induce non-reciprocal effects in the microwave region, which should be observable in the second harmonic generation and produce gyrotropic birefringency. We calculate the various (non-linear) susceptibilities in terms of a few parameters the order of magnitude of which is under control.

5.1 Introduction

The response of magnetic materials to electromagnetic fields gives rise to a reach variety of interesting phenomena [1]. In particular, non-reciprocal optical effects in antiferromagnets have received considerable attention during the last years [2, 3]. The possible existence of certain phenomena, like second harmonic generation (SHG) or gyrotropic birefringency (GB), is dictated by the magnetic group of the given material, which may (or may not) allow suitable (non-linear) susceptibilities to be different from zero [4, 5]. The optical wavelengths induce atomic transitions which provide a potential microscopic mechanism to obtain non-vanishing susceptibilities. Indeed, this is the case for the observed non-reciprocal effects in Cr_2O_3 [2, 3]. However, alternative mechanisms to produce such effects cannot be ruled out *a priori*, and may even become dominant at certain wavelengths. It is our aim to demonstrate that this is indeed the case for certain antiferromagnets when the electromagnetic fields are in the microwave region. This region is very sensitive to collective magnetic effects which makes a field theoretical description appropriate.

The low temperature low energy properties of antiferromagnets (with spontaneous staggered magnetization) are dominated by spin waves. The spin wave dynamics at low momenta and energy is very much constrained by group theoretical considerations [6]. The symmetry breaking pattern $SU(2) \to U(1)$ tells us that the spin waves must transform under a non-linear realisation of $SU(2)$ [7]. In addition to that the space group and time reversal must be respected by the dynamics. The continuum approach ensures that it is enough to consider the rotational part of the space group, namely, the point group, and the primitive translations as well as time reversal. A systematic description of the spin wave dynamics fully exploiting the above group theoretical constraints has been provided in the previous chapter [8].

In this chapter we apply the general framework described before [8] to work out the electromagnetic response of certain antiferromagnets in the microwave region. We have chosen a crystal with no primitive translations mapping points with opposite magnetisations. The point group is taken to be $\bar{3}m$, but repeating the analysis for any other point group is straightforward. This choice is motivated by the Cr_2O_3 crystal, which shows interesting non-reciprocal effects in the optical region as mention before. We have calculated the linear and non-linear electric and magnetic susceptibilities, which turn out to depend non-trivially on the frequency of the incoming radiation. In parti-

cular non-reciprocal phenomena in the SHG as well as the GB are predicted to occur. These results apply to any antiferromagnet (with spontaneous staggered magnetisation) of arbitrary spin and crystal point group $\bar{3}m$ such that the magnetic ions lie on the z-axis and no primitive translation mapping points with opposite magnetisation exists.

In order to simplify the notation we will take $\hbar = c = 1$, which lead to a relativistic notation. So $x = (t, \mathbf{x})$ and $q = (\omega, \mathbf{k})$. Subindices $\mu = 0, 1, 2, 3$, where the first one represents the time component. Furthermore we work with holomorphic coordenates $z = x + iy$ and $\bar{z} = x - iy$. We distribute the chapter as follows. In section 5.2 we briefly review some basic aspects of electromagnetic wave propagation in media in order to explain the appearance of non-reciprocal effects in SHG as well as GB. In section 5.3 we quickly review the framework described in full detail in the previous chapter [8]. In section 5.4 we present the effective lagrangian. In section nre:interaction we work out the effective action which describes the response to the electromagnetic field and give the (non-linear) electric and magnetic susceptibilities. Section 5.6 is devoted to a discussion. Finally, in the appendix we list all the terms which are not displayed sections 5.4 and 5.5 in order to make the presentation simpler.

5.2 Electromagnetic Waves Propagation in Media

It is the aim of this section to briefly review some features of electromagnetic wave propagation in media, which are relevant for the rest of the chapter. In particular the phenomena of gyrotropic birefringence (GB) and second harmonic generation (SHG), in connection with non-reciprocal effects, which arise due to time reversal violation in the medium.

Let us recall the Maxwell equations in insulating and chargeless media

$$\begin{aligned} \nabla \mathbf{D} &= 0 \\ \nabla \times \mathbf{H} &= \partial_0 \mathbf{D} \\ \nabla \times \mathbf{E} &= -\partial_0 \mathbf{B} \\ \nabla \mathbf{B} &= 0, \end{aligned} \tag{5.2.1}$$

which are to be supplemented with the constitutive equations

$$\begin{aligned} \mathbf{D} &= \mathbf{E} + \mathcal{P} \\ \mathbf{H} &= \mathbf{B} - \mathcal{M}, \end{aligned} \tag{5.2.2}$$

where $\mathcal{P}$ and $\mathcal{M}$ are the electric and magnetic response of the medium respectively. $\mathcal{P}$ and $\mathcal{M}$ are functionals of the electric and magnetic fields and, of course, depend on the physical properties of the medium. From the two equations above we obtain

$$\nabla \times \nabla \times \mathbf{E} + \partial_0^2 \mathbf{E} = -\left(\partial_0^2 \mathcal{P} + \nabla \times \partial_0 \mathcal{M}\right), \tag{5.2.3}$$

which is going to be the basic equation in our discussion. Once $\mathcal{P}$ and $\mathcal{M}$ are given this equation describes the propagation of electromagnetic waves in the medium.

5.2.1 Gyrotopic birefringence

For definiteness, consider first the linear response of a homogeneous medium to electric fields only. In this case, the most general form for the electric response is [9]

$$\mathcal{P}^a(z) = \int dx \chi^{ab}(z-x) E^b(x), \tag{5.2.4}$$

where x and z are space-time vectors. The tensor $\chi^{ab}(z-x)$ depends not only on time, but also on space coordinates, which caracterises the spatial dispersive medium. We shall make the standard assumption that it varies slowly over the medium. This is equivalent to an expansion of the tensor $\chi^{ab}(\omega, \mathbf{k})$ in powers of $\mathbf{k}$ in momentum space. We obtain

$$\mathcal{P}^a(t, \mathbf{z}) = \int dt' \chi^{ab}(t-t') E^b(t', \mathbf{z}) + \int dt' \gamma^{abc}(t-t') \partial_c E^b(t', \mathbf{z}) + \cdots. \tag{5.2.5}$$

The first and second term in the electric response are the polarisation and the quadrupolar moment respectively. Notice that the tensors associated to each order of the multipole expansion depend only on the frequency of the electromagnetic wave.

Let us see next how some terms in the multipole expansion of both the electric and magnetic responses give rise to qualitatively new observable effects. Consider (5.2.5) together with the leading term in the multipole expansion of the magnetic response (magnetoelectric term)

$$\begin{aligned} \mathcal{P} &= \chi^{ab} E^b + \gamma^{abc} \partial_c E^b \\ \mathcal{M} &= \alpha^{ab} E^b \end{aligned} \tag{5.2.6}$$

Upon substituting these expressions in (5.2.3), the quadrupolar and magnetoelectric term give rise to the so-called gyrotropic birefringence as we shall show next. Consider the plane wave solution, $E^a(x) = E^a(q) e^{-iqx} + E^a(-q) e^{iqx}$, of the equation (5.2.3). Then $E^b(q)$ fulfills

$$\left[n^2 \delta^{ab} - \left[\epsilon^{ab} - n^c \left(\epsilon^{acd} \alpha^{db} - i\omega \gamma^{abc}\right)\right] - n^a n^b\right] E^b(q) = 0, \tag{5.2.7}$$

where $n^a \equiv k^a/\omega$ gives the propagation direction and its modulus the refraction index (recall that $q = (\omega, \mathbf{k})$). Suppose first that the quadrupolar moment, γ^{abc}, and the magnetoelectric term, α^{bd}, are zero. Non trivial solutions to this equation arise from the condition that the determinant of the matrix on which the electric field acts vanishes. The anisotropy of the permitivity tensor ϵ^{ab} is generally responsible for this condition to yield two values of the refraction index for each propagation direction, which is known as birefringence. Namely, two different plane waves propagate in each direction with two different polarisations and two different velocities [10]. If the quadrupolar and magnetoelectric terms are restored, they enter eq. (5.2.7) through an effective permitivity tensor, $\epsilon^{ab} - n^c \left(\epsilon^{acd}\alpha^{db} - i\omega\gamma^{abc}\right)$, with a linear dependence on the propagation direction, which is known as gyrotropic birefringence [5]. In particular, the equations governing the propagation in directions $\mathbf{n}$ and $-\mathbf{n}$ are different, which implies that the GB is a non-reciprocal effect, since these propagation directions are related by time reversal.

5.2.2 Second harmonic generation

Let us consider next the non-linear response of the system to electric fields. Thus we have to add to (5.2.4) new quadratic, cubic, ..., terms [11]

$$\mathcal{P}^a(z) = \int dx \chi^{ab}(z-x)E^b(x) + \int dxdy \chi^{abc}(z-x, z-y)E^b(x)E^c(y) + \cdots. \quad (5.2.8)$$

In particular, the quadratic term in the above equation leads to the appearance of second harmonic generation. Whenever exists in the field $E^a(x)$ a contribution of frequency ω the electric response will have in addition two contributions, one of zero frequency and another one of frequency 2ω. Then, the electric response will be, in general, a superposition of plane waves with frequencies multiple of ω

$$\mathcal{P}^a(z) = \mathcal{P}^a_0(z) + \mathcal{P}^a_q(z) + \mathcal{P}^a_{2q}(z) + \cdots, \quad (5.2.9)$$

leading, in turn, to a similar superposition for the electric field solution of eq. (5.2.3). The contribution to SHG comes from $\mathcal{P}^a_{2q}(z)$ in the expression above, which to lowest order can be written as

$$\begin{aligned} \mathcal{P}^a_{2q}(z) &= P^a(2q)e^{-iqz} + P^a(-2q)e^{iqz} \\ P^a(2q) &= \chi^{abc}(q,q)E^b(q)E^c(q). \end{aligned} \quad (5.2.10)$$

In order to be more explicit consider the non-linear expressions for the electric and magnetic responses

$$\begin{aligned} \mathcal{P}^a &= \chi^{ab}E^b + \chi^{abc}E^bE^c \\ \mathcal{M}^a &= \mu^{abc}E^bE^c, \end{aligned} \tag{5.2.11}$$

Once they are introduced in (5.2.3) we have a complicated non-linear equation. However, the non-linear terms are usually small. Therefore, if we pass the linear part of the response to the l.h.s. we can calculate the electric field solution perturbatively, $\mathbf{E} = \mathbf{E}_{(0)} + \mathbf{E}_{(1)} + \cdots$. $\mathbf{E}_{(0)}$ is the solution of the homogeneous equation (eq. (5.2.7) without the quadrupolar and magnetoelectric terms), i.e., a monochromatic plane wave of frequency ω. Then $\mathbf{E}_{(1)}$ follows from the equation

$$\bar{\omega}^2\left[\bar{n}^2\delta^{ab} - \epsilon^{ab} + \bar{n}^a\bar{n}^b\right]E^b_{(1)}(\bar{q})e^{-i\bar{q}x} = -(2\omega)^2\left[\chi^{abc} + n^d\epsilon^{ade}\mu^{ebc}\right]E^b_{(0)}(q)E^c_{(0)}(q)e^{-i2qx}. \tag{5.2.12}$$

It is clear that the solution of this equation requires in the l.h.s. an electric field of frequency $\bar{\omega} = 2\omega$. This is called second harmonic generation. Notice, moreover, that the second term in the r.h.s. depends linearly on the direction of the wave number. Then when this term is non-vanishing we have non-reciprocal effects in the second harmonic generation.

5.2.3 Generalised susceptibilities

In the discussion above we have presented the simplest situations which lead to non-reciprocal effects. In magnetic materials, as the one we are interested in, $\mathcal{P}$ and $\mathcal{M}$ depend both on the electric and magnetic fields. In this case, since $\mathbf{B} = \mathbf{n} \times \mathbf{E}$, the non-reciprocal effects can be obtained from terms depending on the magnetic field in both the electric and magnetic responses [12, 13]. Furthermore, the (generalised) susceptibilities are constrained by the magnetic point group of the crystal. Since we are considering GB and SHG, which are dynamical effects, only the elements without the time reversal operator of the magnetic group are to be considered [2, 4]. For Cr_2O_3 with the spins aligned in the third direction this is the 32 group. The allowed linear susceptibilities (relevant for the GB) are

$$\begin{aligned} P^z &= \chi_E^{z\bar{z}} E^z + \chi_B^{z\bar{z}} B^z \\ P^3 &= \chi_E^{33} E^3 + \chi_B^{33} B^3 \\ M^z &= \gamma_E^{z\bar{z}} E^z + \gamma_B^{z\bar{z}} B^z \\ M^3 &= \gamma_E^{33} E^3 + \gamma_B^{33} B^3, \end{aligned} \tag{5.2.13}$$

and the bilinear ones (relevant for the SHG)

$$\begin{aligned} P^z &= \chi_{EE}^{zzz} E^{\bar{z}} E^{\bar{z}} + 2\chi_{EE}^{z\bar{z}3} E^z E^3 \\ &\quad + \chi_{EB}^{zzz} E^{\bar{z}} B^{\bar{z}} + \chi_{EB}^{z\bar{z}3} E^z B^3 + \chi_{EB}^{z3\bar{z}} E^3 B^z \\ &\quad + \chi_{BB}^{zzz} B^{\bar{z}} B^{\bar{z}} + 2\chi_{BB}^{z\bar{z}3} B^z B^3 \\ P^3 &= 2\chi_{EE}^{3\bar{z}z} E^z E^{\bar{z}} + \chi_{EB}^{3\bar{z}z} (E^z B^{\bar{z}} - E^{\bar{z}} B^z) + 2\chi_{BB}^{3\bar{z}z} B^z B^{\bar{z}} \\ M^z &= \gamma_{EE}^{zzz} E^{\bar{z}} E^{\bar{z}} + 2\gamma_{EE}^{z\bar{z}3} E^z E^3 \\ &\quad + \gamma_{EB}^{zzz} E^{\bar{z}} B^{\bar{z}} + \gamma_{EB}^{z\bar{z}3} E^z B^3 + \gamma_{EB}^{z3\bar{z}} E^3 B^z \\ &\quad + \gamma_{BB}^{zzz} B^{\bar{z}} B^{\bar{z}} + 2\gamma_{BB}^{z\bar{z}3} B^z B^3 \\ M^3 &= 2\gamma_{EE}^{3\bar{z}z} E^z E^{\bar{z}} + \gamma_{EB}^{3\bar{z}z} (E^z B^{\bar{z}} - E^{\bar{z}} B^z) + 2\gamma_{BB}^{3\bar{z}z} B^z B^{\bar{z}}. \end{aligned} \tag{5.2.14}$$

In the remaining sections we shall calculate the contributions to the generalised susceptibilities above due to the spin wave dynamics. We will start with a local effective lagrangian describing the interaction between spin waves and electromagnetic fields. Upon integrating out the spin waves we obtain a non-local effective action for the electromagnetic fields, which is equivalent to having a free energy [12], taking into account that $L_{int} = -H_{int}$. The electric and magnetic response, and hence all the (generalised) susceptibilities, can be easily obtained as follows:

$$P^a = \frac{\delta S_{\mathit{eff}}}{\delta E^a} \quad , \quad M^a = \frac{\delta S_{\mathit{eff}}}{\delta B^a}. \tag{5.2.15}$$

5.3 Building Blocks

In this section we present the basic building blocks in the construction of an effective lagrangian for the interaction between the spin waves and electromagnetic fields, and their transformations under the relevant symmetries. The method we follow has been

thoroughly described in the previous chapter [8]. Here we shall give a brief overview of it.

As it was mentioned in the introduction the spin waves are the lowest lying excited states of the antiferromagnetic ground state associated to the spontaneous symmetry breaking $SU(2) \to U(1)$. This tells us that the associated field, $U(x)$, is an element of the coset space $SU(2)/U(1)$ [7], which transforms under $SU(2)$ as follows:

$$U(x) \to gU(x)h^{\dagger}(g,U), \tag{5.3.1}$$

where $g \in SU(2)$ and $h \in U(1)$ is a local ($U(x)$ dependent) element which restores $gU(x)$ to the coset space. If the alignment direction of the local spin is the third direction $U(x)$ can be written as

$$U(x) = \exp\left\{\frac{i\sqrt{2}}{f_\pi}\left[\pi^1(x)S^1 + \pi^2(x)S^2\right]\right\}, \tag{5.3.2}$$

where $\pi^i(x)$ are the spin wave fields. These fields in the complex representation have the form $\pi^{\pm} = (\pi^1 \pm i\pi^2)/\sqrt{2}$ and the generators are written as $S_{\pm} = S^1 \pm iS^2$.

In addition to the continuous $SU(2)$ transformations the action must be invariant under the space-time transformations. In our case we take the Cr_2O_3 as the underlying crystal in which the spin waves propagate. Cr_2O_3 enjoys the crystallographic point group $\bar{3}m$. The transformation properties of the $U(x)$ field under the $\bar{3}m \otimes T$ elements are

$$\begin{array}{rrcl} C_{3z}^{+}: & U(x) & \to & g_3 U(x) h_3^{\dagger} \\ I: & U(x) & \to & U(x) C h_I^{\dagger} \\ \sigma_y: & U(x) & \to & g_2 U(x) h_2^{\dagger} \\ T: & U(x) & \to & U(x) C h_t^{\dagger} \end{array} \quad , \quad \begin{array}{l} C = e^{-i\pi S^2} \\ C^{\dagger} = -C. \end{array} \tag{5.3.3}$$

The nontrivial transformation under I is due to the fact that this particular transformation maps points with opposite local magnetisation in the antiferromagnetic ground state. The primitive translations act trivially on $U(x)$ and have not been displayed.

The spin-orbit is an important interaction which produces a gap in the spectrum of the spin waves because it breaks explicitly the $SU(2)$ symmetry. The breaking part is given by some additional terms in the Heisenberg hamiltonian [14],

$$H = \sum_{<i,j>} J_{ij}\mathbf{S}_i\mathbf{S}_j + \sum_{<i,j>} \mathbf{D}_{ij}(\mathbf{S}_i \times \mathbf{S}_j) + \sum_{<i,j>} M_{ij}^{ab} S_i^a S_j^b, \tag{5.3.4}$$

where the tensors D_{ij}^a and M_{ij}^{ab} break the $SU(2)$ symmetry. The order of magnitude of such tensors is $D^a \sim (\Delta g/g)J$ and $M^{ab} \sim (\Delta g/g)^2 J$, where for Cr_2O_3, $\Delta g \sim 10^{-2} g$ [15].

In order to introduce them in the effective theory we take their local limit and promote them to sources with proper transformations under $SU(2)$. By combining these sources with the $SU(2)$ generators we obtain objects which transform covariantly under SU(2),

$$\begin{array}{rcl} D_{pq} \equiv D^a_{pq} S^a & \rightarrow & g D_{pq} g^\dagger \\ M \equiv M^{ab}(S^a \otimes S^b + S^b \otimes S^a) & \rightarrow & (g \otimes g) M (g^\dagger \otimes g^\dagger). \end{array} \tag{5.3.5}$$

Finally they must be fixed to their more general form compatible with the point group symmetry, namely,

$$\begin{array}{ll} D_{zz} = D^-_{zz} S_+ & \\ D_{\bar{z}\bar{z}} = D^+_{\bar{z}\bar{z}} S_- & D^-_{zz} = -D^+_{\bar{z}\bar{z}} \\ & \\ D_{3z} = D^+_{3z} S_- & \\ D_{3\bar{z}} = D^-_{3\bar{z}} S_+ & D^+_{3z} = -D^-_{3\bar{z}} \end{array}$$

$$M = M^{-+}(S_+ \otimes S_- + S_- \otimes S_+) + M^{33}(S^3 \otimes S^3). \tag{5.3.6}$$

Therefore the objects from which we construct our theory are the spin waves given by $U(x)$, the derivatives, ∂_μ, and the spin-orbit tensors, D^a_{ij} and M^{ab}_{ij}. Let us arrange them in a simple form which provides us elements with easier transformations properties under $SU(2)$

$$\begin{array}{rcl} U^\dagger(x) i\partial_\mu U(x) & = & a^-_\mu(x) S_+ + a^+_\mu(x) S_- + a^3_\mu(x) S^3 \\ U^\dagger(x) D_{pq} U(x) & = & d^-_{pq}(x) S_+ + d^+_{pq}(x) S_- + d^3_{pq}(x) S^3 \\ \Big(U^\dagger(x) \otimes U^\dagger(x)\Big) M \Big(U(x) \otimes U(x)\Big) & = & m^{--}(x)(S_+ \otimes S_+) \\ & + & m^{++}(x)(S_- \otimes S_-) \\ & + & m^{33}(x)(S^3 \otimes S^3) \\ & + & m^{-+}(x)(S_+ \otimes S_- + S_- \otimes S_+) \\ & + & m^{-3}(x)(S_+ \otimes S^3 + S^3 \otimes S_+) \\ & + & m^{+3}(x)(S_- \otimes S^3 + S^3 \otimes S_-). \end{array} \tag{5.3.7}$$

From (5.3.1) the transformation properties under $SU(2)$ for the coefficients of the generators are

$$\begin{array}{rcl} a^-_\mu(x) & \to & e^{i\theta(x)}a^-_\mu(x) \\ a^3_\mu(x) & \to & a^3_\mu(x)+\partial_\mu\theta(x) \end{array} \tag{5.3.8a}$$

$$\begin{array}{rcl} d^-_{pq}(x) & \to & e^{i\theta(x)}d^-_{pq}(x) \\ d^3_{pq}(x) & \to & d^3_{pq}(x) \end{array} \qquad \begin{array}{rcl} m^{--}(x) & \to & e^{2i\theta(x)}m^{--}(x) \\ m^{-3}(x) & \to & e^{i\theta(x)}m^{-3}(x) \\ m^{-+}(x) & \to & m^{-+}(x) \\ m^{33}(x) & \to & m^{33}(x), \end{array} \tag{5.3.8b}$$

i.e., the non-linear $SU(2)$ transformation is implemented by a $U(1)_{local}$ transformation. The second transformation in (5.3.8a) allows us to introduce a covariant derivative $D_\mu \equiv \partial_\mu \pm ia^3_\mu$ acting on $a^\pm_\mu$. Covariant derivatives acting on ds or ms are redundant and should not be considered (see the previous chapter [8]).

The space-time transformations are given by

$$\xi : \{C^+_{3z}, \sigma_y\} : \quad \left\{ \begin{array}{rcl} a^a_\mu & \to & a^a_{\xi\mu} \\ d^a_{pq} & \to & d^a_{\xi p \xi q} \\ m^{ab} & \to & m^{ab} \end{array} \right. \tag{5.3.9a}$$

$$\xi : \{I\} : \quad \left\{ \begin{array}{rcl} a^a_\mu & \to & -a^{\bar{a}}_{\xi\mu} \\ d^a_{pq} & \to & -d^{\bar{a}}_{pq} \\ m^{ab} & \to & m^{\bar{a}\bar{b}} \end{array} \right. \tag{5.3.9b}$$

$$T : \quad \left\{ \begin{array}{rcl} a^a_\mu & \to & -a^{\bar{a}}_{t\mu} \\ d^a_{pq} & \to & -d^{\bar{a}}_{pq} \\ m^{ab} & \to & m^{\bar{a}\bar{b}}, \end{array} \right. \tag{5.3.9c}$$

where the symbols $\xi\mu$, ξp and $t\mu$ represents the transformation of the subindex under the space and time transformations respectively together with the corresponding coefficient in each case; the $\bar{a}$ superindex is the complex conjugate of a.

Next we present the way of introducing the coupling to the electromagnetic field. Since spin waves have no electric charge they couple to the electromagnetic field through the field strength tensor, i.e., direct couplings to the electric and magnetic fields. This kind of couplings does not break the $SU(2)$ symmetry and in order to maintain the space-time symmetry we impose the field $\mathbf{E}$ transforms like a vector and the field $\mathbf{B}$ transforms like a pseudovector under $\bar{3}m$ point group, whereas under time reversal

these fields transform as:

$$T: \begin{cases} E^a & \rightarrow & E^a \\ B^a & \rightarrow & -B^a. \end{cases} \tag{5.3.10}$$

Since the spin waves are fluctuations of magnetic moments there exists another kind of coupling given by the Pauli term. The Pauli term breaks explicitly the $SU(2)$ symmetry and a source with appropriate transformation properties must be constructed to implement its effect in the effective theory. In the Heisenberg lagrangian with the Pauli interaction, written in the second quantisation language,

$$L = \sum_i \psi^\dagger(x_i) i \left(\partial_0 - i\mu \mathbf{SB}(x_i)\right) \psi(x_i) + \cdots, \tag{5.3.11}$$

a source $A_0(x) \sim \mu \mathbf{SB}(x)$ can be associated to the Pauli term, which transforms like a connexion under time dependent $SU(2)$ transformations,

$$A_0(x) \rightarrow g(t) A_0(x) g^\dagger(t) + i g(t) \partial_0 g^\dagger(t), \tag{5.3.12}$$

such that now the theory will be invariant under time dependent $SU(2)$ transformations. Therefore the effect of the Pauli term is implemented in the effective theory by changing the time derivative by a covariant time derivative,

$$\partial_0 \rightarrow D_0 \equiv \partial_0 - i A_0(x), \tag{5.3.13}$$

and eventually setting $A_0(x) = \mu \mathbf{SB}(x)$. Once this change is performed one has to keep in mind that the $a_0^\pm$ and a_0^3 contain the magnetic field encoded in the covariant time derivative.

5.4 Effective Lagrangian

5.4.1 Power counting

Now we are in a position to construct the spin wave interaction with the electromagnetic field for the antiferromagnet. The way we choose to do this is a perturbative one: the derivative expansion. Carrying out this expansion to a given order is meaningful for low energy and momentum with respect to the typical scales of the antiferromagnet, given respectively by the superexchange constant $J \sim 10meV$ and the inverse of the lattice parameter $1/a \sim 0.1\text{Å}^{-1}$ (the velocity of propagation of the

spin waves relates both parameters, $v = Ja$. It has the following value in Cr_2O_3: $v \sim 10^{-4}c$ [15]). The characteristic energy and momentum of the system are given by the external inputs of the electromagnetic fields, which are the same, namely, ω, and therefore the space derivative is highly suppressed with respect to the time derivative, $v\partial_i \sim 10^{-4}\partial_0$. The suppression of the spin-orbit tensor has already been given, $D \sim 10^{-2}J$ and $M \sim 10^{-4}J$. Terms proportional to D^2 and M force the local magnetisation to be in the third direction an give rise to an energy gap $\sim 10^{-2}J$ for the spin waves. The amplitude of the electromagnetic field must be constrained for the expansion to make sense. First, we consider the Pauli term. Since it is associated to the time derivative it is suppressed by J. We will assume that the remaining couplings of the electromagnetic field come from vector and scalar potential minimal couplings in a microscopic model. The former is associated to a link and hence suppressed by $1/ea$ whereas the latter is associated to a time derivative and hence suppressed by J/e. Therefore the electric field will be suppressed by J/ea, whereas the magnetic field will be suppressed by $1/ea^2$. The microscopic model may also have non-minimal couplings to the electromagnetic field arising from the integration of higher scales of energy and momentum. These terms would be suppressed by the above mentioned higher scales and will be neglected. In any case, as far as they respect the $SU(2)$ and crystal point group symmetries their only effect is to slightly modify the value of the constants in the effective lagrangian, which are anyway unknown.

Any effect due to spin waves is expected to be enhanced when we approach their energy gap. This is why we shall choose the energy of the electromagnetic wave of that order of magnitude. When in addition the amplitude of the electromagnetic wave is tunned so that $E \sim \partial_0$ the following relative suppressions hold:

$$\begin{aligned} \partial_0, eaE, d &\sim 10^{-2}J \\ m &\sim 10^{-4}J \\ \mu B &\sim 10^{-5}J \\ v\partial_i, eavB &\sim 10^{-6}J. \end{aligned} \tag{5.4.1}$$

5.4.2 Effective lagrangian

Once the above relation are given we are prepared to construct the relevant effective lagrangian, invariant under $SU(2)$ and space-time transformations given by (5.3.8), (5.3.9) and (5.3.10), for the effect we want to study: Non reciprocal effects in SHG and GB.

The effective lagrangian at the lowest order in which electromagnetic field appears reads

$$\begin{aligned} S[\pi, E, B] \;=\; \int dx f_\pi^2 \Big\{ & a_0^+ a_0^- \\ & + Z_1 (d^+_{zz} d^-_{\bar{z}\bar{z}} + d^-_{zz} d^+_{\bar{z}\bar{z}}) \\ & + Z_2 [(d^+_{3z} d^-_{zz} + d^-_{3z} d^+_{zz}) + (d^-_{3\bar{z}} d^+_{\bar{z}\bar{z}} + d^+_{3\bar{z}} d^-_{\bar{z}\bar{z}})] \\ & + Z_3 (d^+_{3z} d^-_{3\bar{z}} + d^-_{3z} d^+_{3\bar{z}}) \\ & + Z_4 d^3_{zz} d^3_{\bar{z}\bar{z}} \\ & + Z_5 (d^3_{3z} d^3_{zz} + d^3_{3\bar{z}} d^3_{\bar{z}\bar{z}}) \\ & + Z_6 d^3_{3z} d^3_{3\bar{z}} \\ & + Z_7 m^{-+} \\ & + Z_8 m^{33} \\ & + Z_9 i [(d^+_{\bar{z}\bar{z}} a_0^- - d^-_{\bar{z}\bar{z}} a_0^+) E^z - (d^-_{zz} a_0^+ - d^+_{zz} a_0^-) E^{\bar{z}}] \\ & + Z_{10} i [(d^+_{3z} a_0^- - d^-_{3z} a_0^+) E^z - (d^-_{3\bar{z}} a_0^+ - d^+_{3\bar{z}} a_0^-) E^{\bar{z}}] \\ & + Z_{11} E^z E^{\bar{z}} \\ & + Z_{12} E^3 E^3 \Big\}, \end{aligned} \tag{5.4.2}$$

When we take into account the Pauli coupling in $a_0^\pm$, contributions to SHG arise as 10^{-11} and 10^{-12} effects, and contributions to 10^{-9} appear in the case of GB. As it will be shown these contributions give rise to the desired non-reciprocal effects. Its is important to notice that if a primitive translation mapping points with opposite magnetisation existed the terms with a single time derivative above would not appear in the effective lagrangian.

Our action has been constructed up to third order (10^{-6}) and the contributions to non-reciprocal effects arise only from the Pauli coupling which is much more suppressed in (5.4.1). Therefore we might expect other contributions at higher orders. This is indeed the case, but in order to keep manegable the number of terms in the main text, these remaining contributions are relegated to the appendix.

5.5 Electromagnetic Field Effective Interaction

Our purpose is to describe non-reciprocal effects in SHG and GB mediated by spin waves. Spin waves are responsible for an effective interaction of the electromagnetic field giving rise to susceptibility tensors where the properties of the material (spin waves) are encoded.

Hence we realise that spin waves are not to be observed in this experiments and therefore they must be eliminated from our theory. The way to do this is by integrating them out in the functional (path) integral [16] so that the new action depends only on the electromagnetic field. In order to perform the integration we have to write the action explicitly in terms of the spin waves. This is achieved by expanding (5.3.2), with the following result:

$$\begin{aligned} S[\pi,E,B] \;=\; \int dx\Big[&\partial_0\pi^+\partial_0\pi^- - \Delta^2\pi^+\pi^- \\ &+ i\mu(\pi^+\partial_0\pi^- - \pi^-\partial_0\pi^+)B^3 \\ &- \frac{1}{2}f_\pi[\partial_0\pi^+(\mu B^{\bar z}+\lambda E^{\bar z}) + \partial_0\pi^-(\mu B^z+\lambda E^z)] \\ &- \frac{1}{2}i\mu f_\pi[\pi^+(\mu B^{\bar z}+\lambda E^{\bar z}) - \pi^-(\mu B^z+\lambda E^z)]B^3 \\ &+ \frac{1}{4}\mu\lambda f_\pi^2(E^zB^{\bar z}+E^{\bar z}B^z) \\ &+ f_\pi^2\left(b_1E^zE^{\bar z}+b_2E^3E^3\right)\Big], \end{aligned} \tag{5.5.1}$$

where only the terms contributing to bilinear and trilinear electromagnetic fields in the effective action to be calculated are kept. These terms are the only ones needed to describe the desired effects. The new constants which appear in (5.5.1) are combinations of those in the previous section. Although we do not know their precise values, their order of magnitude is fixed according to the counting rules given in (5.4.1). We list them below:

$$\begin{aligned} f_\pi^2 &\sim \frac{1}{Ja^3} \qquad & \Delta &\sim D \\ b_i &\sim (ea)^2 \qquad & \lambda &\sim ea\frac{D}{J}. \end{aligned} \tag{5.5.2}$$

Recall that $D\sim 10^{-2}J$ stands for the size of the spin-orbit term.

Notice that the contributions to non-reciprocal effects to the leading order (10^{-11} and 10^{-12} for SHG and 10^{-9} for GB) come from terms with at most two spin waves,

which permits us to perform a gaussian integration in the functional generator. In addition to this, it is worth mentioning that at the order given above the effects are produced at tree level, i.e., without loop contributions.

Once the gaussian integration is carried out a perturbative expansion of the spin waves propagator in the presence of electromagnetic fields has to be made, considering the free spin waves propagator,

$$P(x-y) = \int \frac{dq}{(2\pi)^4} P(\omega) e^{-iq(x-y)} \qquad , \qquad P(\omega) = \frac{1}{\omega^2 - \Delta^2}, \tag{5.5.3}$$

as the unperturbed part, leading to the electromagnetic effective interaction lagrangian

$$\begin{aligned} S_{\mathit{eff}}[E,B] &= \int dx f_\pi^2 \left[b_1 E^z E^{\bar{z}} + b_2 E^3 E^3 + \frac{1}{4}\mu\lambda (E^z B^{\bar{z}} + E^{\bar{z}} B^z) \right] \\ &+ \int dx dy f_\pi^2 \left[\frac{1}{4}\mu\lambda \left(E^z \partial_0^2 P(x-y) B^{\bar{z}} + B^z \partial_0^2 P(x-y) E^{\bar{z}} \right) \right] \\ &+ \int dx dy f_\pi^2 \Bigg[-\frac{1}{4} i\mu\lambda^2 E^z \left(B^3 \partial_0 P(x-y) + \partial_0 P(x-y) B^3 \right) E^{\bar{z}} \\ &\qquad - \frac{1}{4} i\mu^2\lambda \Big[E^z \left(B^3 \partial_0 P(x-y) + \partial_0 P(x-y) B^3 \right) B^{\bar{z}} \\ &\qquad\qquad + B^z \left(B^3 \partial_0 P(x-y) + \partial_0 P(x-y) B^3 \right) E^{\bar{z}} \Big] \Bigg]. \end{aligned} \tag{5.5.4}$$

The arguments of the electromagnetic fields have not been explicitly displayed. They must be understood as the nearest in the closest propagator.

Given the transformations under time reversal (5.3.10) it is clear that the SHG, terms with three fields, presents non-reciprocal effects due to the interference of different terms. The same is true for the GB since bilinear terms proportional to the magnetic and electric field appear.

5.5.1 Generalised susceptibilities

From the action above, together with the additional terms given in (5.A.6), the electromagnetic response of the Cr_2O_3 due to spin waves, leading to non-reciprocal effects in SHG and GB, can be easily obtained using (5.2.13)-(5.2.15).

The linear susceptibilities read

$$\begin{aligned}
\chi_E^{z\bar{z}}(\omega) &= 2b_1 f_\pi^2 \\
\chi_B^{z\bar{z}}(\omega) &= \frac{1}{2}\mu\lambda f_\pi^2[1-\omega^2 P(\omega)] \\
\chi_E^{33}(\omega) &= 2b_2 f_\pi^2 \qquad (5.5.5)\\
\\
\gamma_E^{z\bar{z}}(\omega) &= \frac{1}{2}\mu\lambda f_\pi^2[1-\omega^2 P(\omega)].
\end{aligned}$$

Recall that $\chi_B^{z\bar{z}}(\omega)$ and $\gamma_E^{z\bar{z}}(\omega)$ give rise to the GB. Notice that here this effect is proportional to the gap of the spin wave spectrum, which is in turn due to the spin-orbit interaction.

The susceptibilities contributing to SHG read

$$\begin{aligned}
\chi_{EE}^{zzz}(\omega,\omega) &= \lambda e_1 f_\pi^2\omega^3[P(\omega)-4P(2\omega)] + 2\lambda f_1 f_\pi^2\omega[P(\omega)-P(2\omega)] \\
&\quad + \frac{1}{2}\lambda^2 d_1 f_\pi^2\omega^3 P(\omega)[P(\omega)+2P(2\omega)] \\
\chi_{EE}^{z\bar{z}3}(\omega,\omega) &= \frac{1}{2}\lambda e_2 f_\pi^2\omega^3[P(\omega)+4P(2\omega)] - \lambda e_3 f_\pi^2\omega^3[P(\omega)-2P(2\omega)] \\
&\quad - \frac{1}{2}\lambda f_2 f_\pi^2\omega[P(\omega)+2P(2\omega)] - \frac{3}{2}\lambda^2 d_2 f_\pi^2\omega^3[P(\omega)P(2\omega)] \\
&\quad - 3\lambda^2 c f_\pi^2\omega^5 P(\omega)P(2\omega) - 3h f_\pi^2\omega \\
\chi_{EB}^{zzz}(\omega,\omega) &= \lambda g_1 f_\pi^2\omega[P(\omega)-2P(2\omega)] \\
\chi_{EB}^{z\bar{z}3}(\omega,\omega) &= \frac{1}{2}\mu\lambda^2 f_\pi^2\omega[P(\omega)+2P(2\omega)-6\omega^2 P(\omega)P(2\omega)] \\
&\quad - \lambda g_2 f_\pi^2\omega[P(\omega)+2P(2\omega)] - 6j_1 f_\pi^2\omega \\
\chi_{EB}^{z3\bar{z}}(\omega,\omega) &= -2\lambda g_3 f_\pi^2\omega P(2\omega) + 2j_2 f_\pi^2\omega \qquad (5.5.6)\\
\chi_{BB}^{z\bar{z}3}(\omega,\omega) &= \frac{1}{4}\mu^2\lambda f_\pi^2\omega[P(\omega)+2P(2\omega)-6\omega^2 P(\omega)P(2\omega)] \\
\chi_{EE}^{3\bar{z}z}(\omega,\omega) &= -\lambda e_2 f_\pi^2\omega^3 P(\omega) + \frac{1}{2}\lambda e_3 f_\pi^2\omega^3 P(\omega) \\
\chi_{EB}^{3\bar{z}z}(\omega,\omega) &= -\frac{1}{2}\lambda g_3 f_\pi^2\omega P(\omega) - 2j_2 f_\pi^2\omega \\
\\
\gamma_{EE}^{zzz}(\omega,\omega) &= \lambda g_1 f_\pi^2\omega P(\omega) \\
\gamma_{EE}^{z\bar{z}3}(\omega,\omega) &= -\frac{1}{2}\lambda g_3 f_\pi^2\omega P(\omega) + j_2 f_\pi^2\omega \\
\gamma_{EB}^{z\bar{z}3}(\omega,\omega) &= \frac{1}{2}\mu^2\lambda f_\pi^2\omega[P(\omega)+2P(2\omega)-6\omega^2 P(\omega)P(2\omega)].
\end{aligned}$$

Notice the non-trivial dependence in ω of the above susceptibilities. (This dependence is slightly more involved if one calculates the general susceptibilities $\chi(\omega,\omega')$ and $\gamma(\omega,\omega')$ since the limit $\omega=\omega'$ produces a few cancellations.) For this to be so it is crucial that no primitive translation mapping points with opposite magnetisation exists. Otherwise only the local terms proportional to j_i would survive. Notice also that the terms proportional to h arise due to the explicit spin-orbit breaking. Even thought this term gives rise to a local term in the electromagnetic fields at this order, it also contains explicit interactions with spin waves at higher orders.

Let us finally mention that the terms proportional to k_i in (5.A.6) give rise to contributions to the quadrupolar momentum [9, 12] which are of the same order as the ones considered above. In fact, the quadrupolar terms give the unique contribution to SHG in a crystal which contains a center of symmetry as it is the case for Cr_2O_3 above the Neel temperature [12]. The associated susceptibilities can be easily calculated. They are local and will not be displayed explicitly.

5.6 Discussion

We have used an effective field theory for spin waves in an antiferromagnetic material to describe its response to electromagnetic fields in the microwave region. The starting point is a local effective lagrangian which fully exploits the fact that spin waves are Goldstone modes of a $SU(2)\to U(1)$ symmetry breaking pattern together with the crystal space group symmetry and time reversal. By integrating out the spin waves we obtain a non-local effective action which encodes the response of the material to the electromagnetic field. From this effective action the various linear and non-linear electric and magnetic susceptibilities can be immediately obtained. We have given explicitly those relevant to the GB and SHG experiments. These susceptibilities depend on a relatively large number of unknown constants (~ 23) and a microscopic calculation is required to assign definite numbers to them. However, their order of magnitude can be readily established in terms of the typical lattice spacing a and the energy of the first gapped excitation J. Notice also that these susceptibilities present a rather non-trivial dependence on ω, the frequency of the incoming radiation. This dependence cannot be obtained from the magnetic group symmetries alone and it is a direct consequence of the existence of spin waves in an antiferromagnetic crystal where: (i) no primitive translation mapping points with opposite magnetisations exist, and (ii)

spin-orbit effects are sizable.

We have not been able to locate experimental results in the literature to test our formulas against. We expect them to become available at some point. It would be particularly interesting to be able to browse the microwave region with several frequencies so that the ω dependence in (5.5.5) and (5.5.6) could be checked and the free parameters fitted. If the incoming radiation is directed along the third axis then only $\gamma^{zzz}_{EE}(\omega,\omega)$, $\chi^{3\bar{z}z}_{EB}(\omega,\omega)$, $\chi^{3\bar{z}z}_{EE}(\omega,\omega)$, $\chi^{zzz}_{EB}(\omega,\omega)$ and $\chi^{zzz}_{EE}(\omega,\omega)$ are relevant.

Although for definiteness we have focused on the Cr_2O_3 crystal, which has spin 3/2, our results hold for any antiferromagnetic crystal (with spontaneous staggered magnetisation) with crystal point group $\bar{3}m$ and arbitrary spin, as long as no primitive translations mapping points with opposite magnetisation exist. This includes for instance V_2O_3 (spin 1). It is also worth emphasising that the method we have used is general enough to become applicable to any antiferromagnet of any spin and crystal point group, as long as there is spontaneous staggered magnetisation. The allowed terms in the effective lagrangian, however, depend on the particular crystal point group and on the particular distribution of the magnetic ions in the crystal.

5.A Complete Electromagnetic Interaction

In this appendix we will present the higher order terms in the effective action (5.4.2) which contribute to the SHG and GB to the same order as those in (5.5.1).

Contributions to fourth order (10^{-8}):

$$i(a_0^+ D_0 a_0^- - a_0^- D_0 a_0^+)E^3 \tag{5.A.1a}$$

$$\begin{aligned}
&d^3_{zz}(d^+_{zz}a_0^- + d^-_{zz}a_0^+)E^z + d^3_{\bar{z}\bar{z}}(d^-_{\bar{z}\bar{z}}a_0^+ + d^+_{\bar{z}\bar{z}}a_0^-)E^{\bar{z}}\\
&d^3_{zz}(d^+_{3\bar{z}}a_0^- + d^-_{3\bar{z}}a_0^+)E^z + d^3_{\bar{z}\bar{z}}(d^-_{3z}a_0^+ + d^+_{3z}a_0^-)E^{\bar{z}}\\
&d^3_{3\bar{z}}(d^+_{3\bar{z}}a_0^- + d^-_{3\bar{z}}a_0^+)E^z + d^3_{3z}(d^-_{3z}a_0^+ + d^+_{3z}a_0^-)E^{\bar{z}}\\
&[d^3_{zz}(d^+_{\bar{z}\bar{z}}a_0^- + d^-_{\bar{z}\bar{z}}a_0^+) + d^3_{\bar{z}\bar{z}}(d^-_{zz}a_0^+ + d^+_{zz}a_0^-)]E^3\\
&[d^3_{zz}(d^+_{3z}a_0^- + d^-_{3z}a_0^+) + d^3_{\bar{z}\bar{z}}(d^-_{3\bar{z}}a_0^+ + d^+_{3\bar{z}}a_0^-)]E^3\\
&[d^3_{3\bar{z}}(d^+_{3z}a_0^- + d^-_{3z}a_0^+) + d^3_{3z}(d^-_{3\bar{z}}a_0^+ + d^+_{3\bar{z}}a_0^-)]E^3.
\end{aligned} \tag{5.A.1b}$$

To fifth order (10^{-10}):

$$\begin{aligned}
&(d^+_{zz}D_0a_0^- + d^-_{zz}D_0a_0^+)E^zE^z + (d^-_{\bar{z}\bar{z}}D_0a_0^+ + d^+_{\bar{z}\bar{z}}D_0a_0^-)E^{\bar{z}}E^{\bar{z}}\\
&(d^+_{3\bar{z}}D_0a_0^- + d^-_{3\bar{z}}D_0a_0^+)E^zE^z + (d^-_{3z}D_0a_0^+ + d^+_{3z}D_0a_0^-)E^{\bar{z}}E^{\bar{z}}\\
&(d^+_{zz}D_0a_0^- + d^-_{zz}D_0a_0^+)E^{\bar{z}}E^3 + (d^-_{\bar{z}\bar{z}}D_0a_0^+ + d^+_{\bar{z}\bar{z}}D_0a_0^-)E^zE^3\\
&(d^+_{3\bar{z}}D_0a_0^- + d^-_{3\bar{z}}D_0a_0^+)E^{\bar{z}}E^3 + (d^-_{3z}D_0a_0^+ + d^+_{3z}D_0a_0^-)E^zE^3\\
&(d^+_{zz}a_0^- + d^-_{zz}a_0^+)E^{\bar{z}}\partial_0E^3 + (d^-_{\bar{z}\bar{z}}a_0^+ + d^+_{\bar{z}\bar{z}}a_0^-)E^z\partial_0E^3\\
&(d^+_{3\bar{z}}a_0^- + d^-_{3\bar{z}}a_0^+)E^{\bar{z}}\partial_0E^3 + (d^-_{3z}a_0^+ + d^+_{3z}a_0^-)E^z\partial_0E^3
\end{aligned} \tag{5.A.2a}$$

$$\begin{aligned}
&i(d^+_{zz}d^-_{\bar{z}\bar{z}} - d^-_{zz}d^+_{\bar{z}\bar{z}})(d^3_{zz}E^zE^z - d^3_{\bar{z}\bar{z}}E^{\bar{z}}E^{\bar{z}})\\
&i(d^+_{3z}d^-_{3\bar{z}} - d^-_{3z}d^+_{3\bar{z}})(d^3_{zz}E^zE^z - d^3_{\bar{z}\bar{z}}E^{\bar{z}}E^{\bar{z}})\\
&i(d^+_{zz}d^-_{\bar{z}\bar{z}} - d^-_{zz}d^+_{\bar{z}\bar{z}})(d^3_{3\bar{z}}E^zE^z - d^3_{3z}E^{\bar{z}}E^{\bar{z}})\\
&i(d^+_{3z}d^-_{3\bar{z}} - d^-_{3z}d^+_{3\bar{z}})(d^3_{3\bar{z}}E^zE^z - d^3_{3z}E^{\bar{z}}E^{\bar{z}})\\
&i[(m^{+3}d^-_{zz} - m^{-3}d^+_{zz})E^zE^z - (m^{-3}d^+_{\bar{z}\bar{z}} - m^{+3}d^-_{\bar{z}\bar{z}})E^{\bar{z}}E^{\bar{z}}]\\
&i[(m^{+3}d^-_{3\bar{z}} - m^{-3}d^+_{3\bar{z}})E^zE^z - (m^{-3}d^+_{3z} - m^{+3}d^-_{3z})E^{\bar{z}}E^{\bar{z}}]\\
&i(d^+_{zz}d^-_{\bar{z}\bar{z}} - d^-_{zz}d^+_{\bar{z}\bar{z}})(d^3_{zz}E^{\bar{z}}E^3 - d^3_{\bar{z}\bar{z}}E^zE^3)\\
&i(d^+_{3z}d^-_{3\bar{z}} - d^-_{3z}d^+_{3\bar{z}})(d^3_{zz}E^{\bar{z}}E^3 - d^3_{\bar{z}\bar{z}}E^zE^3)
\end{aligned} \tag{5.A.2b}$$

$$
\begin{aligned}
&i(d^+_{zz}d^-_{\bar{z}\bar{z}} - d^-_{zz}d^+_{\bar{z}\bar{z}})(d^3_{3\bar{z}}E^{\bar{z}}E^3 - d^3_{3z}E^zE^3)\\
&i(d^+_{3z}d^-_{3\bar{z}} - d^-_{3z}d^+_{3\bar{z}})(d^3_{3\bar{z}}E^{\bar{z}}E^3 - d^3_{3z}E^zE^3)\\
&i[(m^{+3}d^-_{zz} - m^{-3}d^+_{zz})E^{\bar{z}}E^3 - (m^{-3}d^+_{\bar{z}\bar{z}} - m^{+3}d^-_{\bar{z}\bar{z}})E^zE^3]\\
&i[(m^{+3}d^-_{3\bar{z}} - m^{-3}d^+_{3\bar{z}})E^{\bar{z}}E^3 - (m^{-3}d^+_{3z} - m^{+3}d^-_{3z})E^zE^3]
\end{aligned}
$$

$$
\begin{aligned}
&i(d^3_{zz}E^zB^z - d^3_{\bar{z}\bar{z}}E^{\bar{z}}B^{\bar{z}})\\
&i(d^3_{3\bar{z}}E^zB^z - d^3_{3z}E^{\bar{z}}B^{\bar{z}})\\
&i(d^3_{zz}E^{\bar{z}}B^3 - d^3_{\bar{z}\bar{z}}E^zB^3)\\
&i(d^3_{3\bar{z}}E^{\bar{z}}B^3 - d^3_{3z}E^zB^3)\\
&i(d^3_{zz}E^3B^{\bar{z}} - d^3_{\bar{z}\bar{z}}E^3B^z)\\
&i(d^3_{3\bar{z}}E^3B^{\bar{z}} - d^3_{3z}E^3B^z).
\end{aligned}
\tag{5.A.2c}
$$

To sixth order (10^{-12}):

$$
\begin{aligned}
&i(d^+_{zz}d^-_{\bar{z}\bar{z}} - d^-_{zz}d^+_{\bar{z}\bar{z}})(E^z\partial_0E^{\bar{z}} - E^{\bar{z}}\partial_0E^z)E^3\\
&i[(d^+_{zz}d^-_{3z} - d^-_{zz}d^+_{3z})E^z\partial_0E^{\bar{z}} - (d^-_{\bar{z}\bar{z}}d^+_{3\bar{z}} - d^+_{\bar{z}\bar{z}}d^-_{3\bar{z}})E^{\bar{z}}\partial_0E^z]E^3\\
&i(d^+_{3z}d^-_{3\bar{z}} - d^-_{3z}d^+_{3\bar{z}})(E^z\partial_0E^{\bar{z}} - E^{\bar{z}}\partial_0E^z)E^3
\end{aligned}
\tag{5.A.3a}
$$

$$
\begin{aligned}
&(E^z\partial_0E^{\bar{z}} - E^{\bar{z}}\partial_0E^z)B^3\\
&E^z\partial_0E^3B^{\bar{z}} - E^3\partial_0E^{\bar{z}}B^z
\end{aligned}
\tag{5.A.3b}
$$

$$
\begin{aligned}
&(E^z\partial_{\bar{z}}E^z + E^{\bar{z}}\partial_zE^{\bar{z}})E^3\\
&E^zE^{\bar{z}}\partial_3E^3\\
&E^zE^{\bar{z}}(\partial_zE^z + \partial_{\bar{z}}E^{\bar{z}})\\
&E^3E^3(\partial_zE^z + \partial_{\bar{z}}E^{\bar{z}}).
\end{aligned}
\tag{5.A.3c}
$$

Where to reduce the number of terms in (5.A.3b) the homogeneous Maxwell equations, which are satisfied automatically, have been used. It is important to notice that if a primitive translation mapping points with opposite magnetisation existed, the terms in (5.A.1a), (5.A.1b), (5.A.2c) and (5.A.3a) would not appear.

In spite of the large number of terms, we will see that most of them contribute in the same way to the effective action for the electromagnetic fields.

Indeed, when we expand the terms, above in order to make explicit the interaction between the spin waves and the electromagnetic field, the terms below must be added to (5.5.1) keeping bilinear and trilinear terms in the electromagnetic fields.

$$\begin{aligned}
\Delta S[\pi,E,B] \;=\; \int dx\Big[& ic(\partial_0\pi^+\partial_0^2\pi^- - \partial_0\pi^-\partial_0^2\pi^+)E^3 \\
& + id_1(\pi^+\partial_0\pi^+E^z - \pi^-\partial_0\pi^-E^{\bar z}) \\
& + id_2(\pi^+\partial_0\pi^-E^3 - \pi^-\partial_0\pi^+E^3) \\
& + ie_1f_\pi(\partial_0\pi^+E^z\partial_0E^z - \partial_0\pi^-E^{\bar z}\partial_0E^{\bar z}) \\
& + ie_2f_\pi(\partial_0\pi^+\partial_0E^{\bar z}E^3 - \partial_0\pi^-\partial_0E^zE^3) \\
& + ie_3f_\pi(\partial_0\pi^+E^{\bar z}\partial_0E^3 - \partial_0\pi^-E^z\partial_0E^3) \\
& + if_1f_\pi(\pi^+E^zE^z - \pi^-E^{\bar z}E^{\bar z}) \\
& + if_2f_\pi(\pi^+E^{\bar z}E^3 - \pi^-E^zE^3) \\
& + ig_1f_\pi(\pi^+E^zB^z - \pi^-E^{\bar z}B^{\bar z}) \\
& + ig_2f_\pi(\pi^+E^{\bar z}B^3 - \pi^-E^zB^3) \\
& + ig_3f_\pi(\pi^+E^3B^{\bar z} - \pi^-E^3B^z) \\
& + ihf_\pi^2(E^z\partial_0E^{\bar z} - E^{\bar z}\partial_0E^z)E^3 \\
& + ij_1f_\pi^2(E^z\partial_0E^{\bar z} - E^{\bar z}\partial_0E^z)B^3 \\
& + ij_2f_\pi^2(E^z\partial_0E^3B^{\bar z} - E^3\partial_0E^{\bar z}B^z) \\
& + k_1f_\pi^2(E^z\partial_{\bar z}E^z + E^{\bar z}\partial_zE^{\bar z})E^3 \\
& + k_2f_\pi^2E^zE^{\bar z}\partial_3E^3 \\
& + k_3f_\pi^2E^zE^{\bar z}(\partial_zE^z + \partial_{\bar z}E^{\bar z}) \\
& + k_4f_\pi^2E^3E^3(\partial_zE^z + \partial_{\bar z}E^{\bar z})\Big].
\end{aligned} \tag{5.A.4}$$

Notice that no terms beyond two spin waves appear in the previous action. This does not change the procedure of gaussian integration carried out in section 5.5. The

constants in (5.A.4) have the following order of magnitude:

$$\begin{aligned} c &\sim \frac{ea}{J^2} & d_i &\sim ea\left(\frac{D}{J}\right)^2 \\ e_i &\sim \left(\frac{ea}{J}\right)^2\frac{D}{J} & f_i &\sim (ea)^2\left(\frac{D}{J}\right)^3 \\ g_i &\sim (ea)^2 Da & h &\sim (ea)^3 D^2 \\ j_i &\sim (ea)^3\frac{a}{J} & k_i &\sim (ea)^3\frac{a}{J}. \end{aligned} \tag{5.A.5}$$

The effective action for the electromagnetic fields in (5.5.4) must be augmented with the following terms:

$$\begin{aligned} \Delta S_{\mathit{eff}}[E,B] = \int dxdyf_\pi^2\Big\{ &-\frac{1}{4}i\lambda e_1\left[E^z\partial_0^3P(x-y)E^zE^z + E^{\bar z}E^{\bar z}\partial_0^3P(x-y)E^{\bar z}\right] \\ &-\frac{1}{2}i\lambda\Big[E^z\partial_0^2P(x-y)(e_2E^{\bar z}\partial_0E^3 + e_3\partial_0E^{\bar z}E^3) \\ &\qquad + (e_2E^z\partial_0E^3 + e_3\partial_0E^zE^3)\partial_0^2P(x-y)E^{\bar z}\Big] \\ &+\frac{1}{2}i\lambda\Big[E^z\partial_0P(x-y)(f_1E^zE^z + f_2E^{\bar z}E^3) \\ &\qquad + (f_1E^{\bar z}E^{\bar z} + f_2E^zE^3)\partial_0P(x-y)E^{\bar z}\Big] \\ &+\frac{1}{2}i\lambda\Big[E^z\partial_0P(x-y)(g_1E^zB^z + g_2E^{\bar z}B^3 + g_3E^3B^{\bar z}) \\ &\qquad + (g_1E^{\bar z}B^{\bar z} + g_2E^zB^3 + g_3E^3B^z)\partial_0P(x-y)E^{\bar z}\Big]\Big\} \end{aligned} \tag{5.A.6}$$

$$\begin{aligned} + \int dxdudyf_\pi^2\Big\{ &-\frac{1}{4}i\lambda^2E^z\Big(\partial_0^2P(x-u)(\mu B^3 + d_2E^3)\partial_0P(u-y) \\ &\qquad + \partial_0P(x-u)(\mu B^3 + d_2E^3)\partial_0^2P(u-y)\Big)E^{\bar z} \\ &-\frac{1}{4}i\mu^2\lambda\Big[E^z\Big(\partial_0^2P(x-u)B^3\partial_0P(u-y) + \partial_0P(x-u)B^3\partial_0^2P(u-y)\Big)B^{\bar z} \\ &\qquad + B^z\Big(\partial_0^2P(x-u)B^3\partial_0P(u-y) + \partial_0P(x-u)B^3\partial_0^2P(u-y)\Big)E^{\bar z}\Big] \\ &+\frac{1}{4}i\lambda^2cE^z\Big(\partial_0^2P(x-u)E^3\partial_0^3P(u-y) + \partial_0^3P(x-u)E^3\partial_0^2P(u-y)\Big)E^{\bar z} \\ &+\frac{1}{8}id_1\lambda^2\Big[E^z\Big(\partial_0^2P(x-u)E^z\partial_0P(u-y) - \partial_0P(x-u)E^z\partial_0^2P(u-y)\Big)E^z \end{aligned}$$

$$- E^{\bar{z}}\Big(\partial_0^2 P(x-u)E^{\bar{z}}\partial_0 P(u-y) - \partial_0 P(x-u)E^{\bar{z}}\partial_0^2 P(u-y)\Big)E^{\bar{z}}\Big]\Big\}$$

$$+ \int dx\, f_\pi^2\Big[ih(E^z\partial_0 E^{\bar{z}} - E^{\bar{z}}\partial_0 E^z)E^3$$

$$+ ij_1(E^z\partial_0 E^{\bar{z}} - E^{\bar{z}}\partial_0 E^z)B^3 + ij_2(E^z B^{\bar{z}} - E^{\bar{z}}B^z)\partial_0 E^3$$

$$+ k_1(E^z\partial_{\bar{z}}E^z + E^{\bar{z}}\partial_z E^{\bar{z}})E^3 + k_2 E^z E^{\bar{z}}\partial_3 E^3$$

$$+ k_3 E^z E^{\bar{z}}(\partial_z E^z + \partial_{\bar{z}}E^{\bar{z}}) + k_4 E^3 E^3(\partial_z E^z + \partial_{\bar{z}}E^{\bar{z}})\Big].$$

These contributions to the electromagnetic effective action have been included in our final results for the generalised susceptibilities in formulas (5.5.5) and (5.5.6).

Bibliography

[1] G. Burns, *"Solid State Physics"* (Academic Press, Inc., San Diego, 1985).

[2] V. N. Muthukumar, R. Valentí and C. Gross, *Phys. Rev.* **B54** (1996) 433;

V. N. Muthukumar, R. Valentí and C. Gross, *Phys. Rev. Lett.* **75** (1995) 2766;

Y. Tanabe, M. Muto and E. Hanamura, *Solid State Comm.* **102** (1997) 643.

[3] B. B. Krichevtsov, V. V. Pavlov, R. V. Pisarev and V. N. Gridnev, *J. Phys.: Cond. Matter* **5** (1993) 8233;

M. Fiebig, D. Fröhlich, B. B. Krichevtsov and R. V. Pisarev, *Phys. Rev.* **73** (1994) 2127;

M. Fiebig, D. Fröhlich and G. Sluyterman v. L., *Appl. Phys. Lett.* **66** (1995) 2906.

[4] R. R. Birss, *"Symmetry and Magnetism"* (North Holland, Amsterdam, 1964).

[5] R. M. Hornreich and S. Shtrikman, *Phys. Rev.* **171** (1968) 1065;

R. Fuchs, *Phil. Mag.* **11** (1965) 647.

[6] P. Hasenfratz and F. Niedermayer, *Z. Physik* **B92** (1993) 91.

[7] S. Coleman, J. Wess and B. Zumino, *Phys. Rev.* **177** (1969) 2239;

C. Callan, S. Coleman, J. Wess and B. Zumino, *Phys. Rev.* **177** (1969) 2247.

[8] J. M. Román and J. Soto, *"Effective Field Theory Approach to Ferromagnets and Antiferromagnets in Crystalline Solids"*, Univ. of Barcelona preprint no. UB-ECM-PF 97/23, cond-mat/9709298.

[9] V. M. Agranovich and V. L. Ginzburg, *"Crystal Optics with Spatial Dispersion, and Excitons"*, Springer Series in Solid State Physics (Springer-Verlag, Berlin, 1984).

[10] M. Born and E. Wolf, *"Principles of Optics"*, (Pergamon Press, Oxford, 1983).

[11] Y. R. Shen, *"The Principles of Nonlinear Optics"* (Wiley, New York, 1984).

[12] P. S. Pershan, *Phys. Rev.* **130** (1963) 919.

[13] E. B. Graham and R. E. Raab, *Phil. Mag.* **B66** (1992) 269;

E. B. Graham and R. E. Raab, *J. Phys.: Cond. Matter* **6** (1994) 6725.

[14] T. Moriya, *Phys. Rev.* **120** (1960) 91.

[15] Landolt-Börnstein, New Series III/27f3 p.128.

[16] E. Fradkin, *"Field Theories of Condensed Matter Systems"* (Addison-Wesley, Reading, MA, 1990);

P. Ramond, *"Field Theory: A Modern Primer"* (Addison-Wesley, Reading, MA, 1990).

Chapter 6

Conclusions and Prospects

In this chapter we put together the main results obtained in this thesis as well as some prospects.

In the chapter 2 we have presented a semianalitic variational RG method for quantum systems called matrix product method (MPM). This method allows us a better understanding of previous numerical results.

1. We have presented a rotational invariant formulation (for 2-leg spin ladders) of the MPM which allow us to express the GS energy density, the correlation length and the string order parameter, in terms of invariant objects. This reduces considerably the number of independent MP parameters used in the minimisation procedure.

2. We have improved the numerical results concerning the GS energy density and spin correlation length obtained previously with other approximate methods. The consideration of MP ansatzs with multiple states per spin will certainly lead to better results.

3. We have shown the equivalence between the ladder $AF_{1/2}$ and the spin 1 antiferromagnetic Heisenberg chain. The MPM applied to both systems shows strong numerical coincidences for the GS energy and correlation length.

4. We have found numerical evidences which favors the existence of duality properties for the spin ladders with magnetic structures AA, AF and FA.

5. We have shown that there is a breaking of the long range topological order of the spin 1 chains when they are coupled in a 2-legged ladder. A physical picture of the GS of the spin 1 ladder is given in terms of resonating closed spin 1 chains.

The relation pointed out between the MPM and the DMRG suggests the possibility of a transformation of the ground state minimisation formalism into an eigenvalue problem for the superblock $B_N \bullet B_N^R$.

In summary we have shown the adequacy of the MPM to study the 2-legged ladder, specially in the strong and intermediate coupling regimes. This is made possible from the fact that these ladders are finitely correlated. Hence one may expect that even spin ladders with a finite number of legs could be described by the same technique, although with a larger number of states m. On the other hand, odd legged ladders are not finitely correlated and they cannot be properly described in the large N limit within the actual formulation of the MPM. An interesting problem is the application of the MPM to 2D systems, which can be thought of as ladders with a large number

of legs. It is clear that one should choose a collection of the most representative states for the rungs to be added after each iteration of the MP recurrence equation.

In the chapter 3 we have presented a study of the ground state properties for the doped manganites.

1. We have presented a continuum model which retains the main characteristics of the doped manganites and permits the exploration of the phase diagram beyond the parameters of the current materials.

2. From the effective potential the phase diagram at zero temperature has been calculated in terms of the chemical potential and doping parameter x. Antiferromagnetic, ferromagnetic, canted and even phase separation regions arise upon changing the doping.

3. The obtained canted phases are thermodynamically stable against phase separation.

The phase diagram at finite temperature is the next thing to be calculated within the model, since we could see how the different phases evolve as temperature rises. It would also be interesting to pin down the different phases which may coexist in the phase separation region.

In the chapter 4 we have presented a systematic study of the spin waves in ferromagnetic and antiferromagnetic crystalline solids.

1. We have presented a systematic way of writing an effective lagrangian describing the spin waves dynamics in crystalline media. To do this we fully exploit the internal symmetry breaking pattern $SU(2) \to U(1)$ as well as space symmetries and time reversal.

2. The formalism presented easily keeps track of elusive topological terms.

3. We have found the remarkable differences between the ferromagnetic and antiferromagnetic spin wave effective lagrangian by the only use of symmetry properties.

4. Within the antiferromagnetic case, we have pointed out that the existence of primitive translations which map points with opposite magnetisations has nontrivial consequences in the effective lagrangian.

5. We have shown how to introduce terms that break the symmetry explicitly. These are given by spin-orbit and magnetic dipole interactions. A gap appears in the excitation spectrum due to these terms.

6. We have introduced the electromagnetic field coupling with the spin waves. On the one hand, through the Pauli coupling, which does not introduces additional parameters in the effective lagrangian, and on the other, by means of a non-minimal coupling to the **E** and **B** fields.

In the chapter 5 we have described the electromagnetic response in the microwave region for Cr_2O_3 based on the previous formalism.

1. By integrating out the spin waves in the path integral we have obtained a non-local action which contains the material response to the electromagnetic field.

2. From this action electric and magnetic susceptibilities relevant for the gyrotropic birefringence and second harmonic generation, with a non-trivial funcionality in the incident light frequency, have been calculated. These susceptibilities depend on unknown constants whose order of magnitude can be readily established in terms of the typical lattice spacing a and the energy of the first gapped excitation J.

3. These susceptibilities give rise to non-reciprocal effects as a direct consequence of the lack of primitive translations connecting the two sublattices in the antiferromagnetic state and the existence of sizable spin-orbit effects.

4. The Cr_2O_3 has spin 3/2, but the results hold for any antiferromagnetic crystal with crystal point group $\bar{3}m$ and arbitrary spin, as, for example, the V_2O_3 (spin 1).

The doped manganites present a phase diagram where canted magnetic structures exist. The previous formalism of effective lagrangians permit us to study the spin waves in these phases. The SSB in this case is $SU(2) \to 1$, which gives three Goldstone fields. These fields arrange themselves as one ferromagnetic and one antiferromagnetic spin wave, whose interactions are described by the effective lagrangian. Conducting fermions also exist in these materials. Thus, the effective interaction mediated by spin waves can be easily calculated.

Capítulo 7

Resumen

En este capítulo resumiremos los puntos más importantes presentados en esta tesis, así como las conclusiones a las que ha dado lugar. En primer lugar, hemos estudiado un conjunto de sistemas cuasi-unidimensionales, que en la actualidad generan un gran interés, como son las escaleras de espín. Este estudio lo hemos realizado mediante un método variacional del grupo de renormalización desde un punto de vista cuántico. En segundo lugar, hemos aplicado un modelo continuo en el estudio de las configuraciones del estado fundamental en cristales de manganitas dopadas. Finalmente, utilizando teorías efectivas hemos desarrollado un formalismo que describe las ondas de espín en medios cristalinos ordenados magnéticamente. Hemos introducido el acoplamiento con el campo elctromagnético en el régimen de microondas para aplicar el formalismo a la descripción de efectos no recíprocos en cristales antiferromagnéticos.

7.1 Introducción

Esta tesis ha sido dedicada al estudio de sistemas magnéticos en Matería Condensada (CM) utilizando diferentes técnicas. La primera es el Grupo de Renormalización (RG), que consiste en una modificación variacional del Grupo de Renormalización de Matriz Densidad (DMRG). El DMRG es muy utilizado en la solución de problemas uni y cuasi-uni-dimensionales, conduciendo a una gran precisión en los resultados, en particular para la energía y longitud de correlación del estado fundamental de cadenas de espín [1]. Posteriormente, hemos introducido un modelo continuo para el estudio de las propiedades magnéticas y conductoras del estado fundamental de las manganitas dopadas, que produce una estructura de fases muy rica. Por último, hemos introducido un formalismo de Teoría Efectiva de Campos, utilizada en Teoría Cuántica de Campos (QFT) satisfactoriamente en la descripción de sistemas en los que se produce ruptura espontánea de simetría (SSB), como es el caso de la dinámica de piones en el espectro de baja energía de QCD [2]. Notese que debido al hecho de que la SSB se produce en sistemas con dimensionalidad mas grande que uno [3] las teorías efectivas anteriores no pueden ser aplicadas en sistemas de dimensión uno. Sin embargo, otros formalismos resultan ser eficientes para el estudio de sistemas de dimension 1, entre ellos el Método de Producto de Matrices que hemos presentado aquí.

Ahora introduciremos los sistemas físicos con los cuales hemos trabajado. Los componentes fundamentales de un sistema físico de CM son los electrones y los núcleos. Estos interaccionan mediante la ley de Coulomb, $1/r$, a la que en ciertas circunstancias debe añadírsele la interacción de espín-órbita y de dipolo magnético. La forma de trabajar en estos sistemas es seleccionando los grados de libertad relevantes para el problema dentro de una precisión requerida. Estos grados de libertad pueden ser diferentes de los fundamentales, al igual que sus interacciones. Por ejemplo, los fonones, polarones o huecos que resultan ser las excitaciones elementales en algunos sistemas, o nuevas interacciones como la de Lennard-Jones, $1/r^6 - 1/r^{12}$. En general trabajamos a energías a las cuales los átomos forman una estructura cristalina, por lo que únicamente los electrones de los orbitales externos serán relevantes, es decir, su estado puede verse modificado en los procesos físicos considerados. A este nivel tenemos, por ejemplo, el modelo de electrones libres, que describe algunos metales conductores. Otro tipo de modelo es el modelo de Hubbard, que describe electrones localizados con la posibilidad de saltar entre átomos vecinos. Este modelo explica fenómenos tales como la transición

de Mott (aislante-conductor). El modelo $t-J$, que se deriva del anterior cuando se prohibe la doble ocupación de cada átomo, se cree que es relevante para la superconductividad de alta temperatura crítica. En un nivel posterior el modelo de Heisenberg procede del modelo $t-J$ cuando estamos a llenado mitad. Las relaciones anteriores entre estos modelos las discutiremos en la próxima sección.

Una vez que hemos seleccionado el modelo "microscópico" efectivo podemos proceder de dos maneras. Por un lado, podemos calcular directamente algunos observables macroscópicos, y por otro, contruir un modelo macroscópico que nos describa el sistema en el régimen de largas distancias. Algunos de estos modelos pueden, eventualmente, ser elevados a la categoría de teorías efectivas. En cualquiera de los casos, el RG [4] es una técnica ámpliamente utilizada en la realización de estos cálculos. Mediante un procedimiento recurrente el RG realza los grados de libertad relevantes en el régimen de baja energía y largas distancias. En el capítulo 2 hemos mostrado como funciona el RG en el primero de los casos, es decir, en el cálculo de observables macroscópicos, como las energías de estado fundamental o sus longitudes de correlación. En lo que respecta a la derivación de la dinámica de baja energía el RG da lugar a teorías efectivas que describen el comportamiento macroscópico. En particular, cuando es aplicado a sistemas de CM aparecen frecuentemente ecuaciones familiares en QFT. Este es el caso de la ecuación de Majorana para fermiones en la teoría del líquido de Fermi de 2 dimensiones, o la teoría de Chern-Simons en el efecto Hall cuántico (QHE) [5].

Los modelos macroscópicos que podamos construir se basan en evidencias fenomenológicas. Los modelos continuos proveen una descripción adecuada del régimen de largas distancias. Aún cuando estos modelos no hayan sido derivados sistemáticamente de una aplicaicón del RG incorporan las principales características del sistema. En este sentido hemos construido un modelo continuo en el capítulo 3 para describir el estado fundamental y las propiedades de baja energía de las manganitas dopadas.

Además de los grados de libertad aparentes, en el modelo de Hubbard y sucesivos, existen excitaciones colectivas de baja energía. Estos modos colectivos se generan en redes cristalinas, como los fonones, así como en estructuras magnéticas, como las ondas de espín, y deben ser tenidos en cuenta en el estudio de estos sistemas. La aplicación del RG en estos sistemas produciría este tipo de grados de libertad en la descripción de la dinámica macroscópica. Sin embargo, debido a que estas excitaciones resultan ser modos de Goldstone, cuya dinámica esta fuertemente restringida por propiedades de simetría y descrita por un formalismo general independiente de los detalles de los

modelos subyacentes, es innecesaria una aplicación directa del RG. Aunque se tiene en cuenta de forma indirecta en la selección de los términos que entran en la teoría efectiva. Este formalismo es conocido desde los años sesenta [6, 7], pero no ha sido ampliamente utilizado hasta hace unos años para describir la física de piones de QCD [2]. Ultimamente se ha sugerido que este formalismo puede ser util en CM [8]. En el capítulo 5 describimos la contrucción de este formalismo para cristales ferromagnéticos y antiferromagnéticos.

7.2 Modelo de Hubbard

El "modelo de Hubbard" más sencillo describe las excitaciones que se producen en un cristal en el cual los electrones están localizados alrededor de los nucleos, donde interaccionan coulombianamente con el otro electrón de su orbital con una intensidad U, y pueden saltar a uno de los átomos próximos con una reducción t_{ij} en la energía del sistema [9],

$$H_{Hub} = -\sum_{<i,j>\sigma} t_{ij} c^{\dagger}_{i\sigma} c_{j\sigma} + U \sum_{i} n_{i\uparrow} n_{i\downarrow}. \tag{7.2.1}$$

La interacción de Coulomb esta apantallada fuera del átomo, y su término dominante dentro del mismo puede escribirse

$$U = \int d\mathbf{r} d\mathbf{r}' \phi_i^*(\mathbf{r}) \phi_i^*(\mathbf{r}') V(\mathbf{r}-\mathbf{r}') \phi_i(\mathbf{r}') \phi_i(\mathbf{r}), \tag{7.2.2}$$

donde $V(\mathbf{r}-\mathbf{r}')$ representa la interacción de Coulomb y $\phi_i(\mathbf{r})$ la función de onda del orbital correspondiente al átomo i-ésimo. El coeficiente t_{ij} describe el transporte entre orbitales de diferentes átomos, y este salto se considera sólo entre vecinos próximos,

$$t_{ij} = -\int d\mathbf{r} \phi_i^*(\mathbf{r}) h(\mathbf{r}) \phi_j(\mathbf{r}) = t_{ji}^*, \tag{7.2.3}$$

donde $h(\mathbf{r})$ representa la parte mono-particular del hamiltoniano con el término cinético y los campos externos.

En el límite de "acoplamiento fuerte", $|t_{ij}|/U \to 0$, no está permitida la doble ocupación en cada sitio, ya que esto eleva mucho la energía del sistema. En esta situación se puede demostrar que el hamiltoniano de Hubbard se reduce al "modelo $t-J$", donde la interacción de Coulomb da lugar a otra de tipo Heisenberg entre vecinos próximos.

$$H_{t-J} = -\sum_{<i,j>\sigma} t_{ij} c^{\dagger}_{i\sigma} c_{j\sigma} + \sum_{<i,j>} J_{ij} \left(\mathbf{S}_i \mathbf{S}_j + \frac{1}{4} \right), \tag{7.2.4}$$

donde el operador $\mathbf{S}_i = \sum_i c^\dagger_{i\sigma}\sigma_{\sigma\sigma'}c_{i\sigma'}/2$ y el acoplamiento $J_{ij} = 4|t_{ij}|^2/U$ proviene de dos saltos, uno de ida y otro de vuelta, suprimidos por la energía de Coulomb debida a la doble ocupación "virtual". Debido al hecho de que el modelo de Hubbard solamente permite la doble ocupación cuando los dos electrones tienen diferente espín el acoplamiento de Heisenberg resultante es antiferromagnético. De este modo vemos como la interacción de Heisenberg tiene un origen electrostático. De hecho el campo magnético generado por los dipolos magnéticos es de una intensidad de 10^4 veces inferior a la *inducida* por las constantes de Heisenberg típicas [10].

Cuando consideramos el sistema a "llenado mitad", es decir, un electrón por cada átomo, al no estar permitida la doble ocupación por el modelo $t-J$ no pueden producirse saltos de los electrones, obtenemos el modelo de Heisenberg,

Estos modelos describen gran parte de la física de sistemas cristalinos magnéticos. Por ejemplo, se cree que el modelo $t-J$ es el que describe la superconductividad de alta temperatura crítica. El modelo de Heisenberg por su parte describe satisfactoriamente las características físicas de los cristales ferromagnéticos y antiferromagnéticos.

Uno de los trabajos en que se basa esta tesis se refiere al estudio de las escaleras de espín, que interaccionan mediante un modelo de Heisenberg. Estas escaleras de espín consisten en el acoplamiento de varias cadenas de espín paralelas. El estudio de las mismas puede arrojar un entendimiento más profundo sobre la transición entre 1 y 2 dimensiones. En este sentido mientras las escaleras con un número impar de cadenas presentan una transición continua (longitud de correlación infinita, no presentan gap) las de un número par la tienen discontinua (longitud de correlación finita, gap en el espectro de excitaciones) [11]. Además se han descubierto recientemente materiales, como el VOPO, cuyas características físicas están descritas por escaleras de espín, lo cual nos ofrece un campo donde comprobar experimetalmente la validez de los resultados obtenidos.

7.3 Grupo de Renormalización en Sistemas Cuánticos

Para el estudio de las escaleras de espín utilizamos una técnica muy potente y ámpliamente utilizada como es el RG. Este nos permite describir el comportamiento macroscópico de un sistema, es decir, partiendo de una teoría microscópica aplicamos

un algoritmo, conocido como transformación de grupo de renormalización (RGT), que realza los grados de libertad relevantes macroscópicamente (en el régimen de bajas energías y largas distancias), y construye la interacción entre ellos.

7.3.1 Bloqueado y condiciones de contorno

La RGT más habitual es un proceso de "bloqueado". En el bloqueado se divide el sistema por bloques y se escogen los grados de libertad relevantes dentro de cada bloque (después del bloqueado no podemos recuperar los detalles de la información microscópica dentro de cada bloque). Después de repetir el proceso un cierto número de veces se puede alcanzar un punto estacionario, que nos da la descripción macroscópica del sistema.

Cuando consideramos un sistema cuántico [12] podemos resolver el problema cuántico en el bloque y escoger los estados representativos entre las soluciones, en principio, los de más baja energía. Para la resolución del problema cuántico del bloque hemos de imponer condiciones de contorno (BC). Si imponemos unas BC particulares el conjunto de funciones de onda de los bloques no reproducirá la función de onda del sistema global. Una forma de evitar este problema es considerando el método de combinación de condiciones de contorno (CBC), que consiste en resolver el bloque para varias BC y al final hacer una combinación de todas la soluciones. Ahora hemos de decidir el criterio para hacer la combinación.

7.3.2 Grupo de renormalización de matriz densidad

El grupo de renormalización de matriz densidad (DMRG) desarrollado por White en 1992 [1] es el método de CBC más eficiente para sistemas unidimensionales. El DMRG sigue el proceso de renormalización desarrollado por Wilson para el estudio del problema de Kondo, que consiste en generar una cadena unidimensional por un método recursivo añadiendo un sitio en cada paso del RG, es decir, dada una cadena B (descrita por m estados, $|\beta\rangle$) le añadimos un sitio $\bullet$ (descrito por m^* estados, $|s\rangle$) para obtener una nueva cadena B' (descrita por m estados, $|\alpha\rangle$), $B\bullet \rightarrow B'$.

El algoritmo de DMRG resuelve el sistema $B\bullet$ para varias BC y decide el criterio de combinación de las mismas de una sola vez.

1. Dobla el sistema $B\bullet$ para formar el llamado superbloque $B \bullet \bullet B^R$, donde B^R es la reflexión de la cadena B.

2. Calcula el estado fundamental del superbloque $|\Psi_0\rangle$.

3. Realiza la traza parcial de la matriz densidad $|\Psi_0\rangle\langle\Psi_0|$ sobre la ampliación del sistema $\bullet B^R$,
$$\rho = tr_{\bullet B^R}|\Psi_0\rangle\langle\Psi_0|. \tag{7.3.1}$$

4. Diagonaliza la matriz ρ, que describe la física del sistema $B\bullet$.

5. Toma los m estados de autovalor más grande como los representantes del nuevo sistema B'.

Esta truncación del espacio de Hilbert se refleja en la siguiente relación recurrente para los estados:
$$|\alpha\rangle_N = \sum_{\beta s} A^{(N)}_{\alpha\beta}[s]\ |s\rangle_N \otimes |\beta\rangle_{N-1}, \tag{7.3.2}$$
donde las matrices $A^{(N)}_{\alpha\beta}[s]$ son calculadas en cada paso del RG y están directamente relacionadas con las matrices de cambio de base que diagonalizan la matriz densidad ρ.

La expresión (7.3.2) es el punto de partida para el trabajo expuesto en el capítulo 2 que resumiremos en la próxima sección.

7.4 Método de Producto de Matrices

En el cápitulo 2 hemos presentado un método basado en el DMRG que pretende arrojar un entendimiento más profundo sobre el funcionamiento de este último. Al ser el DMRG un método numérico es dificil seguir la evolución del proceso físico y extraer alguna intuición de él. El método de producto de matrices (MPM) es un método recurrente variacional que asume la existencia de un punto fijo para la equación (7.3.2) de tal forma que $\lim_{N\to\infty} A^{(N)}_{\alpha\beta}[s] = A_{\alpha\beta}[s]$. En este caso, dado un conjunto de estados $|\beta\rangle$ para B y $|s\rangle$ para $\bullet$, utilizamos la fórmula recurrente
$$|\alpha\rangle_N = \sum_{\beta s} A_{\alpha\beta}[s]\ |s\rangle_N \otimes |\beta\rangle_{N-1} \tag{7.4.1}$$
para calcular los observables (energía del estado fundamental, longitud de correlación, etc.) para el sistema unidimensional, que dependerán de las matrices $A_{\alpha\beta}[s]$. Estas matrices las tomamos como parámetros variacionales y las calculamos mediante la minimización de la energía del estado fundamental.

El sistema sobre el que trabajamos son las escaleras de espín de dos cadenas, que pueden ser asimiladas a sistemas unidimensionales considerando cada peldaño de la escalera como un sitio en una cadena unidimensional. Los espines de estas cadenas interacionan entre si mediante el hamiltoniano de Heisenberg

$$H_N = J_\perp \sum_{n=1}^{N} \mathbf{S}_1(n) \cdot \mathbf{S}_2(n) + J_\parallel \sum_{n=1}^{N-1} \left(\mathbf{S}_1(n) \cdot \mathbf{S}_1(n+1) + \mathbf{S}_2(n) \cdot \mathbf{S}_2(n+1) \right), \quad (7.4.2)$$

donde $\mathbf{S}_a(n)$ es un operador de espín S actuando en el escalón $n = 1, \ldots, N$ y en la cadena $a = 1, 2$ de la escalera.

Debido al hecho de que el hamiltoniano conmuta con el operador de espín total podemos escoger estados de espín bien definido para describir el sistema,

$$|J_1 M_1\rangle_N = \sum_{\lambda J_2} A^{\lambda}_{J_1 J_2} \, |(\lambda J_2), J_1 M_1\rangle_N, \quad (7.4.3)$$

donde

$$|(\lambda J_2), J_1 M_1\rangle_N = \sum_{\mu} \langle \lambda\mu, J_2 M_2 | \lambda J_2, J_1 M_1 \rangle \;\; |\lambda\mu\rangle_N \otimes |J_2 M_2\rangle_{N-1} \quad (7.4.4)$$

y $A^{\lambda}_{J_1 J_2}$ son los parámetros variacionales. De este modo el formalismo se simplifica enormemente al poder utilizar todas las propiedades del grupo de rotaciones (teorema de Wigner-Eckart).

Mediante este método hemos calculado la energía del estado fundamental, la longitud de correlación y algunos otros observables similares para diferentes tipos de escaleras, dependiendo del caracter ferromagnético (F) o antierromagnético (A) de los acoplamientos de Heisenberg a lo largo de las cadenas y los peldaños de la escalera. Los casos considerados son $AA_{1/2}$, $AF_{1/2}$, $FA_{1/2}$, AA_1 y $AA_{3/2}$ (por ejemplo $AF_{1/2}$ es una escalera de espín $1/2$ con acoplamiento A en las cadenas y F en los peldaños). Además ciertas relaciones de simetría propuestas en [13] para las escaleras de espín $1/2$, que denominamos "dualidades", son puestas de manifiesto al menos para algunas regiones de los acoplamientos $J_\parallel$ y $J_\perp$.

7.5 Manganitas Dopadas

Las manganitas constituyen un grupo genérico de aleaciones que presentan un estado fundamental con una gran riqueza en su estructura magnética, que va desde el

antiferromagnetismo hasta el ferromagnetismo, pasando por fases *canted* (es decir, las magnetizaciones en las dos subredes forman un ángulo θ, $0 < \theta < \pi$) o regiones de separación de fases. Estas aleaciones se basan en la fórmula general $La_{1-x}A_xMnO_3$, donde $A = Ca, Sr$, o Ba y $0 \leq x \leq 1$ representa el número de átomos de La que son sustituidos por átomos del tipo A. La valencia con la que actuan los diferentes elementos es La^{3+}, A^{2+}, Mn^{3+} ($[Ar]3d^4$) o Mn^{4+} ($[Ar]3d^3$) y O^{2-}. Por lo tanto, cada sustitución $La^{3+} \rightarrow A^{2+}$ corresponde a una sustitución en el átomo de manganeso $Mn^{3+} \rightarrow Mn^{4+}$, el cual al jugar el papel de átomo magnético en el compuesto produce un cambio en el espín $S = 2 \rightarrow S = 3/2$ (el principio de Pauli ayuda a minimizar la energía electrostática en las capas de tipo d, si los electrones permanecen desapareados dando lugar al máximo espín posible. Esta es la conocida Regla de Hund).

Pasaremos ahora a resumir brevemente las estructuras cristalográficas y magnéticas de estos materiales. Por lo general, las manganitas cristalizan en una estructura de tipo Perovskita deformada. La estructura de Perovskita tiene los átomos de Mn en los vértices de un cubo, mientras el otro elemento metálico (La, Ca, Sr o Ba) está colocado en el centro del cubo y los átomos de O en el centro de las caras. Desde esta estructura el grupo espacial ideal $Pm\bar{3}m$ se deforma ligeramente dando lugar a un grupo espacial ortorrómbico. El campo cristalino produce el desdoblamiento de la banda d, con degeneración 5, en dos nuevas bandas, t_{2g}, con degenaración 3, y e_g, con degeneración 2. Para valores pequeños de x una nueva deformación (deformación de Jahn-Teller) produce un nuevo desdoblamiento de la banda e_g.

La estructura de bandas anterior implica que los compuestos de los extremos, es decir, $LaMnO_3$ ($x = 0$) y $AMnO_3$ ($x = 1$) se comportan como semiconductores. Estos compuestos además presentan un estado fundamental antiferromagnético, debido al acoplamiento antiparalelo que se produce entre los electrones de las capas d de átomos vecinos. En cambio, para $0.2 < x < 0.4$ el estado fundamental resulta ser ferromangnético. En este rango del *doping* se observan propiedades de conducción, lo que sugiere una relación entre ambos fenómenos. De hecho, Zener en su "modelo de doble intercambio" [14] postula que el intercambio de electrones entre el Mn^{3+} y el Mn^{4+} a través de los átomos de O produce una disminución de la energía del sistema, y debido a que los intercambios no modifican el espín de los electrones el estado ferromagnético resulta ser el más favorecido.

Las anteriores características son las que definen un problema de Kondo con interacción antiferromagnética, descritos por el modelo $s - d$. Este modelo considera los

electrones el la banda e_g como fermiones dinámicos cuánticos de espín 1/2, con una amplitud de transición t_{ij} y una interacción local ferromagnética de Heisenberg con un espín clásico, generado por los electrones de la banda t_{2g}, que tiene en cuenta la regla de Hund. Los espines clásicos interaccionan, a su vez, antiferromagnéticamente con sus vecinos próximos.

$$H_{s-d} = -\sum_{<i,j>\sigma} t_{ij} c^\dagger_{i\sigma} c_{j\sigma} - \frac{J_H}{2} \sum_i c^\dagger_i \boldsymbol{\sigma} c_i \mathbf{S}_i + \sum_{<i,j>} J_{ij} \mathbf{S}_i \mathbf{S}_j. \tag{7.5.1}$$

7.6 Modelo de Campos para Manganitas Dopadas

Basándonos en el modelo anterior, en el capítulo 3 hemos introducido un modelo continuo que describe las propiedades de baja energía de las manganitas dopadas. En primer lugar, introducimos dos campos de magnetización, $\mathbf{M}_1(x)$ y $\mathbf{M}_2(x)$, que varian suavemente, asociados a las dos subredes del cristal. Después añadimos dos campos fermiónicos para describir los huecos conductores producidos por el dopaje, que interaccionan localmente con la correspondiente magnetización. El número de huecos dopantes es controlado por un potencial químico.

$$\begin{aligned} \mathcal{L}(x) &= \psi_1^\dagger(x) \left[(1+i\epsilon) i\partial_0 + \frac{\partial_i^2}{2m} + \mu + J_H \frac{\boldsymbol{\sigma}}{2} \mathbf{M}_1(x) \right] \psi_1(x) \\ &\quad + \psi_2^\dagger(x) \left[(1+i\epsilon) i\partial_0 + \frac{\partial_i^2}{2m} + \mu + J_H \frac{\boldsymbol{\sigma}}{2} \mathbf{M}_2(x) \right] \psi_2(x) \\ &\quad + t \left(\psi_1^\dagger(x) \psi_2(x) + \psi_2^\dagger(x) \psi_2(x) \right) - J_{AF} \mathbf{M}_1(x) \mathbf{M}_2(x), \end{aligned} \tag{7.6.1}$$

En ella hemos considerado la aproximación parabólica de la banda para *doping* pequeño.

Asumimos que tomando $t = 0$ los potenciales químicos asociados a pequeños *dopings* se encuentran por debajo de la banda llena. Cuando permitimos valores finitos del parámetro t la banda puede bajar cruzando el potencial químico, lo que dará lugar a conductividad, así como ferromagnetismo o fases *canted*.

El potencial efectivo para los campos $\mathbf{M}_1(x)$ y $\mathbf{M}_2(x)$, obtenido después de integrar los grados de libertad femiónicos en la integral de camino, da lugar a diferentes fases: AFI (AF-Aislante), $AFC2$ (AF-Conductora, 2-bandas), $CC2$ ($Canted$-Conductora, 2-bandas), $CC1$ and $FC1$, así como una región de separación de fases.

7.7 Ruptura Espontánea de Simetría

Como digimos en la introducción, ciertas excitaciones colectivas de baja energía, que son conocidas como modos de Goldstone, pueden existir en los sistemas de CM. Por ejemplo, los fonones, en cualquier sistema cristalino, o las ondas de espín, en sistemas ordenados magnéticamente. Estas excitaciones colectivas están presentes, en general, en sistemas en los que se produce una ruptura espontánea de la simetría. Existen teorías efectivas de campos especialmente adecuadas para describir su dinámica, que está totalmente determinada (salvo algunos coeficientes que deben ser medidos experimentalmente o calculados desde primeros principios) por propiedades de simetría, que son independientes de los detalles del modelo microscópico que describe el sistema.

7.7.1 Teorema de Goldstone

Dado un sistema decimos que existe ruptura espontánea de simetría (SSB) cuando la teoría presenta un grupo de simetría G, mientras que el estado fundamental de dicho sistema tiene un grupo de simetría menor H, $H \subset G$. En estas circunstancias el teorema de Goldstone nos dice que aparecen modos de excitación sin gap en el espectro del sistema.

Estos modos están descritos por campos que transforman bajo el grupo G como elementos del coset G/H. El número de campos reales que describen estos modos es igual al número de generadores que rompen la simetría, es decir, $n_G - n_H$, donde n_G y n_H son el número de generadores de los grupos G y H respectivamente. Mientras el número de campos es conocido, el número de modos descritos por estos campos no puede ser conocido *a priori*, pues depende del tipo de ecuación que verifiquen los campos. Una ecuación de onda (de tipo Klein-Gordon) describe un modo por medio de un campo real, mientras que una ecuación de Schödinger describe un modo por medio de un campo complejo, o lo que es lo mismo dos campos reales [15]. El tipo de ecuación que describe la dinámica viene determinado por las propiedades de transformación espacio-temporales.

7.7.2 Lagrangianos efectivos

Ya hemos mencionado anteriormente la importancia de los modos de Goldstone en la descripción de un sistema físico. Debido a la ausencia de gap en su espectro de

excitación son susceptibles de aparecer en cualquier fenómeno. Por esta razón debemos dotarnos de un formalismo que describa tanto su presencia como su interacción con el resto de los componentes. En primer lugar trataremos de describir matemáticamente los modos de Goldstone.

Los modos de Goldstone, como los fonones u ondas de espín, son fluctuaciones de un estado fundamental que tiene un grupo de simetría, H, inferior al de la teoría, G. Esta fluctuación puede imaginarse como un elemento de G, donde los parámetros del grupo varían lentamente sobre la estructura espacio-temporal del estado fundamental. Aquellos parámetros que producen una fluctuación a lo largo de las direcciónes de H serán irrelevantes, pues dejan invariante el estado fundamental, por lo que el elemento resultante pertenece al coset G/H.

$$U(x) = \exp\left\{\frac{i}{f_\pi}\pi^a(x)X^a\right\} \quad \in \quad G/H \qquad , \qquad (a = 1, \ldots, n_G - n_H). \tag{7.7.1}$$

Los elemntos del coset G/H transforman bajo un elemento del grupo G según una transformación no lineal dada por

$$U(x) \longrightarrow gU(x)h^\dagger(g,U) \qquad , \qquad h^\dagger(g,U) \in H, \tag{7.7.2}$$

de forma que el elemento $h^\dagger(g,U)$ retorna al coset el campo transformado $gU(x)$.

Ahora que conocemos el campo que describe los modos de Goldstone y sus transformaciones pasaremos a construir un lagrangiano efectivo que describa la dinámica de estos modos. Los modos de Goldstone son soluciones de baja energía de la teoría subyacente que tiene un grupo de simetría G, por lo tanto, una teoría efectiva que reproduzca el espectro de baja energía del sistema ha de ser invariante bajo el mismo grupo de simetría, G. El lagrangiano efectivo es un escalar bajo el grupo de invariancia de la teoría, por lo que hemos de construir un desarrollo de términos invariantes en potencias de derivadas. Además podemos admitir la presencia de términos topológicos o invariantes salvo una derivada total, que dan lugar a acciones invariantes. Estos términos juegan un papel esencial como hemos visto en el capítulo 4.

El número de modos de Goldstone descritos por el campo $U(x)$ está determinado por las propiedades de transformación de este bajo el grupo de simetría espacio-temporal. Estas propiedades están relacionadas con la forma en que se produce la ruptura espontánea de la simetría espacio-temporal. En sistemas relativistas [6] el grupo de simetría espacio-temporal está dado por el grupo de Poincaré, lo que nos lleva a ecuaciones de onda (de tipo Klein-Gordon) para los modos de Goldstone, donde

cada modo está descrito por un campo. Además en estos casos el estado fundamental no rompe la invariancia Poincaré. En el caso no relativista la situación es más compleja. En principio podría parecer que el grupo de simetría tendría que ser el de Galileo, y por tanto los modos estarían descritos por una ecuación de Schödinger (habría la mitad de modos que de campos), pero la realidad es que los grupos espaciales cristalográficos son los relevantes. El estado fundamental puede romper espontáneamente esta simetría cristalográfica, lo cual permite la aparición de ecuaciones de onda para la descripción de los modos de Goldstone.

7.8 Ondas de Espín en Cristales Magnéticos

En el capítulo 4 hemos desarrollado la teoría presentada en la sección anterior para el caso de las ondas de espín en cristales ferromagnéticos y antiferromagnéticos. Las ondas de espín son modos de Goldstone debidos a la SSB de $SU(2) \to U(1)$, es decir, pasamos de la invariancia bajo rotaciones de espín a la invariancia bajo una sola dirección, la dirección de alineamiento de los espines en los estados ferromagnético y antiferromagnético que la tomamos en la tercera dirección del espín, $U(1) = \langle e^{i\theta S^3} \rangle$. En este caso estos modos están descritos por

$$U(x) = exp\left\{ \frac{i\sqrt{2}}{f_\pi} \left[\pi_1(x) S^1 + \pi_2(x) S^2 \right] \right\}, \tag{7.8.1}$$

donde S^i son los generadores de $SU(2)$ y $\pi_i(x)$ son los campos que describen las ondas de espín (f_π es un factor dimensional).

Por conveniencia, para la aplicación que hemos desarrollado en el capítulo 5, hemos tomado como grupo de transformaciones espacio-temporal $R\bar{3}c \otimes T$, que es el grupo correspondiente al Cr_2O_3. Este grupo se rompe espontáneamente de forma distinta en el caso ferromagnético o antiferromagnético. Para el caso ferromagnético el espín apunta en el mismo sentido en todos los puntos del cristal, así podemos considerar que el campo $U(x)$ permanece invariante bajo cualquier transformación espacial. Por otro lado, en el caso antiferromagnético podemos decir que existen dos subredes en las cuales los espines apuntan en sentidos opuestos. Así una transformación espacial que nos lleve de una subred a la otra (la inversión espacial I para el Cr_2O_3) debe reflejarse en la transformación de $U(x)$. En efecto, en este caso $U(x) \to U(x)C$, donde $C = e^{-i\pi S^2}$ es una matriz que invierte el espín.

Estas transfomaciones junto con los términos topológicos mencionados en el apartado anterior dan lugar a la diferencia entre las ondas de espín ferromagnéticas y antiferromagnéticas. Consideremos $a_0^3(x) \sim tr(U^\dagger(x) i\partial_0 U(x) P_+)$ (P_+ es un proyector sobre la componente más alta del espín) que bajo la transformación (7.7.2) resulta ser un término topológico. Este es el único término que puede dar lugar a una ecuación de primer orden en la derivada temporal. Para el estado ferromagnético es así, pues $a_0^3(x)$ es invariante bajo las transformaciones espaciales, en particular I. Por el contrario, en el estado antiferromagnético $a_0^3(x) \to -a_0^3(x)$ bajo I, lo que prohibe este término en el lagrangiano efectivo, y por lo tanto el ecuación será de segundo orden en derivadas temporales, lo que nos lleva a una ecuación de onda para describir las ondas de espín de un estado antiferromagnético.

En el capítulo 4 también hemos introducido pequeñas perturbaciones, provenientes del acoplamiento espín-órbita y de dipolo magnético, que no respetan la simetría $SU(2)$ (decimos que rompen explicitamente la simetría). Estas perturbaciónes dan lugar a un gap en el espectro de las ondas de espín que depende del parámetro de acoplamiento.

Por último, y tratando de enlazar con el trabajo presentado en el capítulo 5, presentamos el acoplamiento de las ondas de espín con el campo electromagnético. Existen dos mecanismos, uno el acoplamiento de Pauli, que rompe explicitamente la simetría $SU(2)$, el otro es un acoplamientos no mínimo (acoplamiento directos al tensor de campo electromagnético $F_{\mu\nu}$, o lo que es lo mismo a $\mathbf{E}$ y $\mathbf{B}$).

En el capítulo 5 hemos aplicamdo el formalismo del capítulo 4 al estudio de la posible detección de efectos no recíprocos en cristales antiferromagnéticos en la región de microondas, donde el espectro está dominado por las ondas de espín. Los efectos no recíprocos son aquellos que no son invariantes bajo inversión temporal. En nuestro caso si enviamos un haz de microondas con un número de onda $\mathbf{k}$ y otro con $-\mathbf{k}$ los efectos físicos producidos son diferentes. Observamos que estos efectos se producen en la generación de segundo armónico y en la birefringencia girotrópica.

7.9 Conclusiones y Perspectivas

En esta sección recogeremos los resultados más importantes obtenidos en los trabajos de esta tesis.

En el capítulo 2 hemos presentado un método variacional semianalítico del RG para sistemas cuánticos denominado MPM. Este método nos permite un mejor en-

tendimiento de resultados numéricos anteriores.

1. Hemos presentado una formulación invariante rotacional (para escaleras de espín de dos cadenas) del MPM que nos permite expresar la densidad de energia del estado fundamental, la longitud de correlación y el parámetro de orden de *string* en términos de objetos invariantes, lo que reduce considerablemente el número de parámetros independientes del MP utilizados en el proceso de minimización.

2. Hemos mejorado los resultados numéricos para la densidad de energía y la longitud de correlación del estado fundamental obtenidos en trabajos anteriores. La consideración de *ansatzs* de MP con multiples estados por espín mejoraría los resultados.

3. Hemos mostrado la equivalencia entre la escalera $AF_{1/2}$ y la cadena antiferromagnética de Heisenberg de espín 1. Los resultados del MPM en ambos casos nos ofrecen grandes coincidencias en los resultados numéricos.

4. Hemos encontrado nuevas evidencias numéricas que refuerzan la idea de la existencia de propiedades de dualidad entre las escaleras con estructuras magnéticas AA, AF y FA.

5. Hemos mostrado que el orden topológico de largo alcance es destruido en las cadenas de espín 1 cuando dos de estas cadenas se acoplan para formar un escalera. Además hemos dado una visión física de la escalera de espín 1 en función de cadenas cerradas resonantes de espín 1.

La relación que apuntabamos al principio entre el MPM y el DMRG nos permite suponer la posibilidad de realizar una transfomación del formalismo de minimización de la energía del estado fundamental convirtiéndolo en un problema de valores propios para el superbloque $B_N \bullet B_N^R$.

Hemos demostrado que el MPM es adecuado para estudiar las escaleras de espín de dos cadenas en los regímenes de acoplamiento fuerte e intermedio. Esto se debe al hecho de que estas escaleras tienen una correlación finita, al igual que todas las cadenas con un número par de cadenas, lo que hace suponer que el método será igualmente valido para ellas. Sin embargo las escaleras con un número impar de cadenas tienen una correlación infinita, y por lo tanto es difícil que el método de buenos resultados en el límite de N grande con el formalismo actual. Los sistemas de dos dimensiones

son interesantes para su estudio mediante el MPM, ya que pueden imaginarse como escaleras con un número muy grande de cadenas. Esto nos llevaría a seleccionar los estados a añadir en los peldaños en cada iteración de entre todos los posibles.

En el capítulo 3 hemos presentado un estudio de las propiedades del estado fundamental para las manganitas dopadas.

1. Hemos presentado un modelo continuo que incorpora las características principales de las manganitas dopadas y nos permite la exploración del diagrama de fases incluso más alla de los parámetros de los materiales actuales.

2. Hemos calculado el diagrama de fases a temperatura cero, partiendo del potencial efectivo, en términos del potencial químico y el parámetro de *doping* x. Aparecen fases antiferromagnéticas, ferromagnéticas y *canted*, incluso una region de separación de fases, según variamos el *doping*.

3. Las fases *canted* obtenidas son termodinámicamente estables frente a la separación de fases.

El siguiente objetivo dentro del modelo será calcular el diagrama de fases a temperatura finita, con lo que podríamos ver como evolucionan las diferentes fases al autementar la temperatura. También sería interesante precisar las diferentes fases que pudieran coexistir en la región de separación de fases.

En el capítulo 4 hemos presentado un estudio sistemático de las ondas de las espín en sólidos cristalinos ferromagnéticos y antiferromagnéticos.

1. Hemos presentado una forma sistemática de escribir un lagrangiano efectivo que describa la dinámica de las ondas de espín en médios cristalinos haciendo un uso extensivo del patrón de SSB $SU(2) \to U(1)$ así como de las simetrías espaciales y la inversión temporal.

2. El formalismo presentado mantiene bajo control los términos topológicos.

3. Las diferencias entre los lagrangianos efectivos para las ondas de espín ferromagnéticas y antiferromagnéticas han sido obtenidos únicamente mediante criterios de simetría.

4. En el caso antiferromagnético hemos mostrado que la existencia de traslaciones primitivas que conecten las dos subredes tiene consecuencias no triviales en el aspecto del lagrangiano efectivo.

5. Hemos mostrado como introducir términos que rompen explicitamente la simetría, dados por la interacción de espín-órbita y la de dipolo magnético. Estos términos dan lugar a un gap en el espectro de excitación de las ondas de espín.

6. Hemos introducido el acoplamiento de las ondas de espín con el campo electromagnético. Por un lado, mediante una interaccón de Pauli que no introduce parámetros adicionales en el lagrangiano efectivo, y por otro, mediante un acoplamiento no mínimo con los campos $\mathbf{E}$ y $\mathbf{B}$.

En el capítulo 5 hemos descrito la respuesta electromagnética en la región de microondas del Cr_2O_3 basándonos en el formalismo anterior.

1. Integrando las ondas de espín en la integral de camino hemos obtenido una acción no-local que contiene la respuesta del material al campo electromagnético.

2. A partir de esta acción hemos calculado las susceptibilidades eléctricas y magnéticas relevantes para la birefringencia girotrópica y la generación de segundo armónico, las cuales presentan una funcionalidad no trivial en la frecuencia de la luz incidente. Estas dependen de constantes arbitrarias, cuyo orden de magnitud está determinado por el parámetro de red a y la energía de la primera excitación con gap J.

3. Estas susceptibilidades dan lugar a efectos no recíprocos como consecuencia directa de la ausencia de traslaciones primitivas que conecten las dos subredes del estado antiferromagnético y la existencia de acoplamiento espín-órbita.

4. El Cr_2O_3 tiene espín 3/2, pero este resultado es válido para cualquier cristal antiferromagnético con un grupo puntual $\bar{3}m$ y un espín arbitrario, como, por ejemplo, el V_2O_3 (espín 1).

Las manganitas dopadas presentan un diagrama de fases en los que existen estructuras magnéticas *canted*. Con el formalismo de lagrangianos efectivos podemos estudiar la dinámica de las ondas de espín en estas fases. La SSB en este caso es $SU(2) \to 1$, con lo que existirán tres campos de Goldstone. Estos darán lugar a una onda de espín

ferromagnética y una antiferromagnética, con interacciones entre ellas que vendrán descritas por el lagrangiano efectivo. En estos materiales también existen fermiones conductores, por lo que podemos calcular fácilmente su interacción efectiva mediada por las ondas de espín.

Bibliografía

[1] S. R. White, *Phys. Rev. Lett.* **69** (1992) 2863;

S. R. White, *Phys. Rev.* **B48** (1993) 10345.

[2] J. Gasser and H. Leutwyler, *Ann. Phys. (N.Y.)* **158** (1984) 142.

[3] N. D. Mermin and H. Wagner, *Phys. Rev. Lett.* **22** (1966) 1133.

[4] K. G. Wilson, *Rev. Mod. Phys.* **47** (1975) 773.

[5] R. Shankar, *"Effective Field Theory in Condensed Matter Physics"*, cond-mat/9703210.

[6] J. Goldstone, *Nuovo Cim.* **19** (1961) 145.

[7] G. S. Guralnik, C. R. Hagen and T. W. B. Kibble, *"Advances in Particle Physics"*, Vol.2, p.567, ed. R. L. Cool and R. E. Marshak (Willey, New York, 1968).

[8] H. Leutwyler, *Phys. Rev.* **D49** (1994) 3033.

[9] Balachandran *et al.*, *"Hubbard Model and Anyon Superconductivity"* (World Scientific, Singapore, 1990).

[10] N. W. Ashcroft and N. D. Mermin, *"Solid State Physics"* (Saunders College Publishing, Forth Worth, 1976);

C. Kittel, *"Introduction to Solid State Physics"* (John Wiley & Sons, Inc., New York, 1971);

G. Burns, *"Solid State Physics"* (Academic Press, Inc., San Diego, 1985).

[11] G. Sierra, *J. Phys.* **A29** (1996) 3299.

[12] J. González *et al.*, *"Quantum Electron Liquids and High-T_c Superconductuvity"* (Springer, Berlin, 1995).

[13] G. Sierra, M. A. Martín-Delgado, *"Dualities in Spin Ladders"*, cond-mat/9706104, to appear in *J. Phys.* **A**.

[14] C. Zener, *Phys. Rev.* **82** (1951) 403.

[15] H. B. Nielsen and S. Chada, *Nucl. Phys.* **B105** (1976) 445.